X-470-66-509

TMX-55988

DELTA VEHICLE
FLIGHT FAILURE REPORT
LAUNCH 33

GPO PRICE $ ____________

CFSTI PRICE(S) $ ____________

Hard copy (HC) 3.00

Microfiche (MF) ____________

ff 653 July 65

OCTOBER 1966

NASA

GODDARD SPACE FLIGHT CENTER
GREENBELT, MARYLAND

FACILITY FORM 602

N67-40193 (ACCESSION NUMBER)

(THRU) 1

80 (PAGES)

(CODE) 31

TMX-55988 (NASA CR OR TMX OR AD NUMBER)

(CATEGORY)

X-470-66-509

DELTA VEHICLE

FLIGHT FAILURE REPORT

LAUNCH 33

October 1966

GODDARD SPACE FLIGHT CENTER
Greenbelt, Maryland

DELTA VEHICLE

FLIGHT FAILURE REPORT

LAUNCH 33

SUMMARY

The Delta three-stage vehicle that launched the OSO-C spacecraft from complex 17, Pad E, at Cape Kennedy, Florida on August 25, 1965, experienced a flight failure. A review of vehicle T/M data indicated nominal performance of the first and second stages up to 0.61 seconds after spin-up of the third stage. At this time the third stage chamber pressure rose indicating premature ignition of the third stage motor. Simultaneously, severe second stage attitude disturbances were experienced accompanied by second stage T/M dropout. Separation of the third stage from the second stage was probably effected by burning through the spin table.

Investigation of the possible causes for the premature ignition established that malfunction of the six second time delay squib used to ignite the third stage motor was the most probable cause of the failure. Tests conducted on this type of squib during the failure investigation revealed that the most probable mode of failure was blow-by of the hot gases from the ignition charge passed the six (6) second time delay train and igniting the main output charge of the squib.

CONTENTS

DELTA VEHICLE FLIGHT FAILURE REPORT

LAUNCH 33

INTRODUCTION

The objective of the Delta 33 launch vehicle was to inject the OSO-C spacecraft into a 300 nautical mile circular orbit with an inclination of 33 degrees. The DSV-3C three-stage vehicle used to launch OSO-C was composed of a MB-3 Block II first stage, and Aerojet General Corporation AJ10-118A second stage, and an ABL X-258-C third stage motor. A mission peculiar telemetry system was incorporated on the third stage to obtain performance data on the X-258 motor. (See Appendix A for a description of the third stage telemetry system and third stage flight performance).

Vehicle flight data indicates nominal performance and sequencing of the first and second stages up until 0.61 seconds after second stage programmer Sequence #4. Table 1 shows the predicted and actual sequence of events. Sequence #4 fires the eight spin rockets on the spin table, initiates the third stage time delay (6 seconds) squibs, starts the mechanical payload timer that effects third stage/spacecraft separation, ignites a one second pyrotechnic timer that fires second to third stage wire cutters, and fires a four-second pyrotechnic timer for Sequence #5 back-up. Two seconds later Sequence #5 effects second/third stage separation by firing two explosive bolts on the marmon band holding the stages together and retros the second stage back from the released third stage.

Second stage spin table monitoring switch T/M data shows that approximately one revolution of the spacecraft/third stage assembly occurred before loss of the T/M signal at third stage ignition. At spin-up a normal second stage roll attitude error was experienced due to the exchange of angular momentum through the spin table bearing. Prior to this time all second stage control system limit cycles and limit cycle rates were nominal. At ignition of the third stage a disturbance torque was imparted into both the yaw and roll axis of the second stage. This disturbance is attributed to the second and third stages being still attached during ignition of the third stage. The performance of the third stage was approximately 18 percent low as indicated by the third stage accelerometer data. Consequently, insufficient velocity was obtained and the payload did not achieve orbit.

The conclusion reached from the second and third stage data is that the third stage motor (X-258) ignited prematurely before the second stage signal to

Table 1

SEQUENCE OF LAUNCH EVENTS

Event	Predicted Time	Actual Time
Liftoff	T + 0	T + 0
MECO	T + 148.6	T + 148.2
Stage II Ignition Sequence 1	MECO + 4	MECO + 4
Jettison Fairing Sequence 2	MECO + 34	MECO + 34.8
SECO ETL Cutoff	MECO + 156.34	MECO + 161.1
Sequence 3	MECO + 170.5	MECO + 170.5
Stage III spinup Sequence 4	MECO + 533	MECO + 533.0
Stage II/Stage III separation Sequence 5	MECO + 535	MECO + 534.5
Sequence 5 Back-up	MECO + 537	not observed
Stage III Ignition	MECO + 539	MECO + 533.6
Stage III Burnout	MECO + 561.5	MECO + 556.9
Spacecraft/Stage II Separation	MECO + 659	MECO + 658.7
YO Deployment	MECO + 661	MECO + 661

initiate separation (Sequence #5) had occurred. Hence, the second stage was attached when ignition occurred, and the third stage burned itself free from the second stage.

DISCUSSION

The possible failure modes which could result in the premature ignition of the third stage motor are:

1. Premature Motor Ignition by Means Other Than Squib

The pyrogen igniter used in Delta 33 (shown in Figure 1) was modified after the Delta 32 flight. This modification was made because a marginal ignition condition between the SD60AO squib and the $BKNO_3$ pellets, housed in the head cap of the igniter. This condition was discovered in a test firing at AEDC where an attempt to ignite the X-258 motor, with one squib instead of the customary two squibs, failed. The investigation of this failure revealed that the squib had discharged into the pellet chamber but the $BKNO_3$ pellets failed to ignite. The modifications made to the igniter to correct this marginal ignition condition were:

a. The use of two pellet bags in place of one. The bag material was 1 mil non-conducting polyethylene in lieu of the former 4 mil conducting polyethylene bag.

b. Each bag contained different size pellets to improve the ignition characteristic. Pellet sizes 2A and 2L were used where only 2L was used in the past.

c. A phenolic spacer of larger inside diameter was used instead of the styrofoam spacer to eliminate the possibility of blocking the squib port and also to make additional room available for the additional $BKNO_3$.

d. The metal screen separating the $BKNO_3$ pellets from the igniter propellant grain was redesigned and metal washers were placed under the retaining screws.

Eight pyrogen igniters were fabricated before the Delta 33 flight. Six were tested in combinations of high and low temperature, vibration, sea level and vacuum conditions. The two remaining igniters were scheduled for flight and shipped to AMR. These igniters were x-rayed and one was rejected because of a loose spacer between the squib port and the $BKNO_3$ pellets, the other was used on Delta 33.

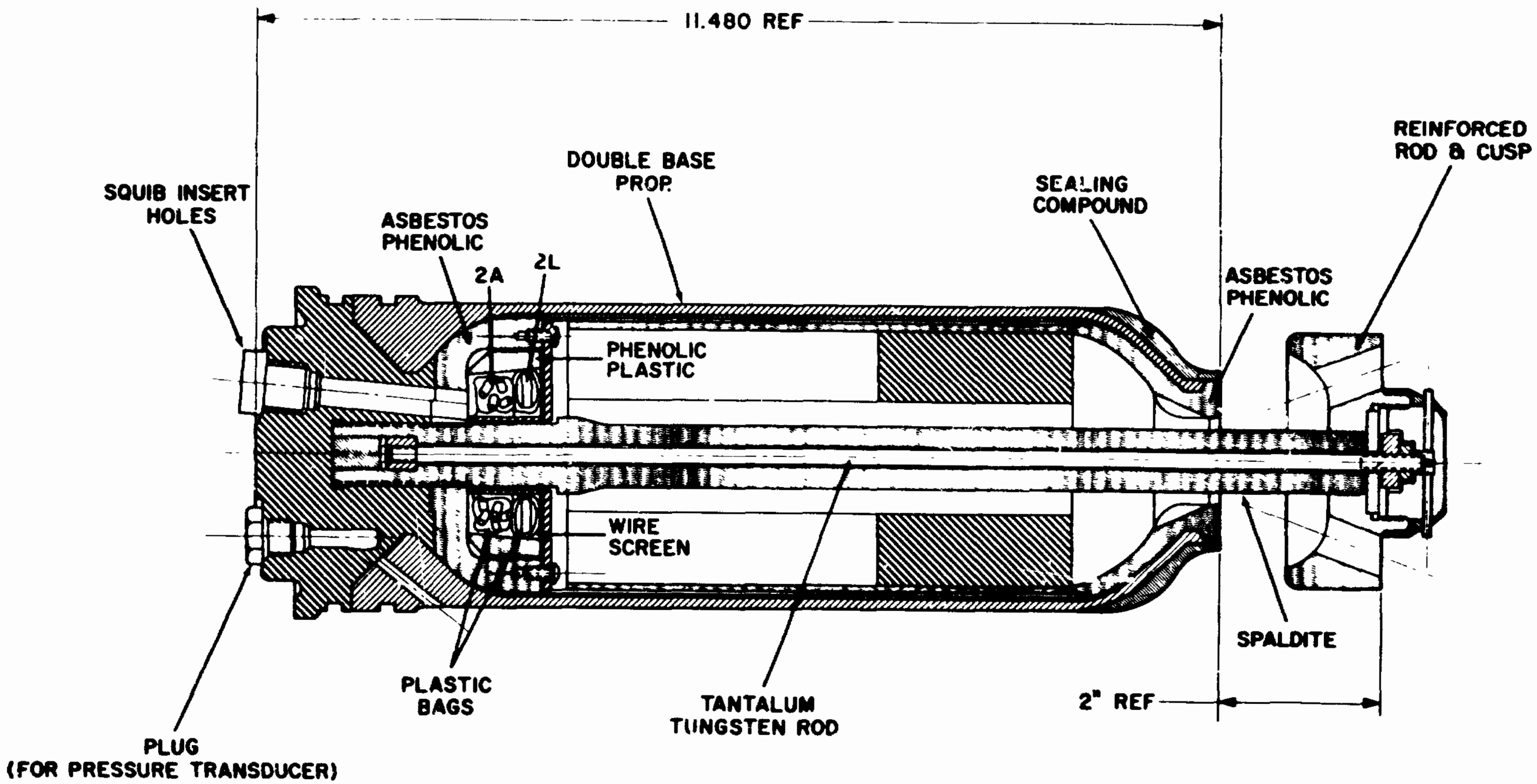
11.480 REF
SQUIB INSERT HOLES
ASBESTOS PHENOLIC
2A
2L
DOUBLE BASE PROP.
PHENOLIC PLASTIC
SEALING COMPOUND
ASBESTOS PHENOLIC
REINFORCED ROD & CUSP
WIRE SCREEN
SPALDITE
PLASTIC BAGS
TANTALUM TUNGSTEN ROD
2" REF
PLUG (FOR PRESSURE TRANSDUCER)

Figure 1

Since the modified igniter did not undergo spin acceleration tests, and since this was the first flight of the modified igniter, the possibility existed that in the process of modifying the igniter it was made sensitive to spin acceleration, impact, or static electric discharge and possibly upon spin up in flight the igniter fired without the aid of the squib.

The pyrogen igniter consists of several elements that operate sequentially. The main charge of the two SD60AO squibs impinge the $BKNO_3$ pellets, which in turn ignite the igniter main charge. If either the $BKNO_3$ or the igniter main charge could be set off by other than a squib firing this would be a possible cause for an early or premature ignition of the X-258 motor. The igniter main charge is sufficiently difficult to ignite that it is highly improbable that it could be ignited by other than burning of the $BKNO_3$ pellets. The pellets on the other hand are particularly suspect, since changes were made from the configuration that had been used previously. In order to increase ignition reliability, the igniter in Delta 33 used two doughnut shaped bags, one with 10 grams of 2L pellets and the other containing 7 grams of 2A pellets. In addition, the bag material was changed from 4 mil conducting polyethylene to 1 mil non-conducting polyethylene. This presented two possibilities; the autoignition sensitivity of the smaller pellets and the possibility of static charge generation by the non-conducting plastic bags. Since spinup was occurring, the angular acceleration could have caused an initiating mechanism related to one of the above mentioned igniter modifications. Therefore, test on the pyrogen igniters were conducted to determine the plausibility of these hypotheses.

Spin tests were conducted at Allegany Ballistics Laboratory to determine igniter sensitivity to angular acceleration. Pyrogen igniter head caps and squibs of the same type used on Delta 33 were spun at angular rates much higher than those experienced in flight. In addition, the angular acceleration used to achieve these rates were much higher than those used in flight. The results of these tests, which are outlined in detail in Appendix B resulted in no autoignition.

In addition to the spin tests, Cornell Aeronautical Laboratory conducted tests to determine the sensitivity of the pyrogen igniter to shock, vibration, and static electric discharge. The results of these tests, which are discussed in detail in Reference B, show that the igniter propellant grain and the $BKNO_3$ pellets to be entirely insensitive to energy levels many times in excess of those available in the flight environment.

The conclusion reached as a result of the tests is that the X-258 pyrogen igniter could not have been ignited by any other means than by squib initiation.

2. Premature Motor Ignition by Electrical System Malfunction

The electrical power system for the second stage of the Delta vehicle consists of the primary direct current sources and the distribution network required to provide power to the various second stage vehicle components and equipments. A block diagram of the power system is shown in Appendix C. The main components of this system are:

a. Battery, instrumentation, HR-5, 28 volts nominal, five ampere-hour.

b. Battery, engine, HR-15, 28 volts nominal, 15 ampere-hour.

c. Battery, control, HR-5, 28 volts nominal, five ampere-hour.

d. Inverter, static, 15/26 volt, three-phase, 400 cps ± 1 percent 0.075 kva; 2 windings 135 volt, single phase, 8.5 volt-ampere (va) outputs synchronized to ± 0.01 percent frequency regulation by programmer timer.

e. Junction boxes, including relays, interconnecting cabling, and circuitry.

f. Wiring harnesses.

g. Umbilical disconnects.

The batteries provide 28 volt dc power to the guidance system, flight controller, engine sequence box, hydraulic pump, telemetry system, pyrotechnic circuits, ordnance systems, and the inverter. The dc wiring is two-wire, grounded negative. The inverter provides both 3 phase and single phase ac power to the flight controller. The ac wiring is four-wire wye-connected with neutral grounded for the three phase inverter output and two-wire for the single phase outputs. During ground operations and checkout, power is provided by means of umbilical connections located on the second stage equipment section airframe. The junction boxes contain relays, terminal blocks, diodes, and resistors as required for the various electrical functions of the second stage. A four receptacle quick-disconnect umbilical assembly is located on the lower right-hand side of the equipment section for connection to external power supplies. The assembly enables switching to the internal battery power prior to vehicle lift off without interruption of power in excess of 10 milliseconds. Electrical wiring is routed from the umbilical assembly to the power distribution box, the sequence distribution box, flight controller, telemetry system, range safety junction box, and guidance system. Interconnecting cables to the engine section of the vehicle, which is separated from the equipment section by the propellant tanks, are routed through external tunnels mounted on the airframe. Interstage wiring to the first stage is routed through the second stage engine section with a quick disconnect at the separation plane. Interstage wiring to the third stage is through a conduit (spin tube) to the spin table terminal board and from the terminal board through two-wire cutters (interface) to the third stage attach fitting terminals.

The third stage electrical system, which is located on the payload attach fitting, consists of the following:

a. A single third stage battery made up of six (6) HR-05 Yardney Silvercel battery cells connected in series. The battery has a nine volt nominal, 0.5 amp-hour at a 0.5 ampere discharge rate capability, but is used in this application to provide high currents for short time periods.

b. Timing, sequencing, and firing circuits required to accomplish paddle deployment, boom deployment, spacecraft separation, and yo weight release or tumble rocket ignition when necessary.

The second to third stage interstage structure includes the electrical circuitry associated with the spin rockets, squib delay switches, separation bolts, third stage squib initiators, and wire cutters. The squib delay switches control power to the wire cutters. The cutters sever the wires crossing the second to third stage interface. The separation bolts fire to release the third stage prior to third stage burn.

The performance of the electrical system on Delta 33 was monitored by on-board instrumentation and appeared to be normal through sequence 4 of the second stage programmer. However, portions of the data were commutated necessitating further analysis and testing of the electrical system to insure a higher probability of proper system performance.

Since the mission failure was associated with the premature ignition of the third stage motor, only those portions of the electrical system which could have contributed to the failure are considered here.

There are two basic failure modes by which the electrical system might cause premature ignition of the third stage motor. They are an early pulse with sufficient energy to initiate normal squib operation, or excessive current causing abnormal squib delay. The third stage firing circuit was analyzed to determine the length of time a pulse could be applied to the circuit and be undetected by the instrumentation system. The results of this study show that the maximum undetected pulse length was 17 milliseconds (See Appendix C). This data was then used in the pulse sensitivity tests performed by the Franklin Institute on the third stage ignition squib (SD60AO), the IMT117 Dimple Motor and Atlas OM379-C14 squib switch which are on the same circuit. The details and the results of these tests are outlined in Reference A. The test data indicates that third stage ignition squib is an order of magnitude less sensitive than the Dimple Motor or the Squib Switch.

Resistance values of the electrical circuit for the third stage ignition squibs, the dimple motors, and the squib switches, were determined by actual measurement. These measurements were made on another vehicle at the Eastern Test Range and the results were used to determine initial current distribution for this circuit. These calculations indicated under normal operating conditions no excessive current would be applied to devices in the circuit. The details of this work are presented in Appendix C.

In addition to the resistance measurements just mentioned, pulse tests were performed on a mock-up of the third stage firing circuit. Electrical pulses of a few milliseconds duration were applied to the circuit and the output was observed across resistors simulating the bridgewires of the electro-explosive devices. The purpose of these tests were to determine the effect of circuit resistance on the signature of a short duration pulse at the output of the electro-explosive devices in the circuit. The results of these tests show the rise times of the pulses at the outputs were less than ten microseconds indicating no appreciable distortion.

The conclusion reached as a result of the tests made on the electrical system is that any spurious electrical signal that will initiate the third stage ignition squib would also initiate the Dimple Motors and the Squib Switches. Since the Dimple Motors or the Squib Switches did not initiate prematurely on the Delta 33 vehicle, it is highly improbable that a premature electrical signal of pulse from the electrical system caused the failure of this mission.

3. Premature Motor Ignition by Squib Malfunction

The third stage ignition squibs used in the Delta Vehicle were manufactured by the Port Ewen Works of the Hercules Powder Company. To date fifteen lots have been manufactured involving a total number of 918 squibs. Of the total number of 918 squibs there have been 228 squibs tested and 690 shipped.

The SD60AO squib shown in Figure 2 contains a six second time delay train, dual bridgewires with a recommended all fire current of 5.0 amperes per bridgewire. The bridgewires are covered with a single lead styphnate spot followed by a primer charge of 125 mg of lead oxide/boron which initiates the delay train composed of tellurium, selenium, and lead. The delay train fires the main charge

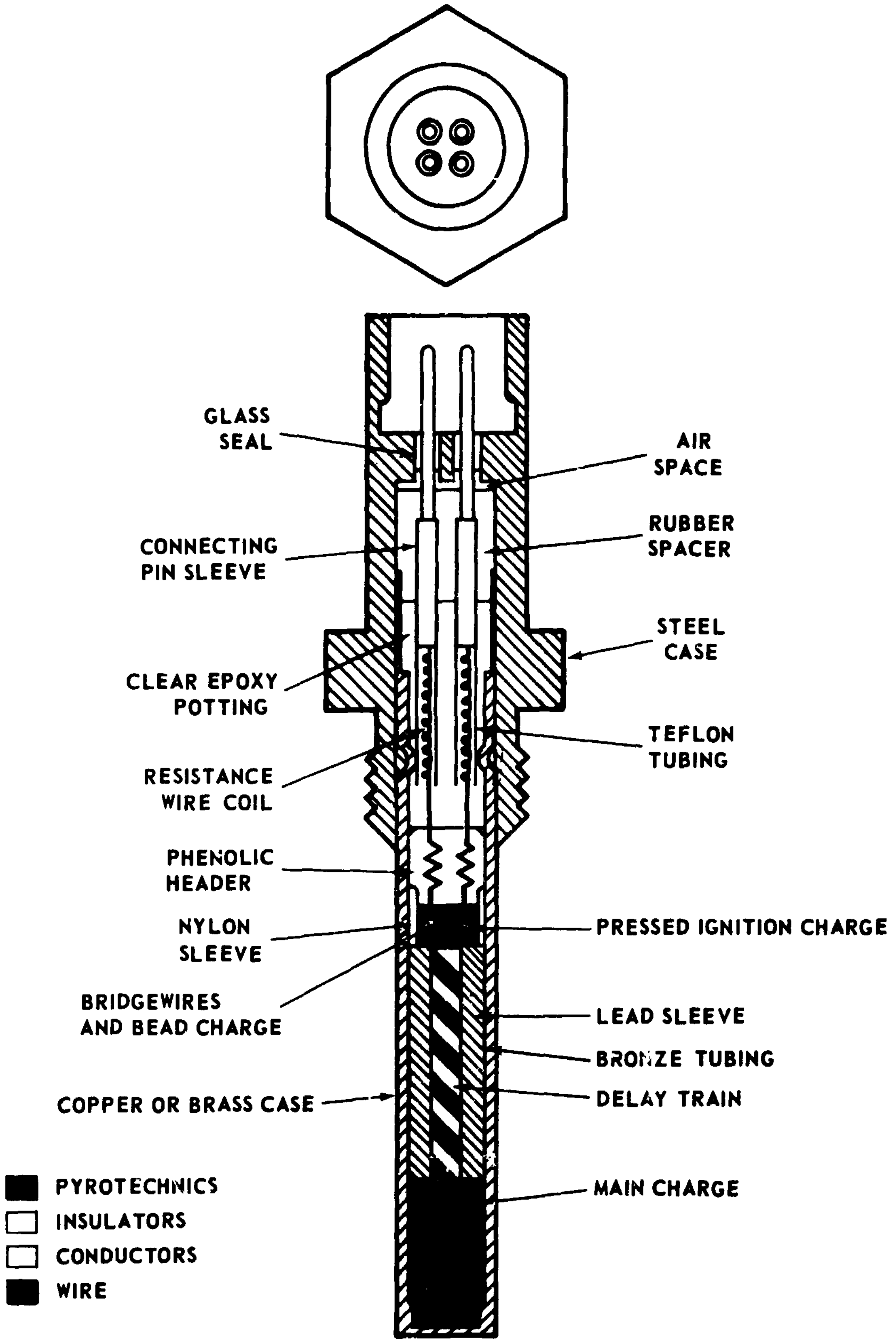

Figure 2—SD60A0 Squib Internal Construction

of 1.5 grams of deflagrating lead oxide/boron which in turn ignites the $BKNO_3$ pellets in the igniter.

The squib body is made up of three concentric brass shells. One end of the inside shell is turned in and a brass button inserted to close the hole. Half of the main charge is then inserted and tamped into place and then the second half is added and the delay train with its lead case is inserted and is used to compress the second half of the charge. The primer charge and rubber plug containing the bridgewire and lead styphnate are then added. The tubes are then crimped, usually just behind the rubber plug. Resistance coils and insulation are added and potting compound is poured into the back end. The squib body is then placed in the header which is made of steel and gold plated. Electrical connections are provided through a glass to metal seal in the end of the header. Epoxy cement is used on the squib body to retain it in the header.

The dual bridge resistance is in the order of 1.0 to 1.8 ohms and will withstand a maximum no fire current specification of 1.0 ampere for a duration of 5 minutes.

Two-hundred and nineteen live and thirty-six expended SD60AO squibs were submitted for radiographic examination. The squibs were from four different production lots identified as 4-1, 5-1, 5-2, and 5-3. The squibs used in the Delta 33 vehicle were from lot 4-1. Each radiograph was examined in detail for discrepancies. Several squibs, both live and expended, were dissected to verify discrepancies detected by radiograph and to inspect those areas which were not clearly illustrated on the radiographic pictures. The following list of discrepancies or irregularities were detected as a result of the above mentioned examination:

(1) Air bubbles in the potting compound behind the bridgewire block.

(2) Short insertion depth of the bronze shell into the steel header.

(3) Incomplete bonding between the outer bronze shell and the steel header.

(4) Large variations in the size and shape of the lead styphnate primer spot over the bridgewires.

(5) Variations in the amount of ignition charge.

(6) Air gap between the ignition charge and the delay train.

(7) Air gap between the delay train and the main charge.

(8) Deposits of lead/boron main charge material between the outside

surface of the lead time delay sleeve and the inside surface of the innermost brass shell.

(9) Bent connector pins and sleeves.

(10) Small ribbons of gold plating shorting across the glass seal of the pin connector (this was the result of burrs on the pin sleeve.)

(11) Large variations in the location and depth of the crimp around the three brass shells.

(12) Large variations from lot to lot in the length of the three brass shells of the squib body.

(13) Air space between the three outer brass shells (present on lot 4-1 only).

This list of discrepancies are indicative of inadequate Quality Control and unaccountable manufacturing practices.

Radiographic pictures of the two squibs used in the Delta 33 vehicle show them to have the following list of discrepancies.

(1) Short insertion depth of the bronze shell into the steel header.

(2) Excessive amount of ignition charge.

(3) Air gap between time delay train and main charge.

Cornell Aeronautical Laboratory and Franklin Institute were the principle investigators on the ordnance devices. The Port Ewen Facility of the Hercules Powder Company provided the test and shipping history of the several manufactured lots of SD60AO squibs. Also, they manufactured several sets of SD60AO squibs having intentional defects for testing purposes.

At Cornell Aeronautical Laboratory squibs were inspected visually both externally and internally. Then several sections of the squib interior were photographed at 1,000 - 5,000 frames per second during firing. Externally, the most apparent unusual feature was a dark deposit on the outside of the outermost sleeve (Figure 3) that appeared to result from a gas leak between the sleeve and the gold plated header. An analysis showed that the deposit did not contain lead or boron (initiator charge) but was carbonaceous in nature. The probable source of the material was revealed when the squib was partially dissected to expose the resistors in the bridge leads and the teflon sleeves around the leads. On film, the resistors glowed red in a few milliseconds after the application of 7.5 amps initiating current in one case and in another, 10 amps caused the dark

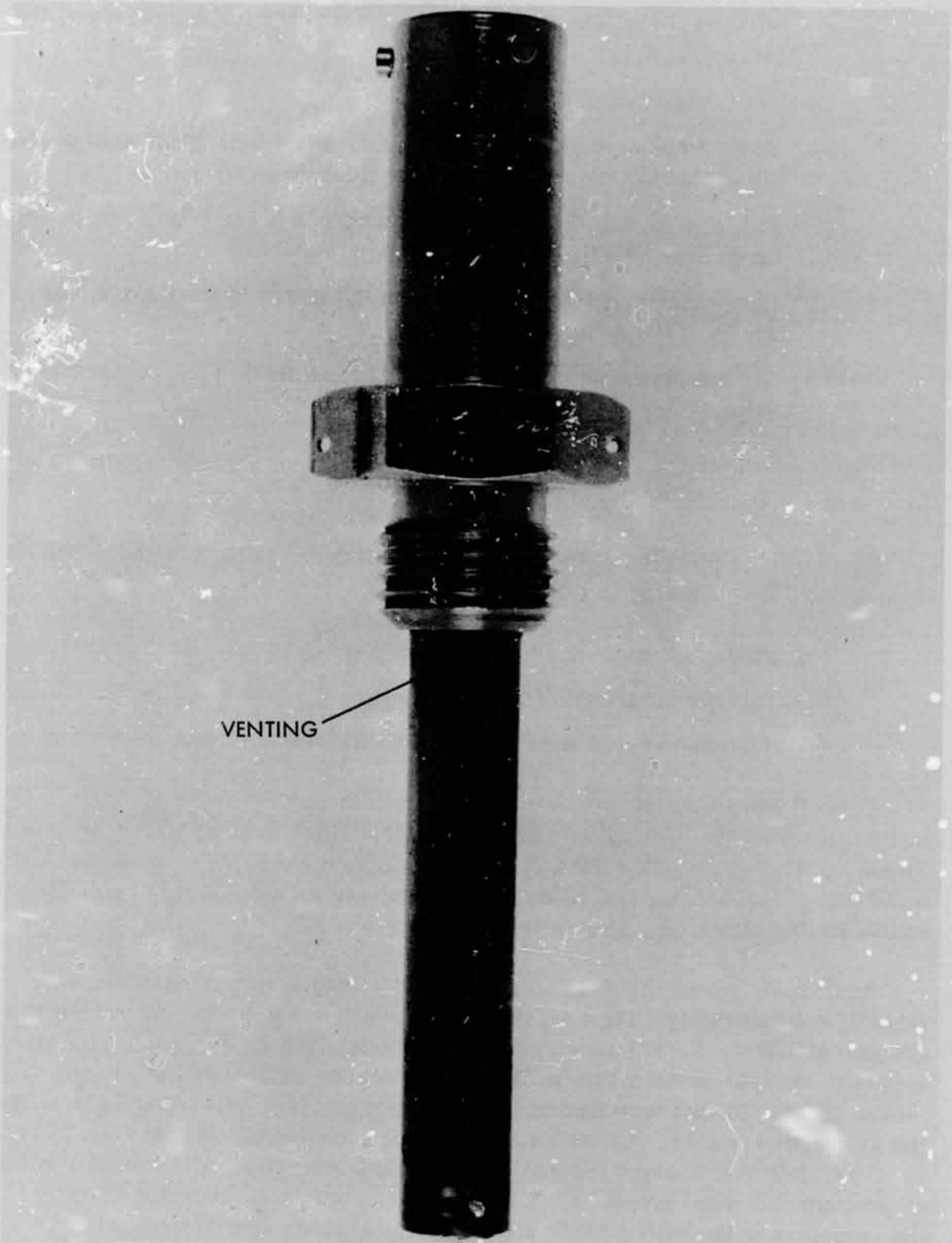

Figure 3. Showing ''Venting'' of "Jetting"

potting compound around the hot wires to boil and break away pieces. Presumably when some squibs are fired hot liquid or gas can be formed and escape between the sleeve and the header. If the sleeve to header bond is weak, a build up of gas pressure could conceivably eject the sleeve. In some tests this malfunction has happened. During a pyrogen static fire test, the squib initiation current remained on and the sleeve was ejected about 8 seconds after the bridgewire fired. Within this time span the other functions were normal. In other cases there is evidence of partial sleeve ejection (Figure 4) from the header.

In another squib firing test all of the PbO/B main charge following the lead ferrule was removed and the sleeves machined back flush with the terminal face of the lead ferrule and delay mix. The squib was fired and the exposed end photographed at 5,000 frames per second (see Figures 5 and 6). Nearly simultaneously with ignition of the PbO/B charge something that appears to be rapidly moving gas emerges from between the lead ferrule and the inner bronze sleeve, then a short pause, and the entire lead ferrule containing the delay train moves out of the tube, perhaps 1/32 of an inch. This entire action takes place in less than a millisecond.

The sequence of internal squib firing events was examined dynamically by slicing it in half on a plane containing the longitudinal axis. One half was mounted tightly in an aluminum block. The sliced flat side of the squib was sealed by a heavy glass plate screwed to the block. Again the firing sequence was photographed at fast frame rates. Three significant events appear: (1) When the PbO/B initiator charge fires, a considerable amount of reaction can be seen taking place outside of the proper chamber between the lead ferrule and the bronze inner sleeve almost all of the way to the terminal end of the ferrule. (2) Rather than a smooth ignition of the delay train a rather violent reaction is observed to penetrate approximately 1/6 of the total train length (the delay train reaction itself is nonluminous and therefore not observable). (3) A similar event occurs when the delay train ignites the final PbO/B charge. It is felt that these reactions may be due to an interdiffusion of the PbO/B at each end with the Selenium/Tellurium mix of the delay.

Some of the more significant results of the Cornell detailed examination of the SD60AO squibs may be summarized as follows:

a. Decomposition of the potting compound in the header due to heating by the resistance coils causes gas generation and internal pressure buildup. Pressure is relieved by "gas leakage" between the shell and header or barrel extension or in some cases barrel ejection.

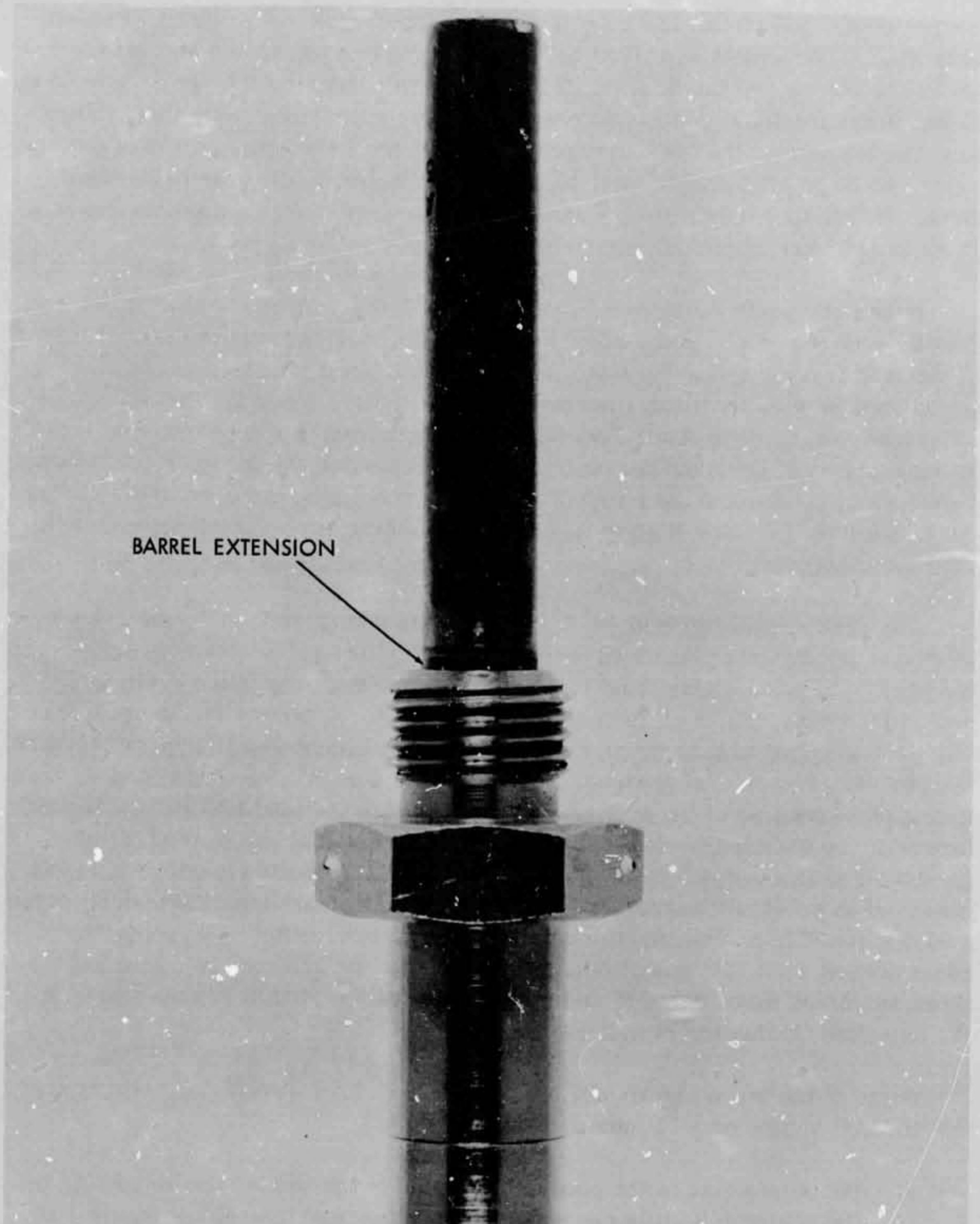

Figure 4. SD60AO Showing Barrel Ejection

Figure 5. High Speed Photograph of Squib Action

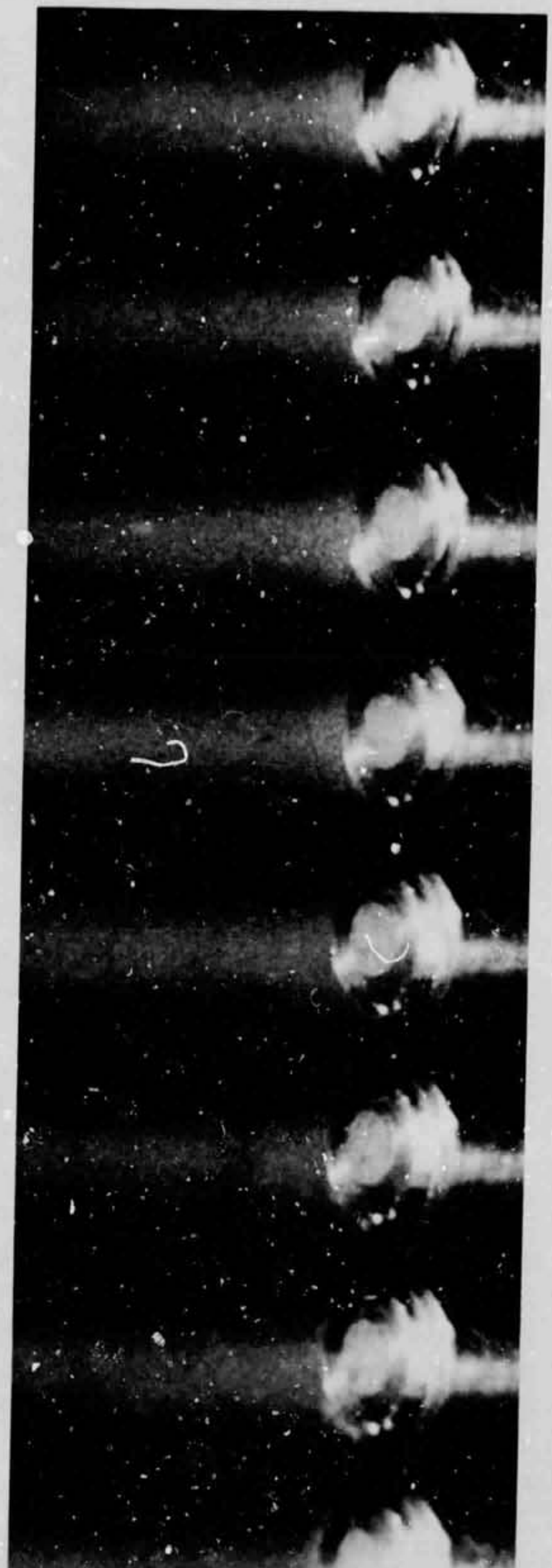

Figure 6. High Speed Photograph of Squib Action

b. Deposition of initiating and/or main charge (lead oxide/boron) material in some instances was observed between the lead ferrule containing the delay train and the brass shell (see Figure 7). Patches and globules have been observed extending from the main charge end up the length of the delay train and concentrated more heavily at both ends. Tests by Cornell indicate a gap greater than .005 inches is required for burning of this material. Gap widths greater than .005 inches are possible between the lead ferrule and the tubing due to fit tolerances, lead oxide/boron deposition and expansion due to temperature and pressure.

c. Phenolic insulator displacement was noted during ignition charge burning. Pressure build-up due to ignition charge can force the phenolic insulator backward toward the header thereby permitting venting of delay train. Venting the delay train increases the time delay between initiation and output.

The most significant results from the tests conducted by the Franklin Institute are:

a. Squibs manufactured with excessive ignition charge may exhibit excessive delay times of about ten (10) seconds or extremely short time delay. The most probable cause for this abnormal behavior is venting of the time delay train past the bridgewire block and potting compound causing a slower burning rate of the time delay mix resulting in excessive time delay or leaking hot gasses past the time delay ferrule to the main charge causing instantaneous firing of the squib.

b. Squibs manufactured without delay trains, eccentric time delay ferrules, and small holes through the delay train fired instantly (in the order of milliseconds).

As a result of the above-mentioned tests on the SD60AO squib, it is concluded that there are several observed discrepancies in the manufacture and assembly of the squib that could result in premature ignition of the X-258 motor. The most significant discrepancies being (a) excessive ignition charge, and (b) deposits of lead/boron main charge material between the outside surface of the time delay lead ferrule and the inside surface of the innermost brass shell.

CONCLUSIONS

The most probable cause of the premature ignition of the X-258 rocket motor and the mission failure was the malfunction of the SD60AO squib. The most probable failure mode of the squib is for the initiation charge to bypass the delay train through a gap between the lead ferrule and the innermost brass shell.

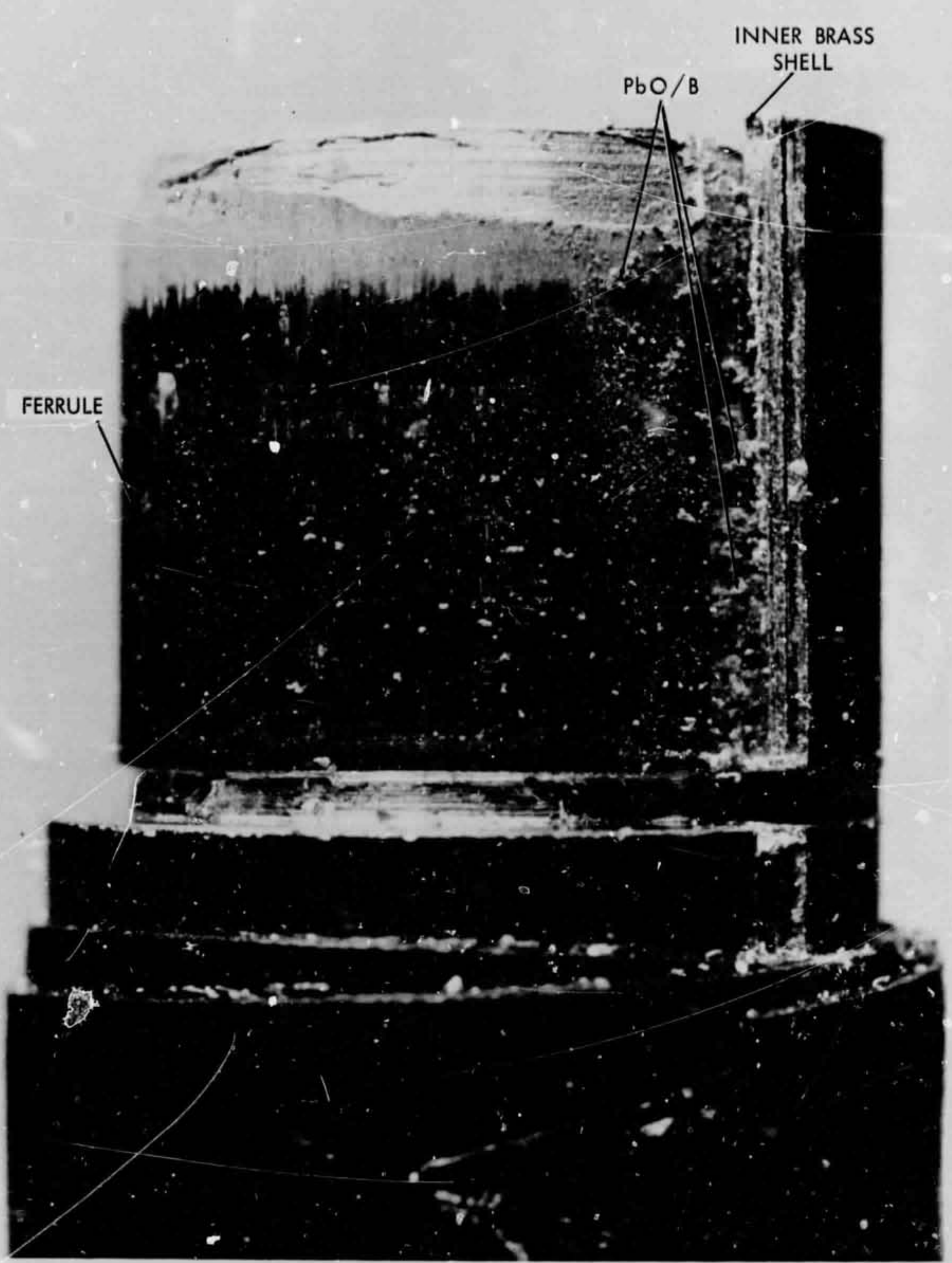

Figure 7. Material Deposition on Lead Ferrule

APPENDIX A

X-258 (S/N RH-78) MOTOR FLIGHT PERFORMANCE

DELTA 33 OSO-C

SUMMARY

The third stage of the Delta 33 launch vehicle was instrumented to measure high range longitudinal acceleration, low range longitudinal acceleration, radial acceleration, chamber pressure, motor case temperature, nozzle deflection, and detection of aluminum propellant slag build up inside the motor chamber.

INTRODUCTION

The Delta Project incorporated on the third stage of the Delta 33 vehicle an instrumentation package (Figures A-1, A-2, and A-3) to investigate the cause for coning of the third stage/spacecraft assembly incurred immediately subsequent to X-258 motor burnout. This coning results in an error in spacecraft injection attitude and, consequently in the case of future missions which are particularly sensitive to dispersions in attitude, can materially degrade the overall probability of mission success.

The three possible causes of this anomaly are:

(1) Nozzle Deflection — Motor case hydrotests have shown that the bond between the nozzle attach ring and the fiberglass aft dome frequently fails and under the influence of chamber pressure the nozzle will move with respect to the motor case. These same tests have shown that when chamber pressure falls-off the nozzle returns to nearly its original position. It is postulated that this lateral movement of the nozzle during motor shutdown could produce a lateral impulse on the motor/spacecraft combination.

(2) Case Temperature — High case temperature in the region of the aft dome may soften the fiberglass motor case and cause misalignment of the thrust axis.

(3) Aluminum Slag Movement — Aluminum propellant slag, trapped during thrusting in the sump formed by the nozzle throat and the aft dome could be spun out to the case sides by centrifugal force when the motor stops thrusting. A nonsymmetrical distribution would cause dynamic unbalance with subsequence coning.

The performance telemetry package carried on-board this mission was designed to provide the following information:

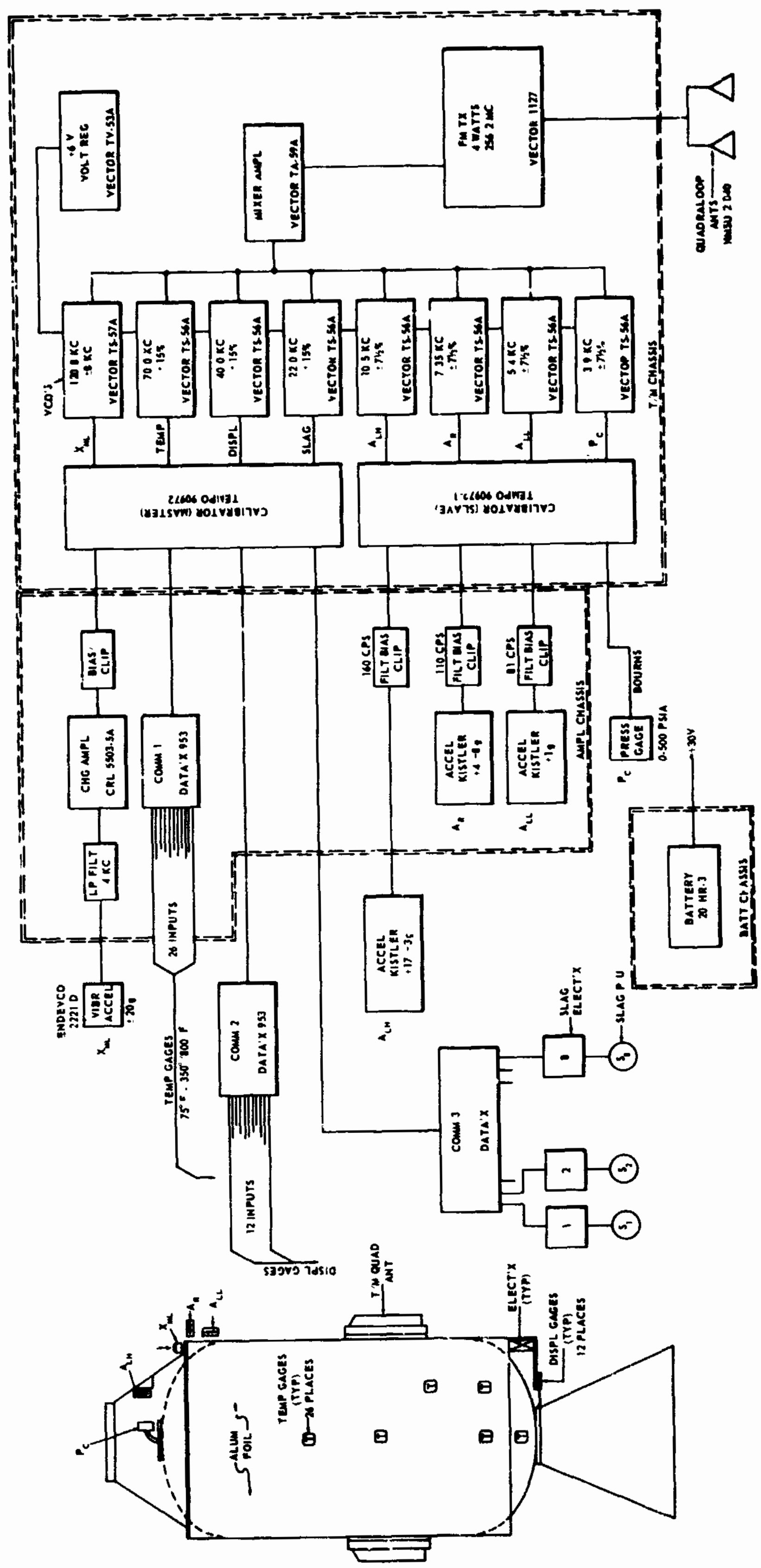
CALIBRATOR (MASTER)
TEMPO 90972
CALIBRATOR (SLAVE)
TEMPO 90972-1
+6 V
VOLT REG
VECTOR TV-53A
MIXER AMPL
VECTOR TA-59A
FM TX
4 WATTS
VECTOR 1127
QUADRALOOP
ANTS
VCO'S
VECTOR TS-57A
VECTOR TS-56A
T/M CHASSIS
AMPL CHASSIS
BATTERY
20 HR-3
BATT CHASSIS
BIAS CLIP
CHG AMPL
CRL 5503-5A
LP FILT
4 KC
COMM 1
DATA'X 953
26 INPUTS
COMM 2
DATA'X 953
12 INPUTS
COMM 3
DATA'X
160 CPS
FILT BIAS
CLIP
110 CPS
81 CPS
ACCEL
KISTLER
PRESS
GAGE
0-500 PSIA
BOURNS
ENDEVCO
2221 D
VIBR
ACCEL
TEMP GAGES
DISPL GAGES
SLAG
ELECT'X
SLAG P U
T/M QUAD
ANT
ELECT'X
(TYP)
DISPL GAGES
(TYP)
12 PLACES
TEMP GAGES
(TYP)
26 PLACES
ALUM
FOIL
TEMP
DISPL
SLAG

Figure A-1

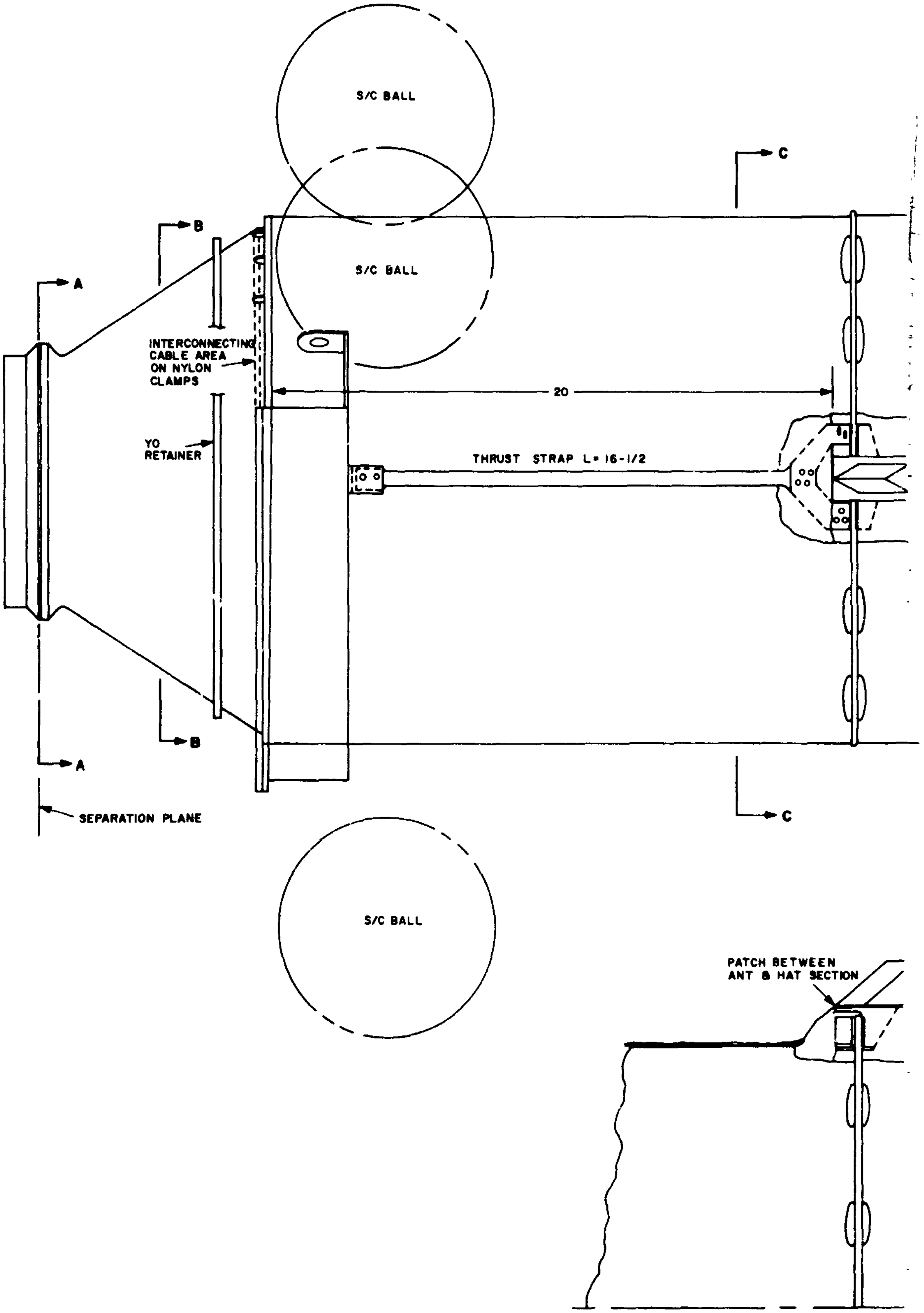

S/C BALL
S/C BALL
S/C BALL
C
C
B
B
A
A
INTERCONNECTING CABLE AREA ON NYLON CLAMPS
YO RETAINER
20
THRUST STRAP L= 16-1/2
SEPARATION PLANE
PATCH BETWEEN ANT & HAT SECTION

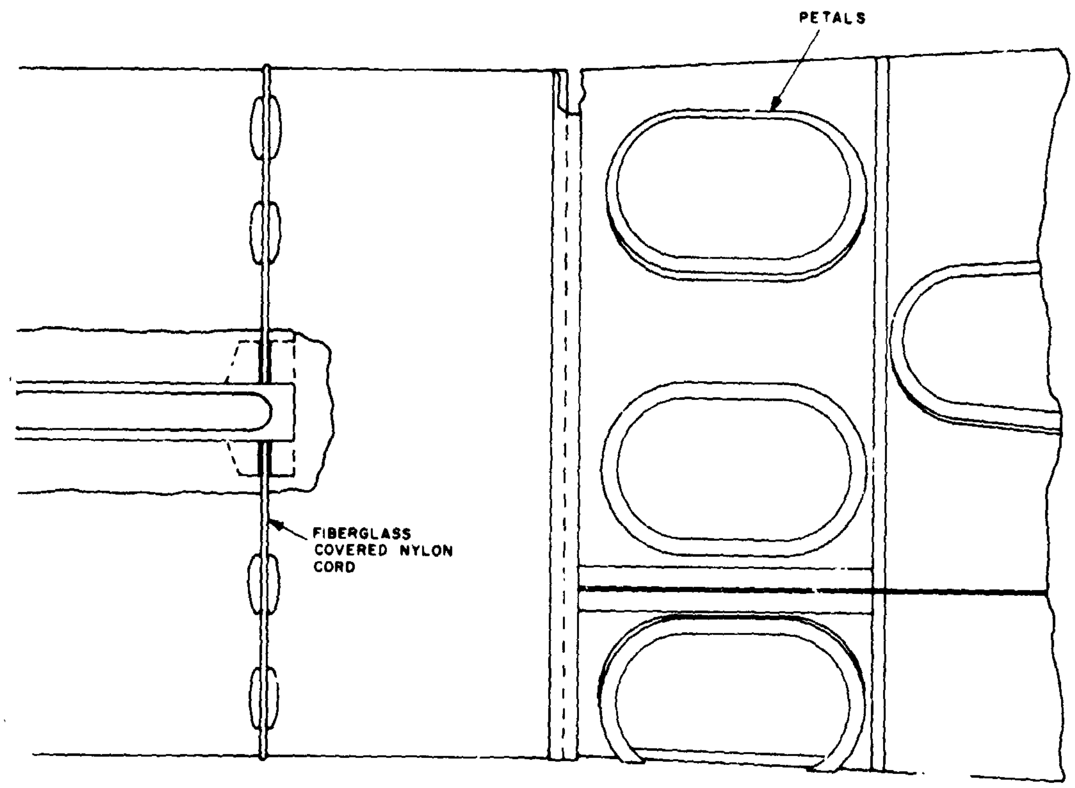

X-258 MOTOR
COVERED WITH ALUMINUM FOIL
TO CREATE GROUND PLANE
FOR QUAD ANTENNAS

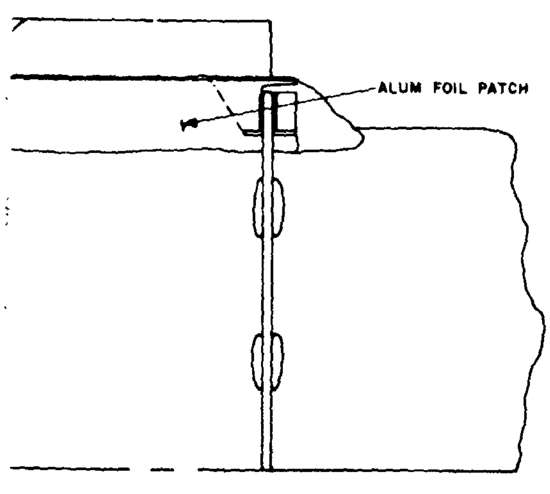

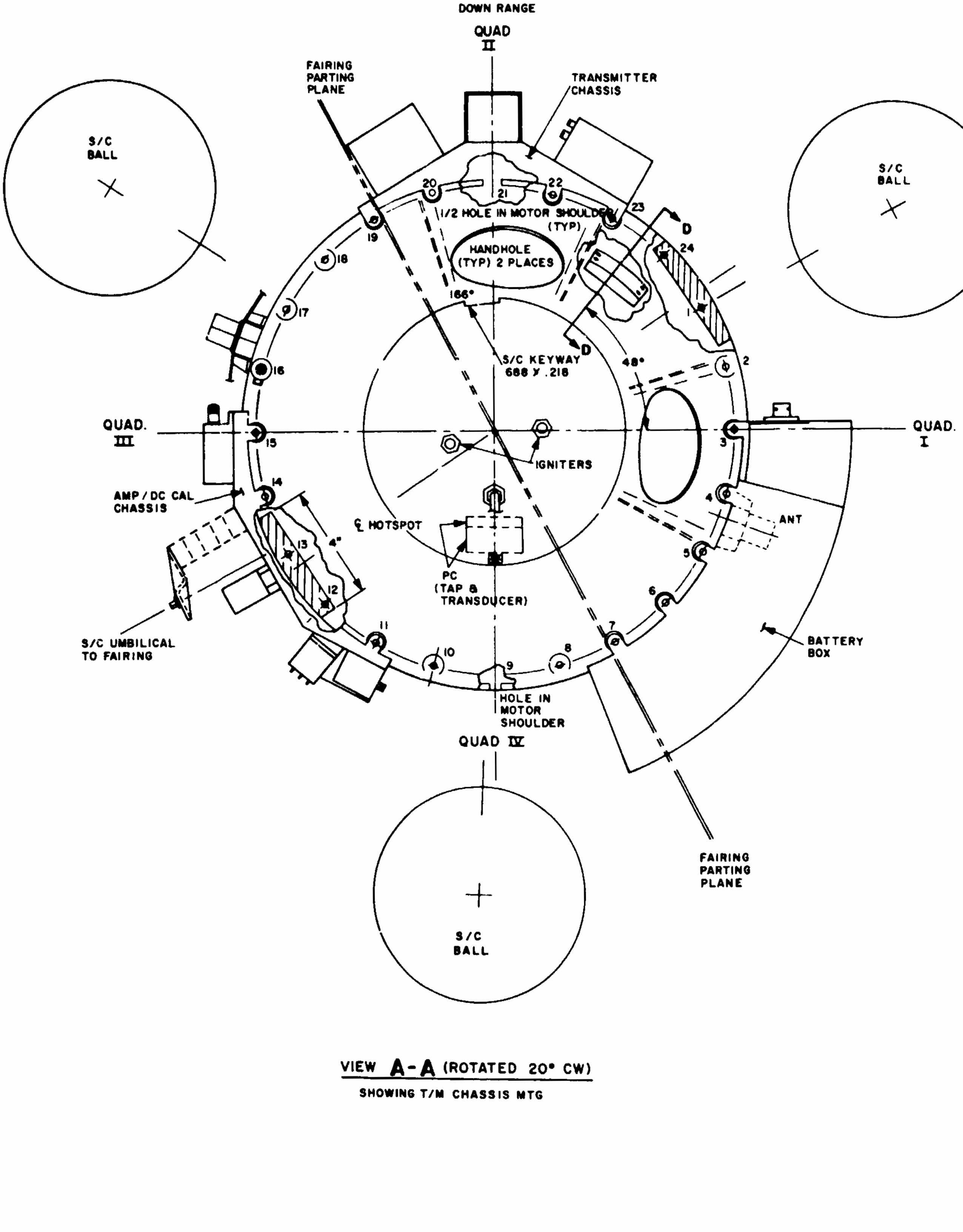

VIEW **A-A** (ROTATED 20° CW)

SHOWING T/M CHASSIS MTG

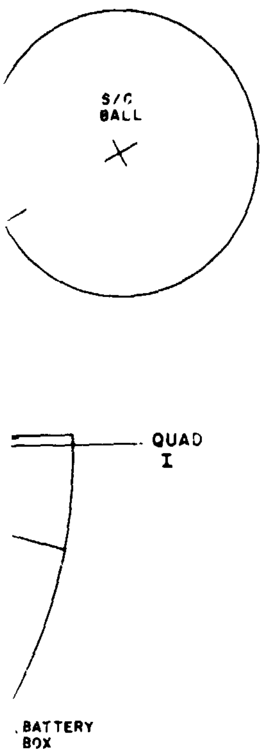

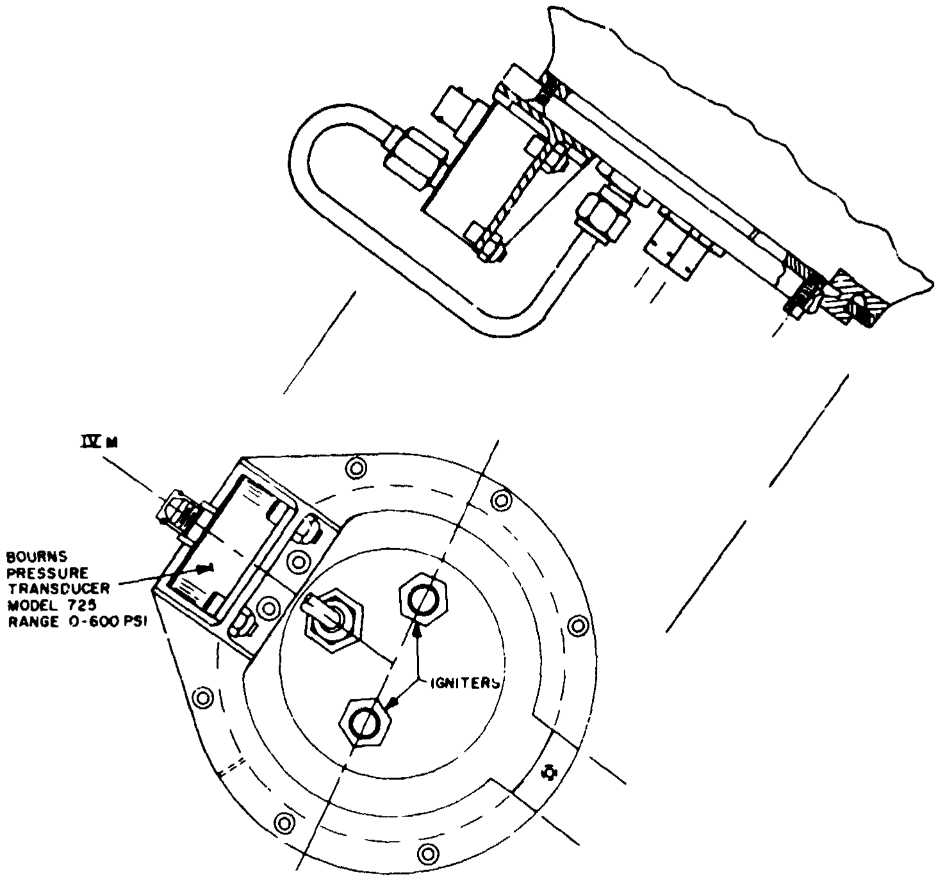

VIEW **B-B**

FULL SIZE -
ROTATED 120° CW

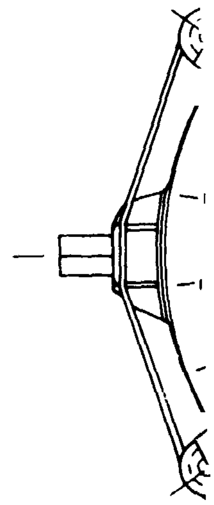

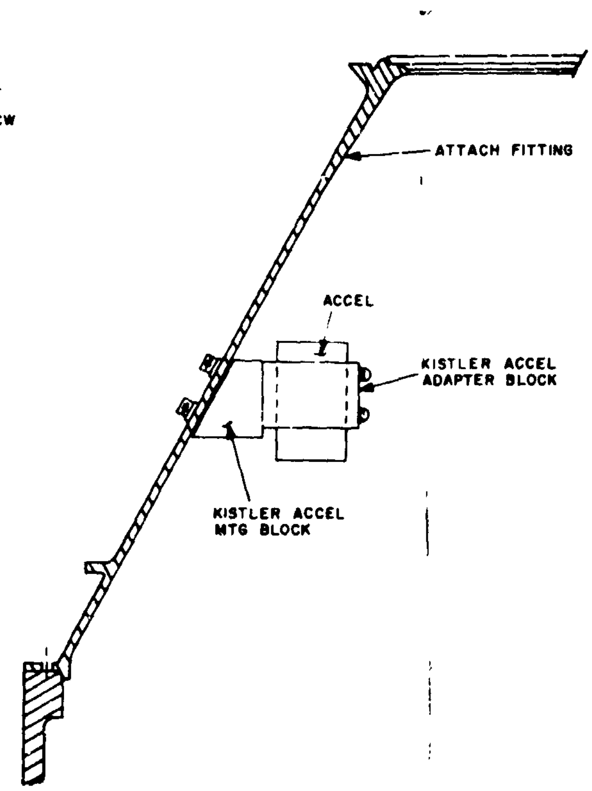

VIEW **D-D**

PAYLOAD ATTACH FITTING SHOWING
ACCELEROMETER MTG BLOCK

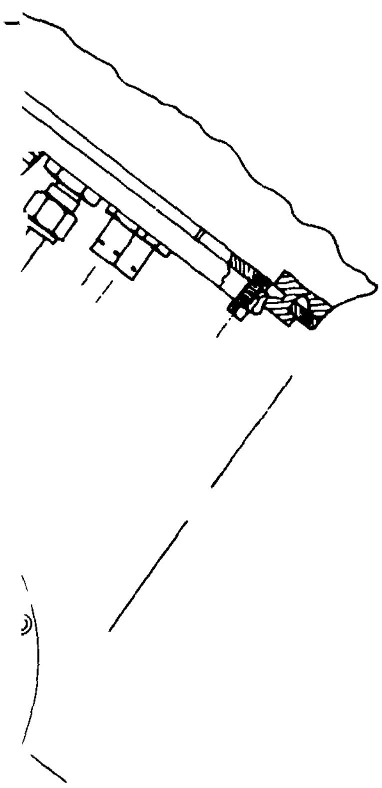

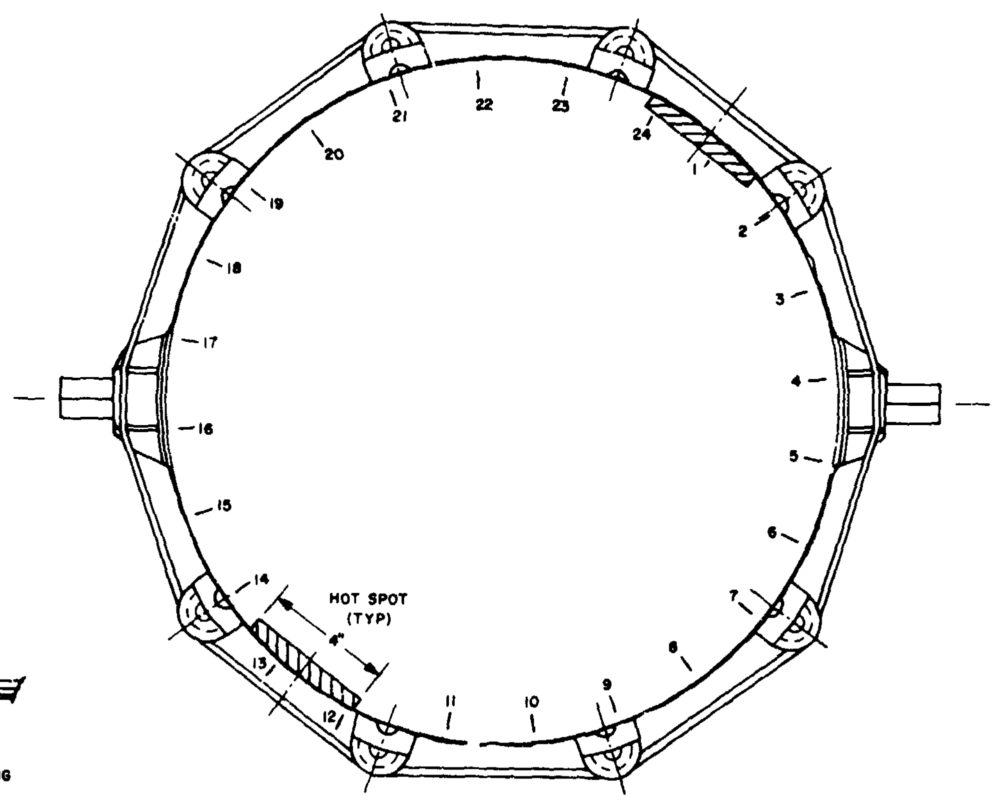

VIEW **C-C**
SHOWING ANTENNA MTG
& FOIL WRAPPING

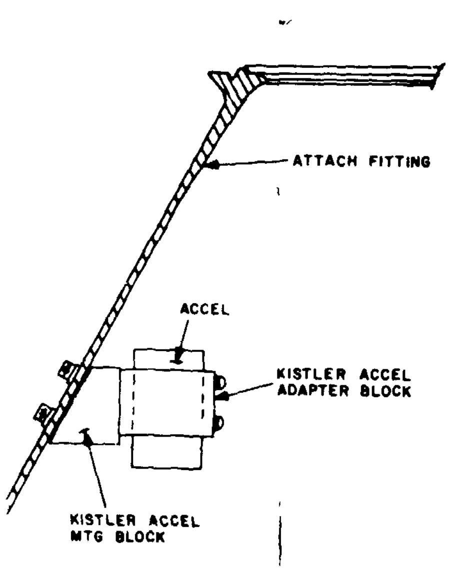

VIEW **D-D**
YLOAD ATTACH FITTING SHOWING
CELEROMETER MTG BLOCK

OSO-C THIRD STAGE PERFORMANCE
TM PACKAGE
FIGURE A-2
PAGE A-3-5

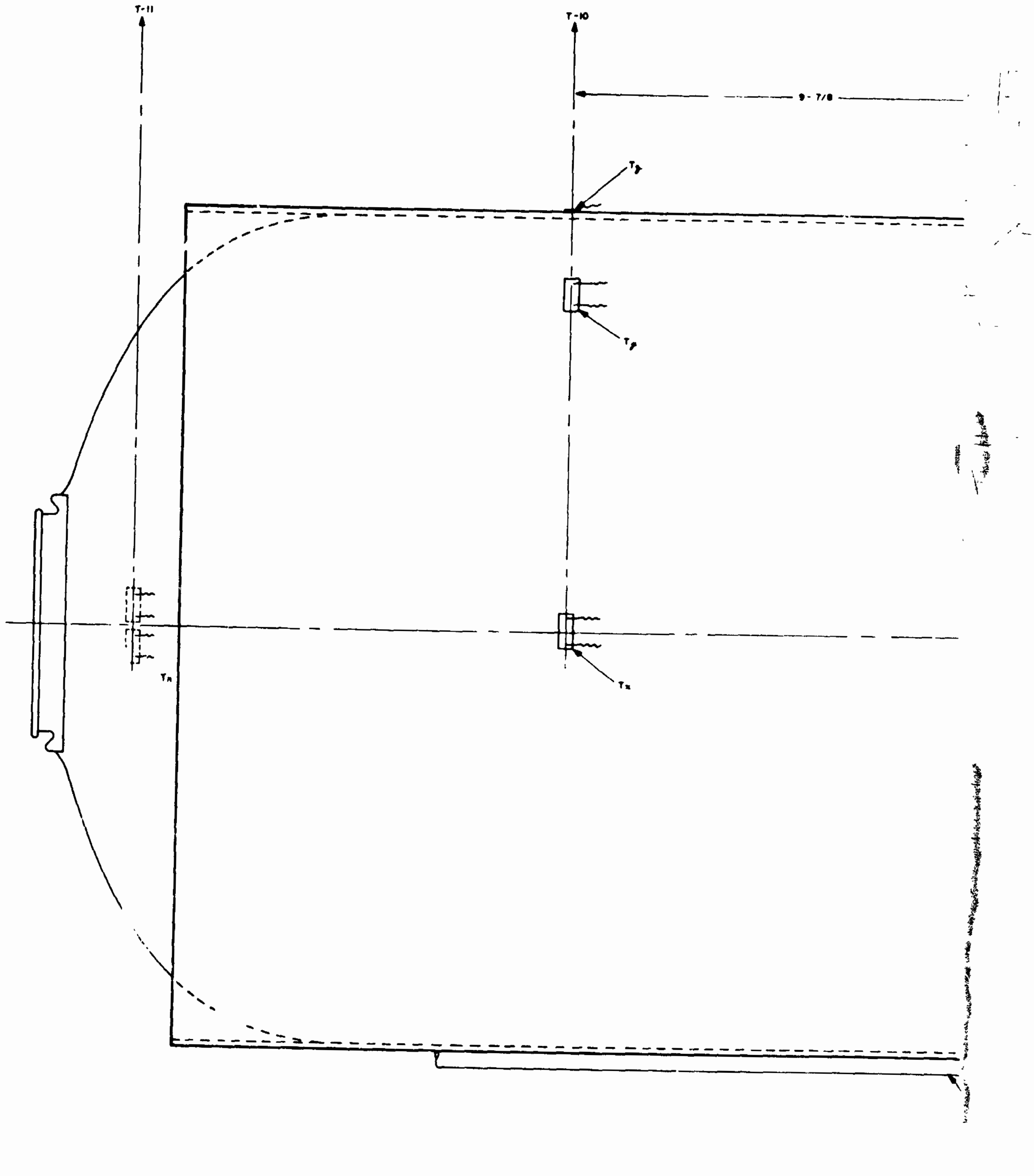
T-11
T-10
9 - 7/8

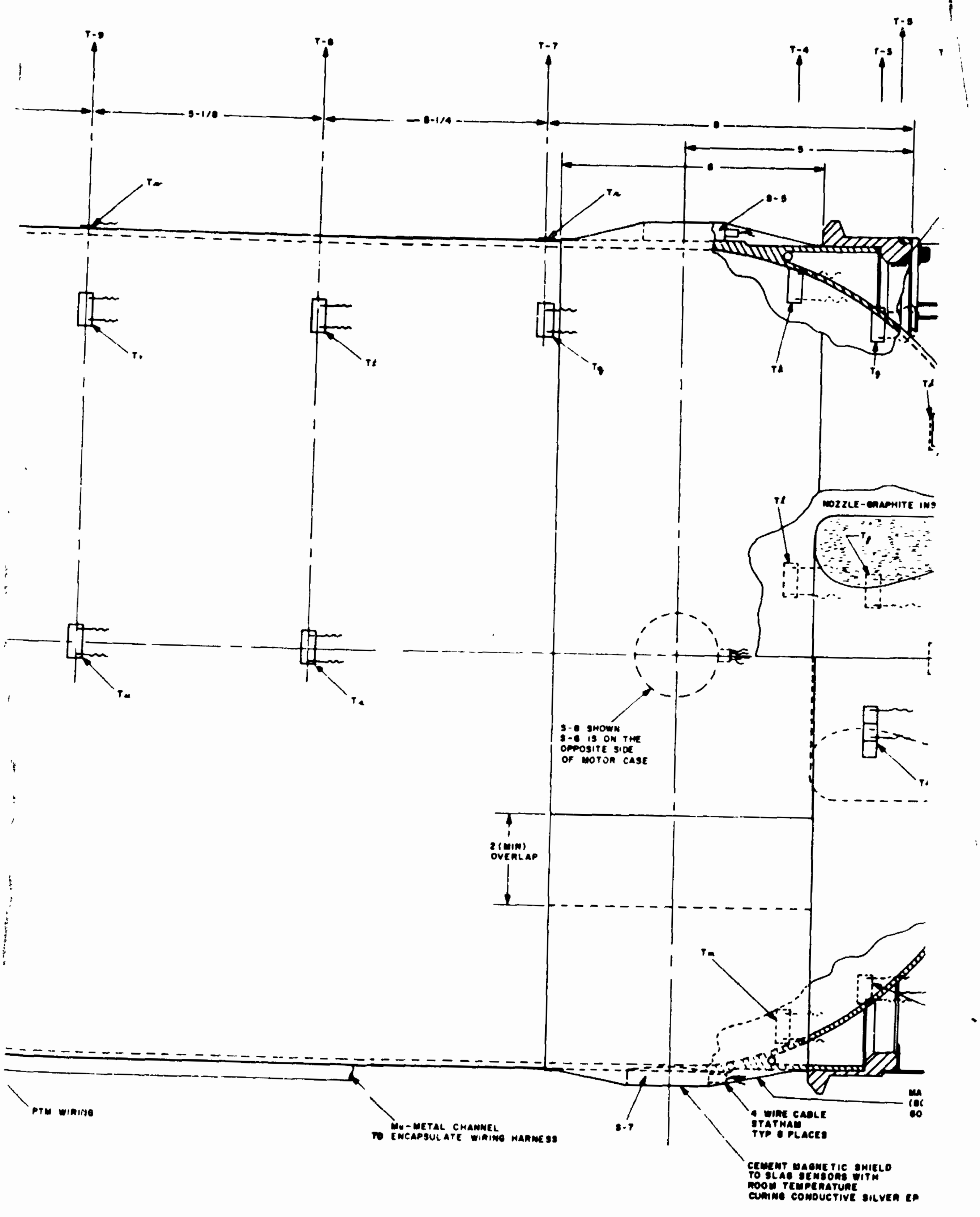

T-9
T-8
T-7
T-4
T-3
T-5
5-1/8
5-1/4
NOZZLE-GRAPHITE INS
S-8 SHOWN
S-6 IS ON THE
OPPOSITE SIDE
OF MOTOR CASE
2 (MIN)
OVERLAP
PTM WIRING
Mu-METAL CHANNEL
TO ENCAPSULATE WIRING HARNESS
S-7
4 WIRE CABLE
STATHAM
TYP 8 PLACES
CEMENT MAGNETIC SHIELD
TO SLAG SENSORS WITH
ROOM TEMPERATURE
CURING CONDUCTIVE SILVER EP

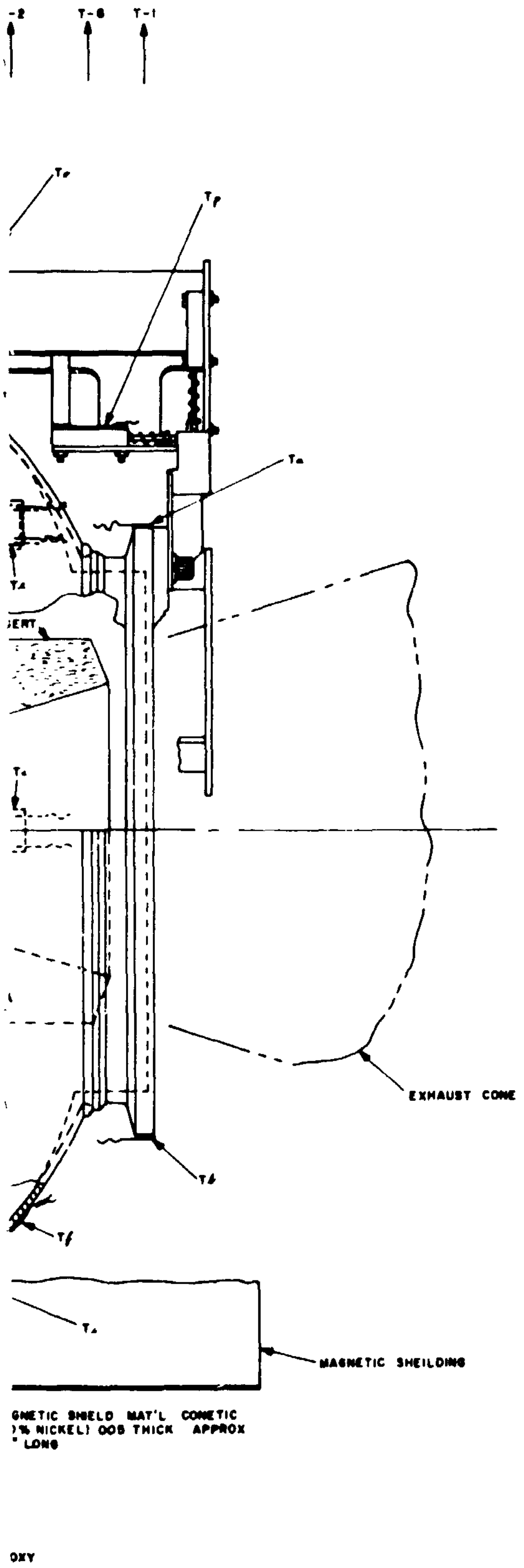
-2
T-6
T-1
EXHAUST CONE
MAGNETIC SHEILDING
GNETIC SHIELD MAT'L CONETIC
)% NICKEL) 005 THICK APPROX
" LONG
OXY

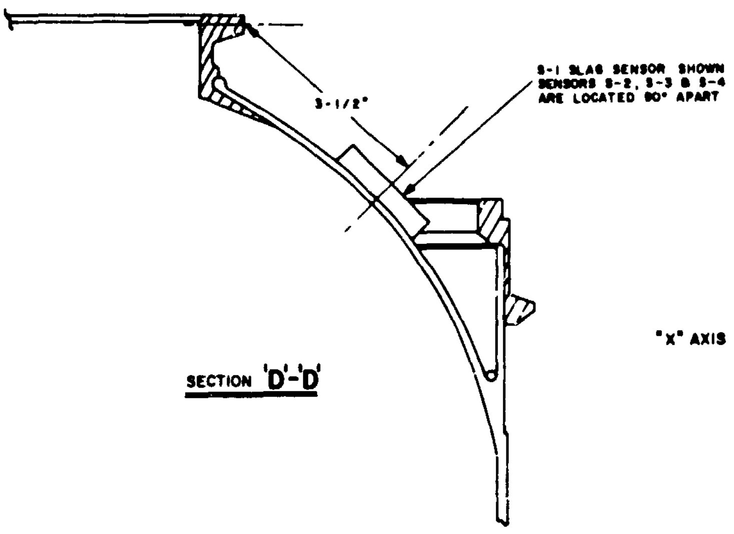
S-1 SLAG SENSOR SHOWN
SENSORS S-2, S-3 & S-4
ARE LOCATED 90° APART
3-1/2"
"X" AXIS

SECTION 'D'-'D'

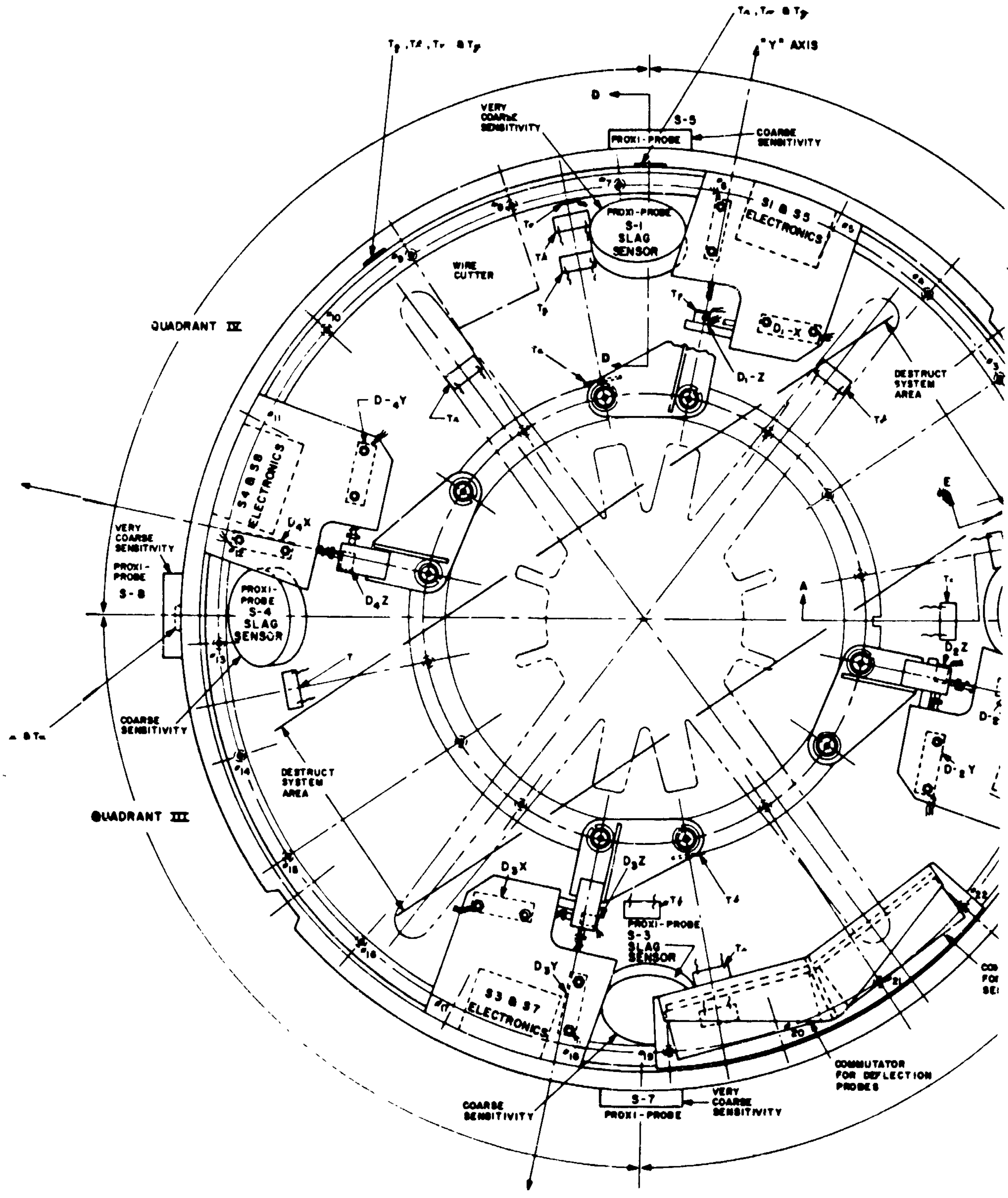
"Y" AXIS
QUADRANT IV
QUADRANT III
S-5
PROXI-PROBE
COARSE SENSITIVITY
VERY COARSE SENSITIVITY
PROXI-PROBE S-1 SLAG SENSOR
S1 & S5 ELECTRONICS
WIRE CUTTER
DESTRUCT SYSTEM AREA
S4 & S8 ELECTRONICS
PROXI-PROBE S-8
PROXI-PROBE S-4 SLAG SENSOR
PROXI-PROBE S-3 SLAG SENSOR
S3 & S7 ELECTRONICS
S-7
COMMUTATOR FOR DEFLECTION PROBES

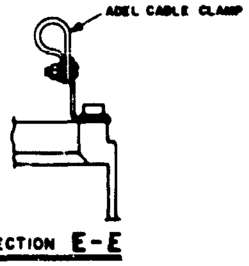

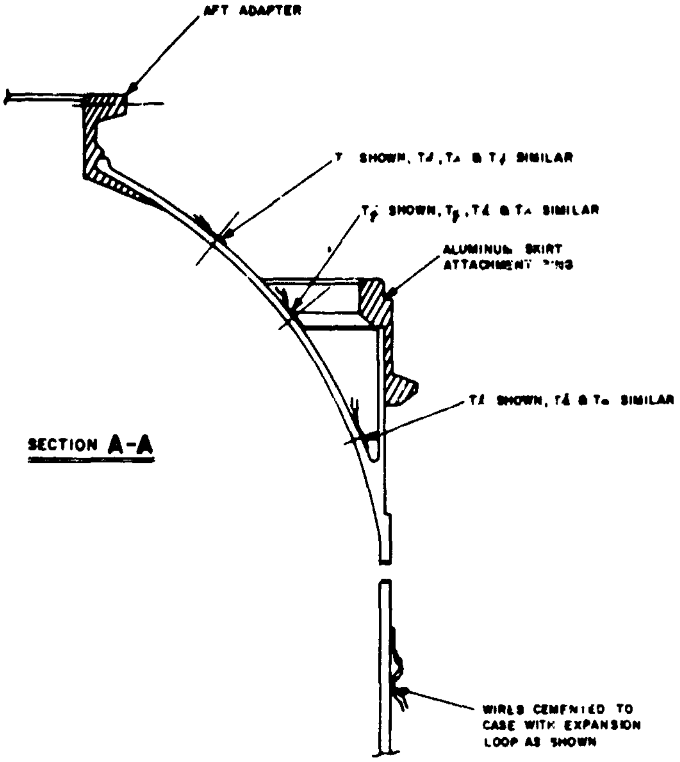

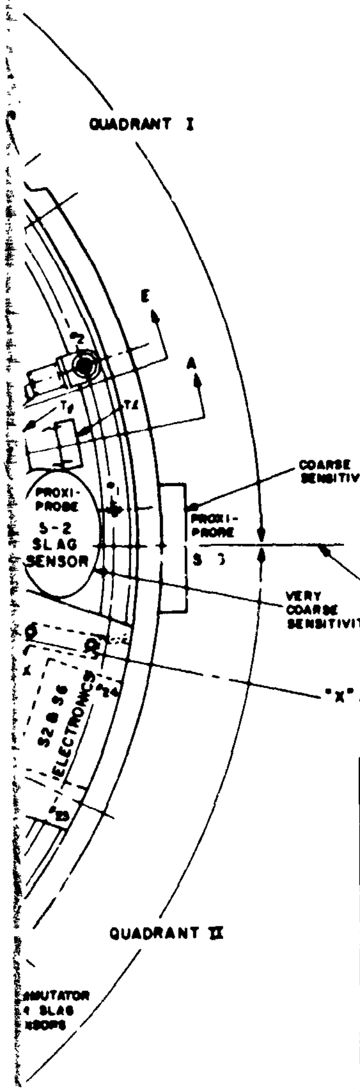

TRANS-SONICS TYPE T4596 SURFACE TEMPERATURE SENSORS 233 OHMS ±1% MEASURED AT ICE POINT DIMENSIONS .31 ± .030 BY .75 ± .030 1/32 NOMINAL THICKNESS 400 MILLI/SEC RESPONSE TWO .010 DIA NICKEL LEADS WITH FIBERGLASS INSULATION 5" LG ± 1/4"		
T-1	2	[illegible]
T-2	4	[illegible]
T-3	4	[illegible]
T-4	3	[illegible]
T-5	1	[illegible]
T-6	1	[illegible]
T-7	2	[illegible]
T-8	2	[illegible]
T-9	3	[illegible]
T-10	3	[illegible]
T-11	1	[illegible]
TOTAL	26	AS PER INPUTS AVAILABLE

D = DEFLECTION POTS
S = SLAG SENSORS
T = THERMOMETERS

FIGURE A-3

a. Measurement of X-258 motor case temperature at 26 representative locations.

b. Measurement of X-258 nozzle displacement with respect to the motor case, in pitch, yaw, and longitudinal displacement.

c. Measurement of slag movements from the X-258 motor aft dome to the lower case area.

d. Measurements of static and low frequency vehicle accelerations in the longitudinal and radial directions.

e. Measurement of third stage chamber pressure.

f. Measurement of the amplitudes, frequencies, and spectral distribution of mechanical vibration of the third stage motor shoulder, resulting from aerodynamic buffeting and motor thrusting.

TRANSDUCERS

1. Vibration Accelerometer, X_{ML}

The vibration accelerometer is a small barium titanate unit mounted to the forward motor shoulder and oriented to measure longitudinal accelerations. Full scale range is adjusted to ± 10 g.

2. Temperature Gages, T_j

The temperature gages are fine platinum wire, resistance thermometers, bounded to a backing strip. Resistance of the gage increases with temperature. Full scale range is 75°F to 800°F.

3. Nozzle Deflection Gages, D_{ij}

Deflection gages are linear displacement, wire wound potentiometers. Full scale range is 7/16 inch.

4. Slag Sensors, S_j

The slag sensor circuits are experimental devices designed for this application to attempt to detect the presence of molten aluminum. They operate on the principle that any metallic material present within the magnetic field of their sensors will upset the null balance condition of oppositely phased pickup coils.

Since the sensors are essentially ferrite antennas, the system is quite susceptible to RF pickup. Mu-metal shields are employed to minimize this effect.

5. Vehicle Accelerometers, A_{LH}, A_R, and A_{LL}

Vehicle accelerometers are servo feed-back units, having a frequence response from static (0 cps) to several hundred cycles per second.

Two longitudinal accelerometers are provided: A_{LH}, a high range, +17 to -3g unit, mounted inside the attach fitting, for measuring overall vehicle thrust levels; and A_{LL}, a low range ± lg unit, mounted to the amplifier chassis, for providing expanded range detail during period of burnout to determine coning information. A radial accelerometer, A_R having a +8 to -4g range, provides spin data.

6. X-258 Chamber Pressure, P_c

A resistance potentiometer type pressure gage, mounted to the X-258 nose ring, and plumbed to the pyrogen unit to measure X-258 chamber burning pressure. Full scale range is 0 to 500 psia.

Table A-1 outlines telemetry channel allocations for the transducers described above.

DATA DISCUSSION

Instrumentation damage resulting from the premature ignition of the X-258 motor and the abnormal separation of the third stage from the second stage precluded any data from slag sensors, nozzle displacement instrumentation, or temperature gauges located at the aft end of the X-258 motor.

CHAMBER PRESSURE DATA

Expanded records of the chamber pressure shown in Figure A-4 were integrated by means of a planimeter over the time interval from ignition to apparent zero pressure. The pressure-time integral obtained by this method is 9,561 PSIA-Sec. Multiplying by an average C_F A_T of 14.5 yields a total impulse of 138,645. This is slightly less than the expected for this motor however the discrepancy can most probably be attributed to overall accuracy of the T/M system and the method of data reduction. The chamber pressure trace indicates that the motor burned to completion with no unusual events occurring after separation.

Table A-1

OSO-C THIRD STAGE PERFORMANCE
TELEMETER CHANNEL ALLOCATIONS

Function	Symbol	Orien-tation	Trans-ducer	FS Range	IRIG Band	Freq. (kc)	DEV	BW (cps)
Vibration Fwd. Motor Shoulder	X_{ML}	Long.	Endevco 2221 D	±20g	14 cx	120.8	±8kc/s	4000
Temperature X-258 (26 Comm.)*	T_i	Aft Dome & Slide	Trans-sonics T4596	75 - 800°F	E	70.00	±15%	2100
Displacement Nozzle (12 Comm.)*	D_{ik}	Long. Pitch & Yaw	Bourns 141	±1/8 in	C	40.0	±15%	1200
Residual Slag X-258 (8 Comm.)++	S_i	Aft Dome & Sides	Proxy-Probe & Budd	yes/no	A	22.0	±15%	660
Acceleration Veh. (Attach Fit-ting)	A_{LH}	Long	Kistler 303A	+17/ -3g	12	10.5	±7½%	160
Acceleration Veh. (Ampl. Chas.)	A_R	Rad.	Kistler 303A	+4/ -3g	11	7.35	±7½%	110
Acceleration Veh. (Ampl. Chas.)	A_{LL}	Long.	Kistler 303A	±1g	10	5.4	±7½%	81
Chamber Pressure X-258	P_c		Bourns 72517	0.500 psi	9	3.9	±7½%	60

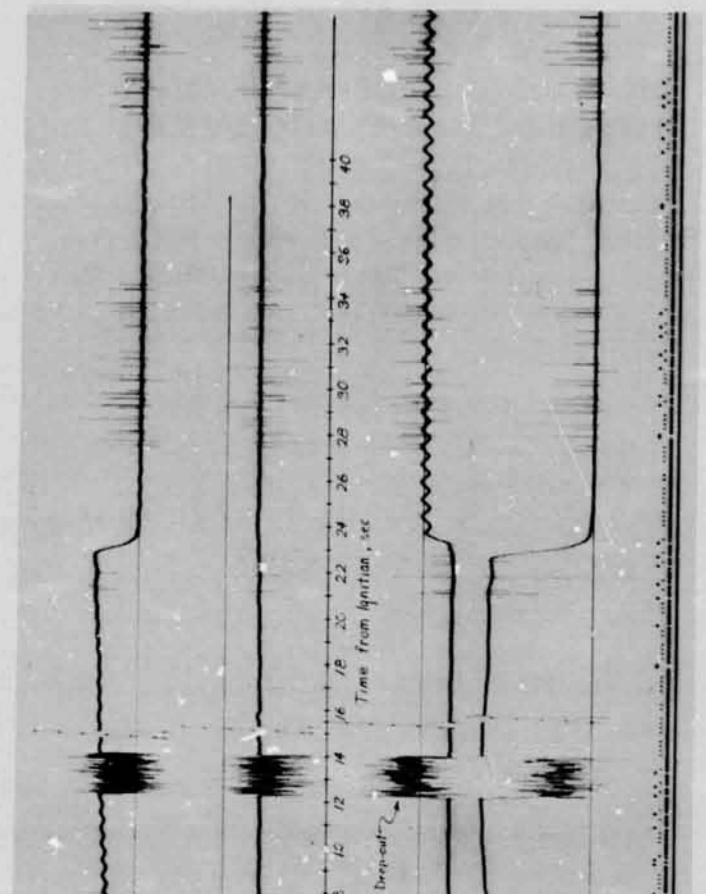
High Level Long Acceleration
Radial Acceleration
Low Level Long Acceleration
Head Cap Chamber Pressure, psia
Time from Ignition, sec
T/M Drop-out
Spin-up
Ignition

Figure A-4

LONGITUDINAL ACCELERATION

Expanded records of the high range longitudinal acceleration shown in Figure A-4 were integrated by means of a planimeter over the time interval from ignition to apparent zero acceleration. The acceleration-time integral obtained is 3,758 ft/sec. which is 18% less than the predicted of 4559 ft/sec. This apparent decrease in performance was probably caused from (a) damage to the X-258 nozzle during separation which would result in a decrease in specific impulse realized and (b) the possibility that parts of the spin table remained attached to the aft end of the motor resulting in an increase in effective payload weight. The acceleration trace indicates large amplitude coning starting at separation and damping out during burning of the motor. This coning is probably caused from from the abnormal second to third stage separation experienced on this mission.

CASE TEMPERATURE MEASUREMENTS

Temperature data received from the ten sensors located on the side of the X-258 motor case indicate a maximum temperature of 475°F at 500 seconds after motor ignition. This is the first time the case temperature has been measured on an X-258-C4 motor and indicates the effectiveness of the added chamber insulation. The motor case was completely covered with aluminum foil which makes this test the most severe thermal condition the motor will be subjected to in flight. Past data indicates that the addition of aluminum foil to the outside of the case will increase the maximum case temperature by approximately 100°F. Figures A-5 and A-6 are temperature-time plots of the case temperature.

CONCLUSION

The data received from the pressure gauge and the high range longitudinal accelerometer show that the motor performed as expected. The decrease in performance noted can be attributed to probable damage to the nozzle at separation and additional weight from parts from the spin table that remained with the motor. The temperature data indicates that the possibility of damage to the case structural integrity due to high temperature after motor burnout is small.

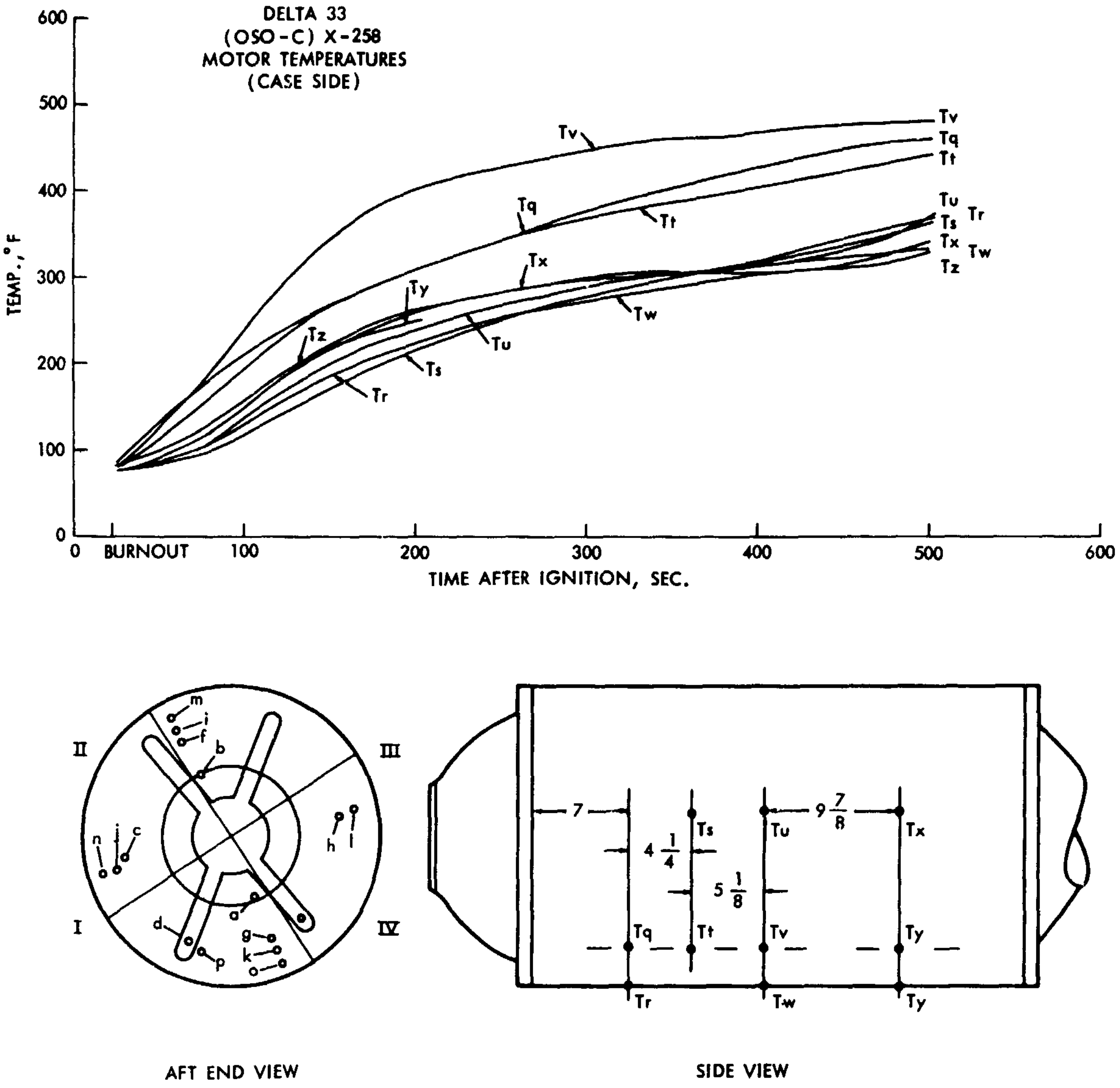
DELTA 33
(OSO-C) X-258
MOTOR TEMPERATURES
(CASE SIDE)
TEMP., °F
TIME AFTER IGNITION, SEC.
BURNOUT
Tv
Tq
Tt
Tu
Ts
Tr
Tx
Tw
Tz
Ty
AFT END VIEW
SIDE VIEW

Figure A-5

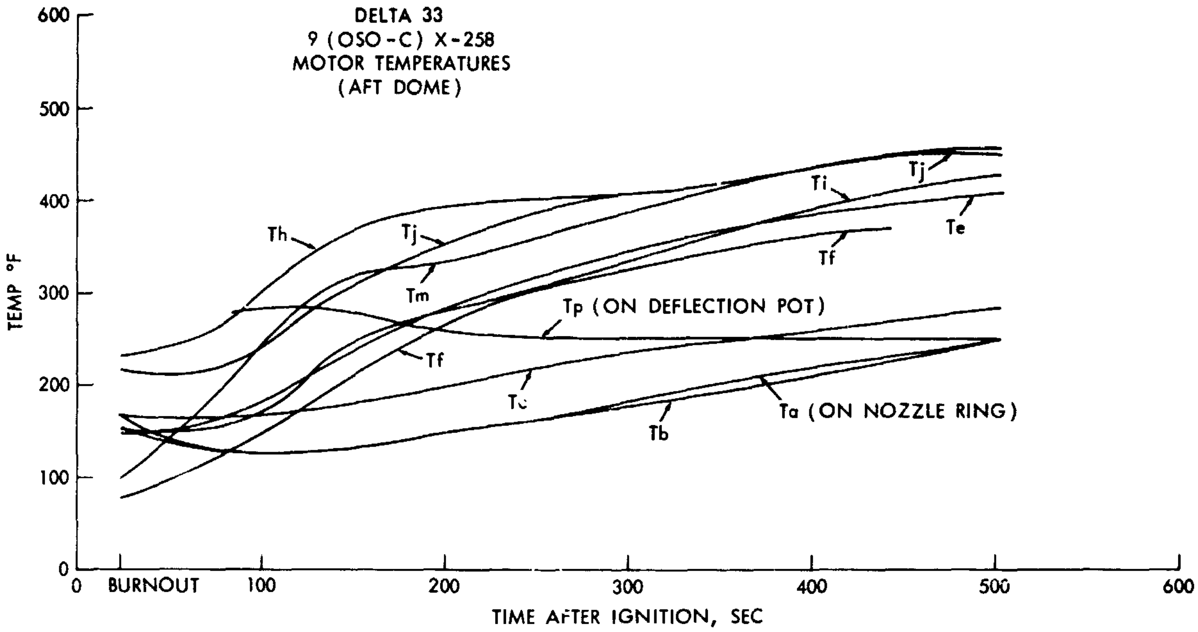
DELTA 33
9 (OSO-C) X-258
MOTOR TEMPERATURES
(AFT DOME)
TEMP °F
TIME AFTER IGNITION, SEC
BURNOUT
Th
Tj
Tm
Ti
Tj
Te
Tf
Tp (ON DEFLECTION POT)
Tf
Tc
Tb
Ta (ON NOZZLE RING)
600
500
400
300
200
100
0
0
100
200
300
400
500
600

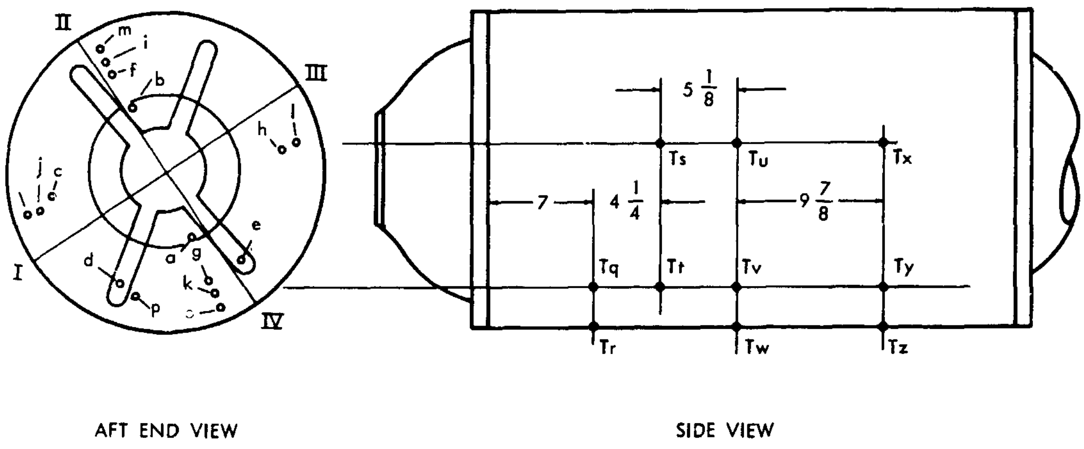
II
III
I
IV
m
i
f
b
h
l
j
c
e
a
g
d
k
p
5 1/8
7
4 1/4
9 7/8
Ts
Tu
Tx
Tq
Tt
Tv
Ty
Tr
Tw
Tz
AFT END VIEW
SIDE VIEW

Figure A-6

APPENDIX B

IGNITER HEAD CAP SPIN TESTS

The X-258 igniter and squib assembly used on Delta 33 was subjected, at spin-up, to an angular acceleration of 12.5 RAD/SEC^2 and an angular velocity of 120 R.P.M. The following spin tests were conducted by the Allegany Ballistics Laboratory to demonstrate the effect of angular acceleration and spin-up shock on the Pyrogen igniter head cap assembly.

Test No.	Angular Acceleration Radian/sec^2	Angular Velocity RPM
1	67	202
2	118	265
3	222	208
4	232	206
5	352	256
6	383	268
7	394	275
8	286	267

NOTE: (1) Prior to test number four (4) the head cap assembly was subjected to vibration per Mil. Standard-353.

(2) Tests six (6) through eight (8) were conducted in a darkened room with live squibs installed. Moving pictures were taken of each test to record any unusual event such as static electric discharge that may have resulted in ignition of the Pyrogen igniter as a result of spin-up.

RESULTS

The results of these tests demonstrate that angular accelerations well in excess of those experienced in flight have no effect on the Pyrogen Igniter.

CONCLUSIONS

As a result of the above-mentioned tests, it is concluded that the premature ignition of the X-258 motor was not the result of spin up acceleration or shock.

APPENDIX C

ELECTRICAL SYSTEM TESTS

INTRODUCTION

The electrical system tests to support the Delta 33 flight failure review were performed to provide sequence 4 information for component tests and for analysis. This appendix includes the tests and the analysis of the results.

Sequence 4 Operation

The normal operation of the sequence 4 circuitry, shown on Figures C-1 and C-2, is as follows:

a. The electrical system is switched to the internal batteries prior to launch.

b. A set of parallel-connected inertia switches transfers second stage engine battery power to an arm bus when the vehicle reaches a predetermined acceleration level. Power from this arm bus is transmitted to the sequence relays located in the second stage sequence distribution box and to the staging relay located in the first stage (through the first to second stage interface).

c. The staging relay is activated at MECO and causes power to be transmitted back to the second stage programmer start relay. The relay starts the programmer and is "locked in" through its own contacts.

d. The programmer then provides the commands at pre-set times for the second stage sequences.

e. The second stage programmer, which was started at first stage main engine cutoff (MECO), applies the negative (ground) side of the Control Battery to the coil of relay K703 at the programmed time for the sequence 4 event (based on mission requirements). Control Battery positive is available from lift-off.

f. Relay K703 is "locked in" through one set of its contacts and applies Engine Battery voltage through two (2) sets of its contacts to parallel circuits composed of the redundant bridge wires and squib switches of sequence 4 ordnance/pyrotechnic items. Each contact provides for all

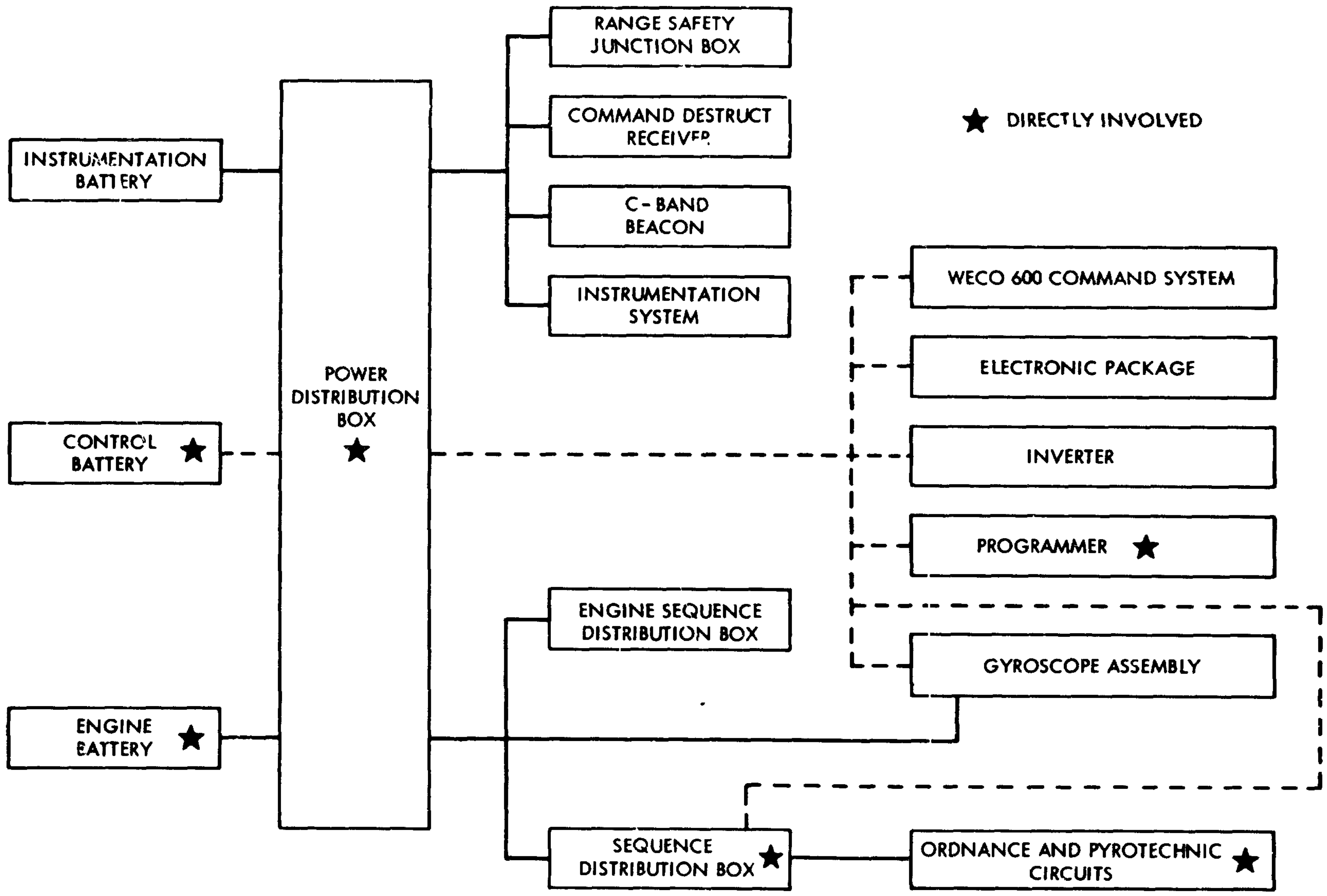

Figure C-1. Electrical System

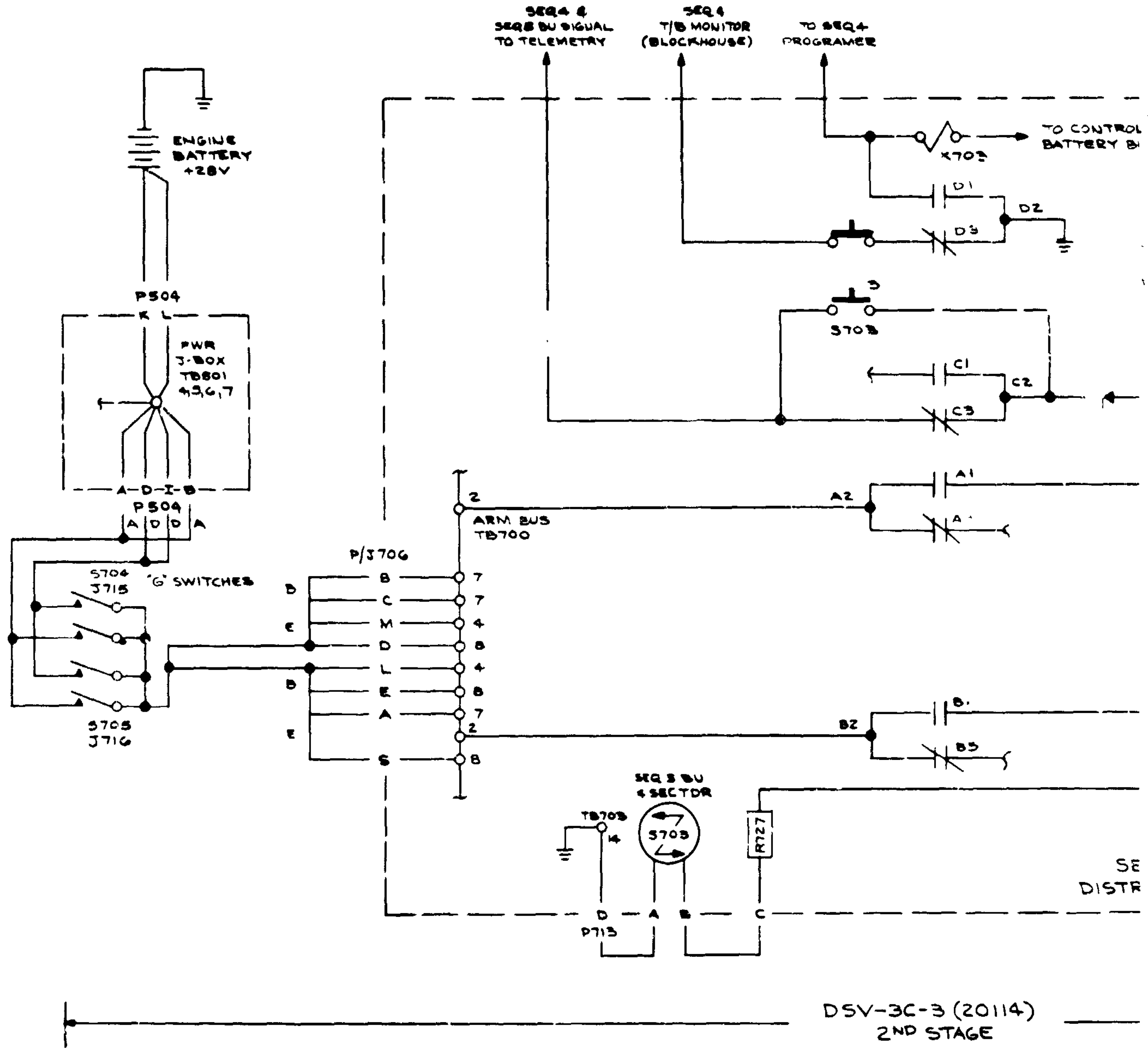

SEQ 4 & SEQ 5 BU SIGNAL TO TELEMETRY
SEQ 4 T/B MONITOR (BLOCKHOUSE)
TO SEQ 4 PROGRAMER
ENGINE BATTERY +28V
TO CONTROL BATTERY B
X703
D1
D2
D3
P504
K L
PWR J-BOX TB801 4,5,6,7
S703
C1
C2
C3
A-D-I-B
P504
A D D A
2
ARM BUS TB700
A2
A1
P/J706
S704 J715
"G" SWITCHES
S705 J716
B C M D L E A S
B2
B1
B3
SEQ 3 BU 4 SECTOR
TB703
S703
R727
D A B C
P713
SE
DISTR
DSV-3C-3 (20114)
2ND STAGE

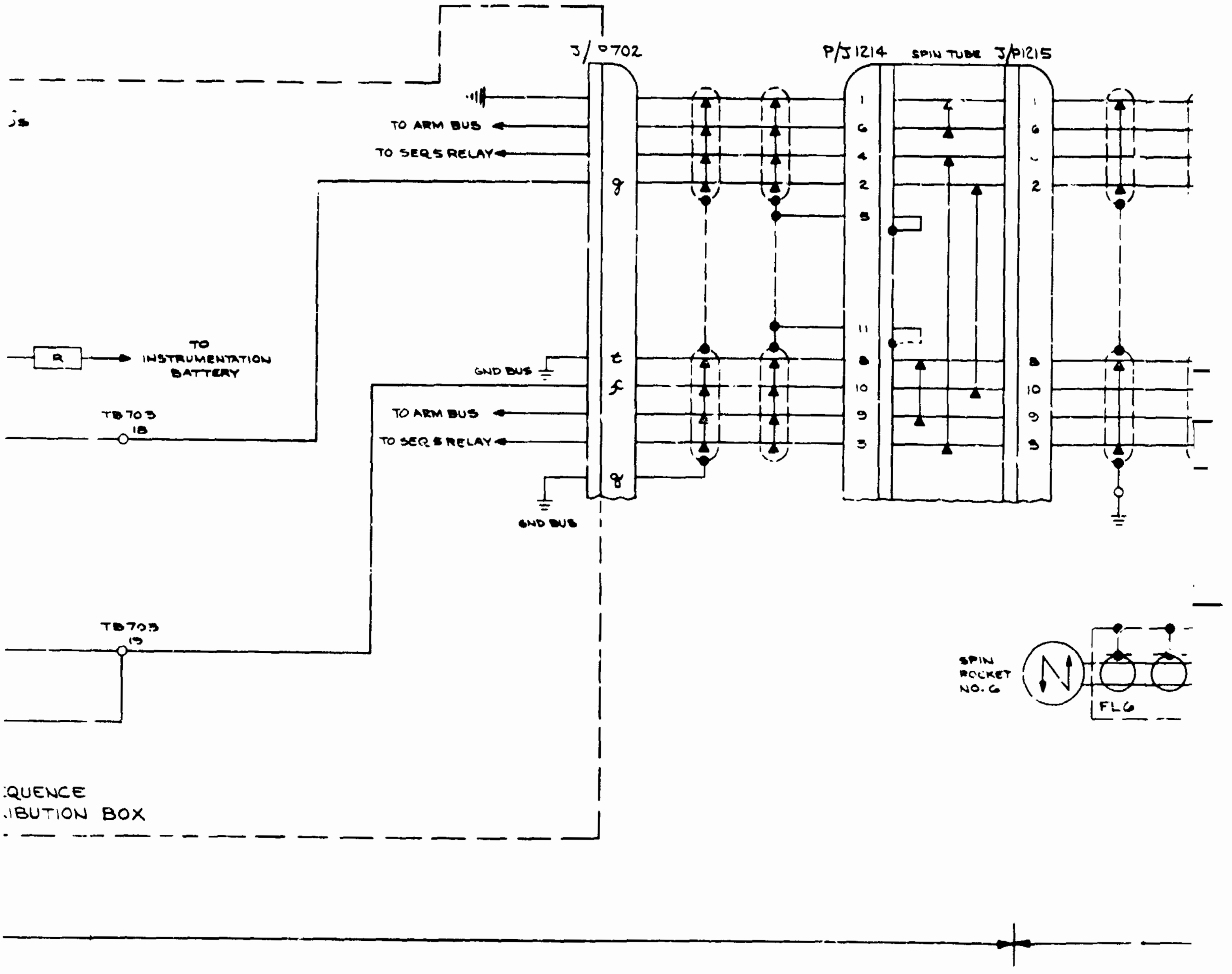

J/P702
P/J1214
SPIN TUBE
J/P1215
TO ARM BUS
TO SEQ S RELAY
TO INSTRUMENTATION BATTERY
R
TB705 18
GND BUS
TB705 19
SPIN ROCKET NO. 6
FL6
QUENCE
IBUTION BOX

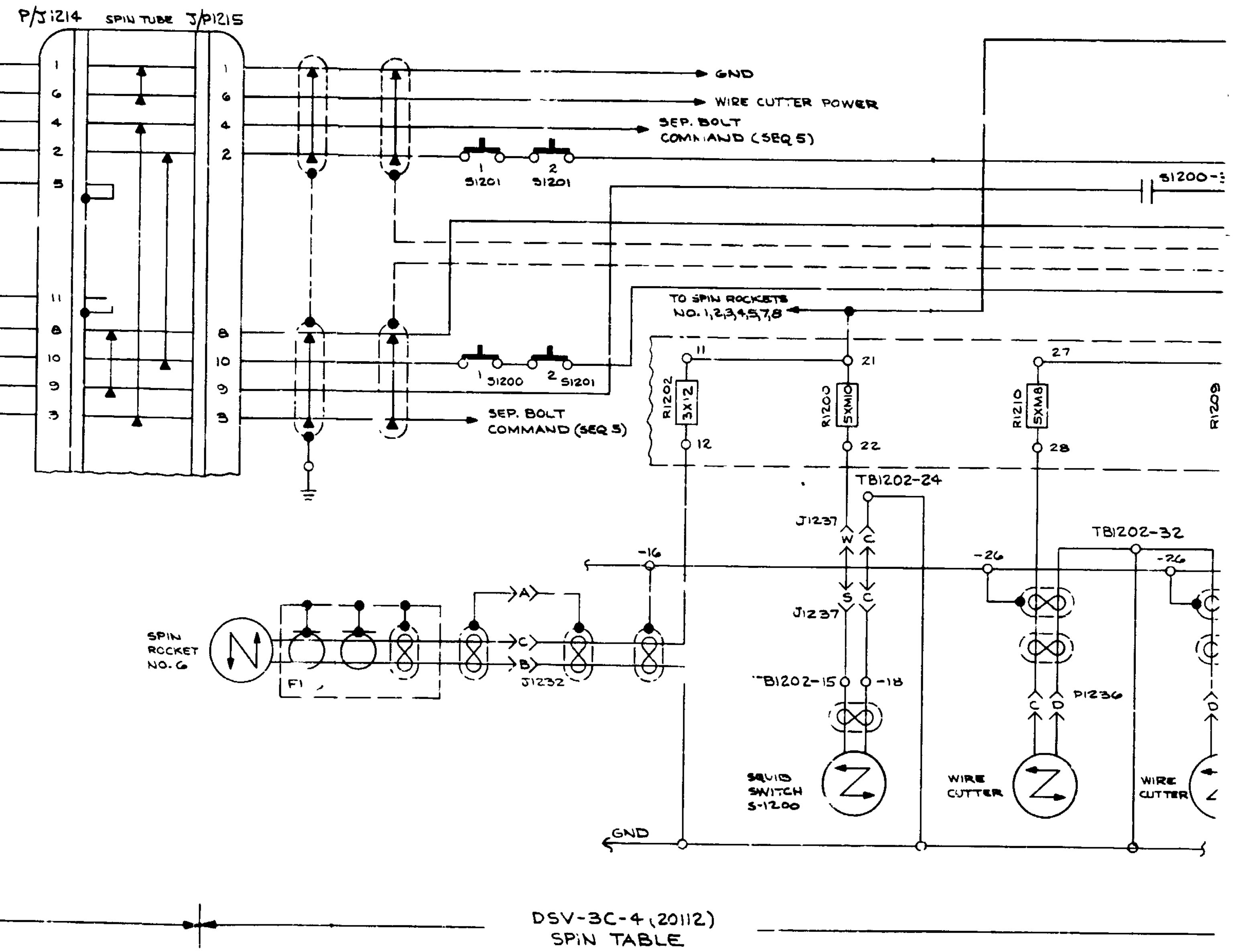

DSV-3C-4 (20112)
SPIN TABLE

OSO—C

△ 33 IGNITION & TIMER ACTUATION CIRCUIT

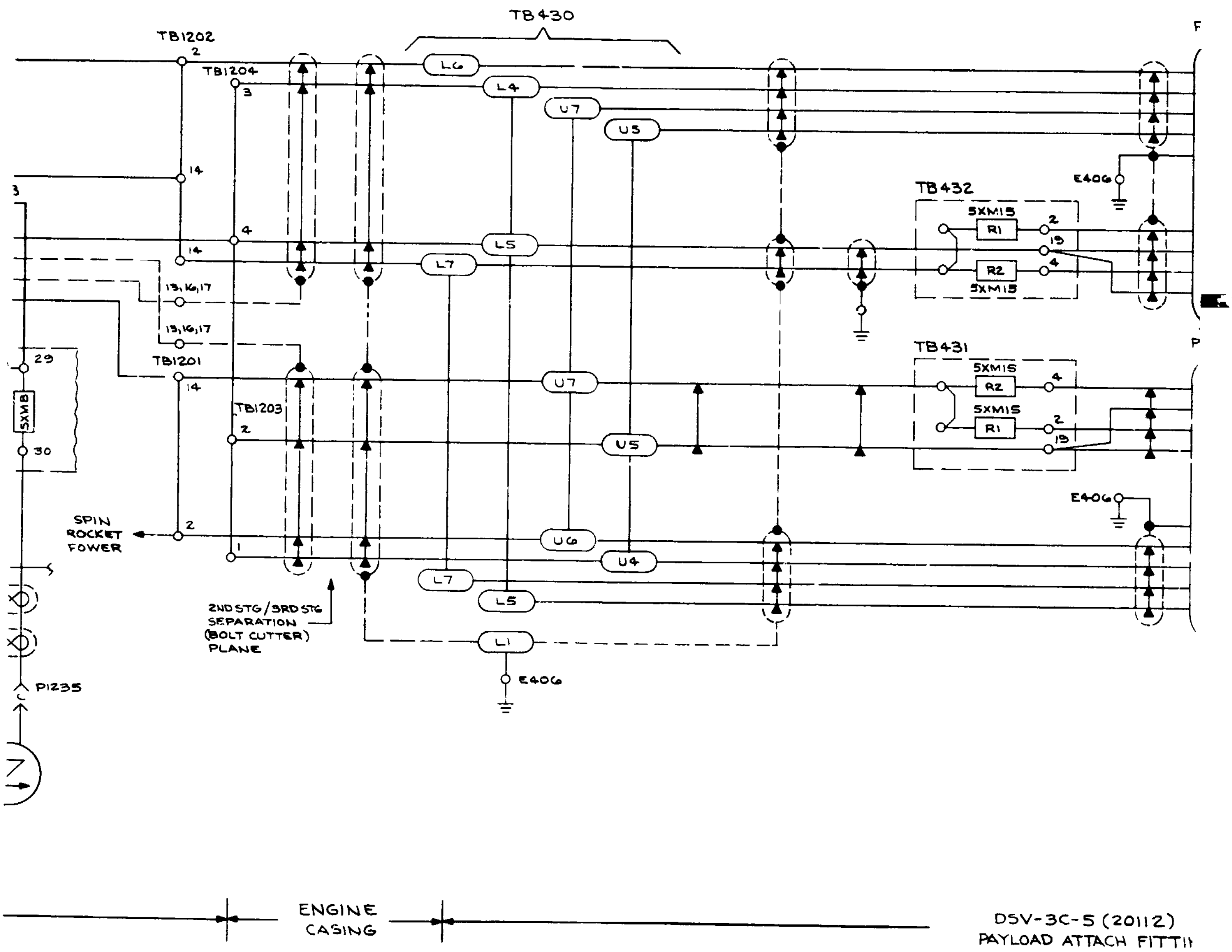

TB430
TB1202
TB1204
TB432
TB431
TB1201
TB1203
L6
L4
U7
U5
L5
L7
U6
U4
L1
5XM15
R1
R2
5XM8
E406
SPIN ROCKET POWER
2ND STG/3RD STG SEPARATION (BOLT CUTTER) PLANE
P1235
ENGINE CASING
DSV-3C-5 (20112)
PAYLOAD ATTACH FITTI

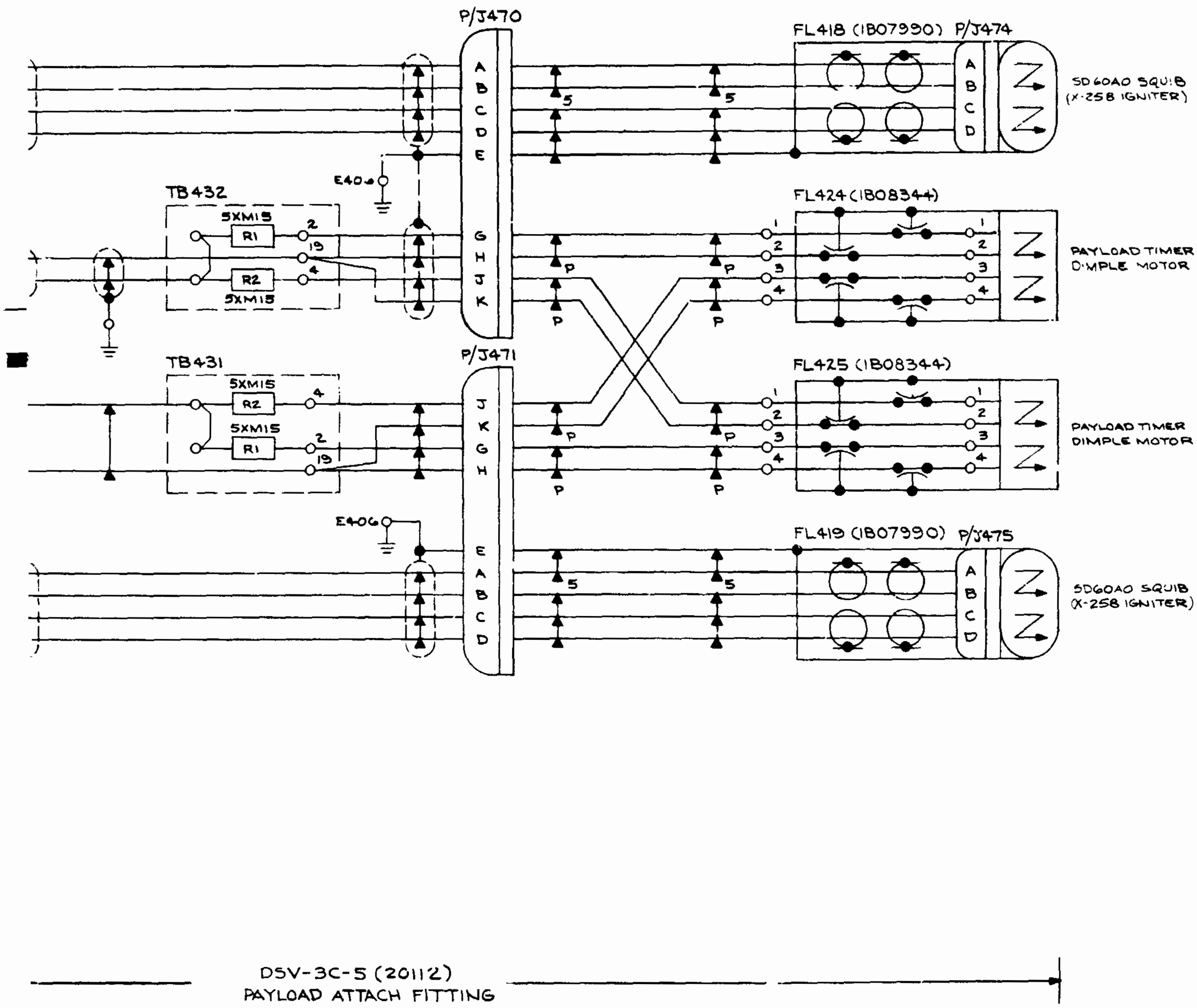

SEQUENCE 4 SCHEMATIC
FIGURE C-2
PAGE C-3

required sequence 4 events. Contact B has an extra function, sequence 5 back-up. Another set of contacts applies Instrumentation Battery voltage to the Instrumentation System to provide an indication of relay operation.

g. The bridgewires "initiate" the following events:

1. The two third stage timers,
2. The pyrotechnic delay which ignites the third stage motor after a nominal 6 second delay,
3. Two squib switches which operate after a nominal 1 second delay to operate two-wire cutters. (This is referred to as sequence 4½).
4. Spin-up (eight spin rockets),
5. The sequence 5 back-up 4 second delay squib switch. (Two (2) seconds after sequence 4 the next programmer event, sequence 5, initiates third stage separation and second stage retro.)

TESTS

Resistance Verification

Measurements for the sequence 4 circuit (where actual values were not available from Delta 33) were made on another vehicle at ETR. A constant current of three (3) amperes was passed through the circuit under test and the voltage drops measured. The resistance values calculated from these measurements are shown in Figure C-3. Measured values from the Delta 33 vehicle log are also shown in this figure and are listed in Table C-1.

Pulse Tests

Purpose: Tests were conducted to determine if a short duration pulse applied at the second stage Sequence J-Box would appear at all sequence 4 ordnance devices.

Mock-up Description: The mock-up consisted of Sections A and B. Section A was a DSV-3C second stage equipment compartment section as shown in Figure C-4. Sequence 4 circuitry including programmer, sequence J-box, engine battery, spin tube and wiring was installed. Section B, shown in Figure C-5, consisted of a flight qualified interstage, an X-258 dummy motor case, a flight qualified attach fitting, and third stage instrumentation Sequence 4 circuitry was complete except for ordnance items and most R. F. filters. These were simulated

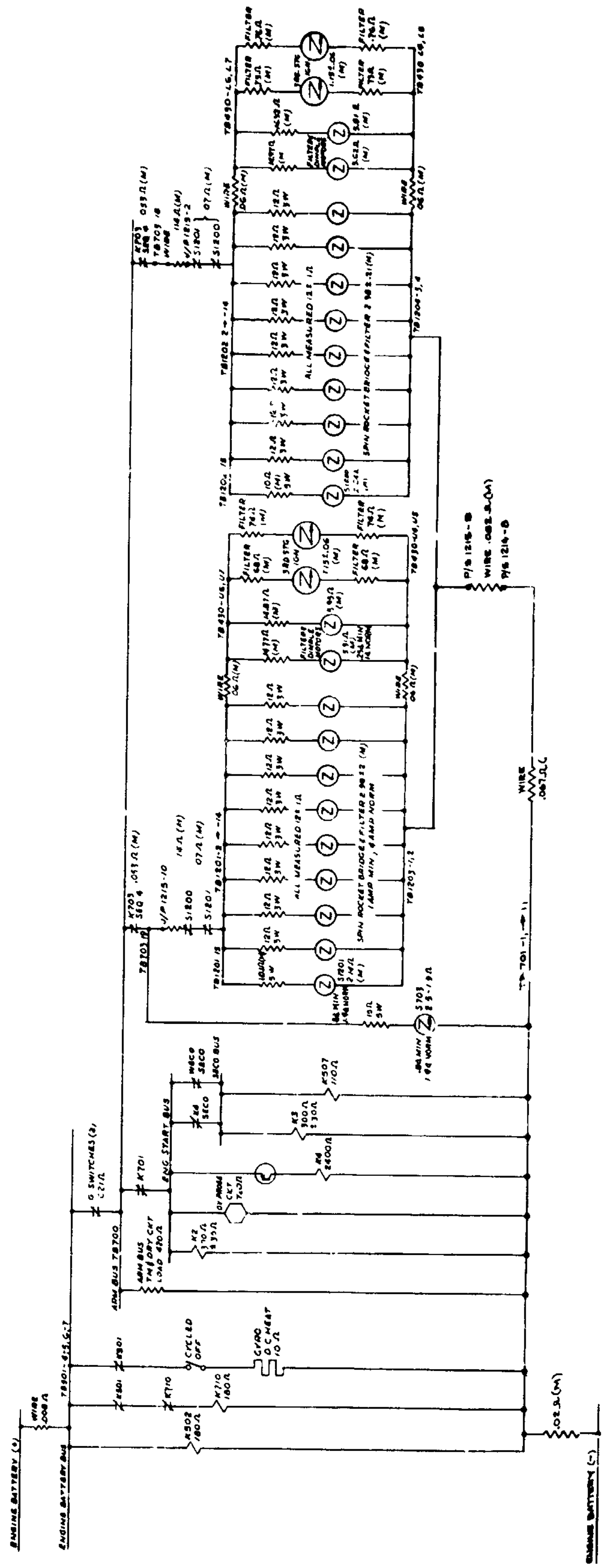

Figure C-3. Sequence 4 Engine Battery Circuit

TABLE C-1

DELTA 33 RESISTANCE VALUES FROM LOG SHEETS		
QUANTITY MEASURED	BETWEEN	RESISTANCE (OHMS)
ATTACH FITTING CONNECTIONS, X-258	P475 A TB430 U6	0.68
	P475 B TB430 U4	0.68
	P475 C TB430 L7	0.73
	P475 D TB430 L5	0.73
	P474 A TB430 L6	0.76
	P474 B TB430 L4	0.76
	P474 C TB430 U7	0.74
	P474 D TB430 U5	0.74
ATTACH FITTING CONNECTIONS WITH J1214 SHORTED	P471 A AND B	0.30
	P471 C AND D	0.26
IGNITER BRIDGEWIRE	SERIAL NO. 99 PIN A AND B	1.09
	SERIAL NO. 99 PIN C AND D	1.12
	SERIAL NO. 100 PIN A AND B	1.17
	SERIAL NO. 100 PIN C AND D	1.20

SPIN ROCKET RESISTANCE IN OHMS				
	BC	D-E	A-F	A-CASE
(1) 5650207	3.00	3.02	.01	.68
(2) 210	3.19	2.92	.02	.05
(3) 211	2.80	3.06	.02	.09
(4) 212	2.98	2.97	.02	.04
(5) 213	2.84	2.93	.02	.04
(6) 214	3.07	2.92	.02	1.29
(7) 215	2.97	2.96	.02	.09
(8) 5650216	3.08	2.98	.02	.04
(2.42 - 3.72) (NOMINAL)				

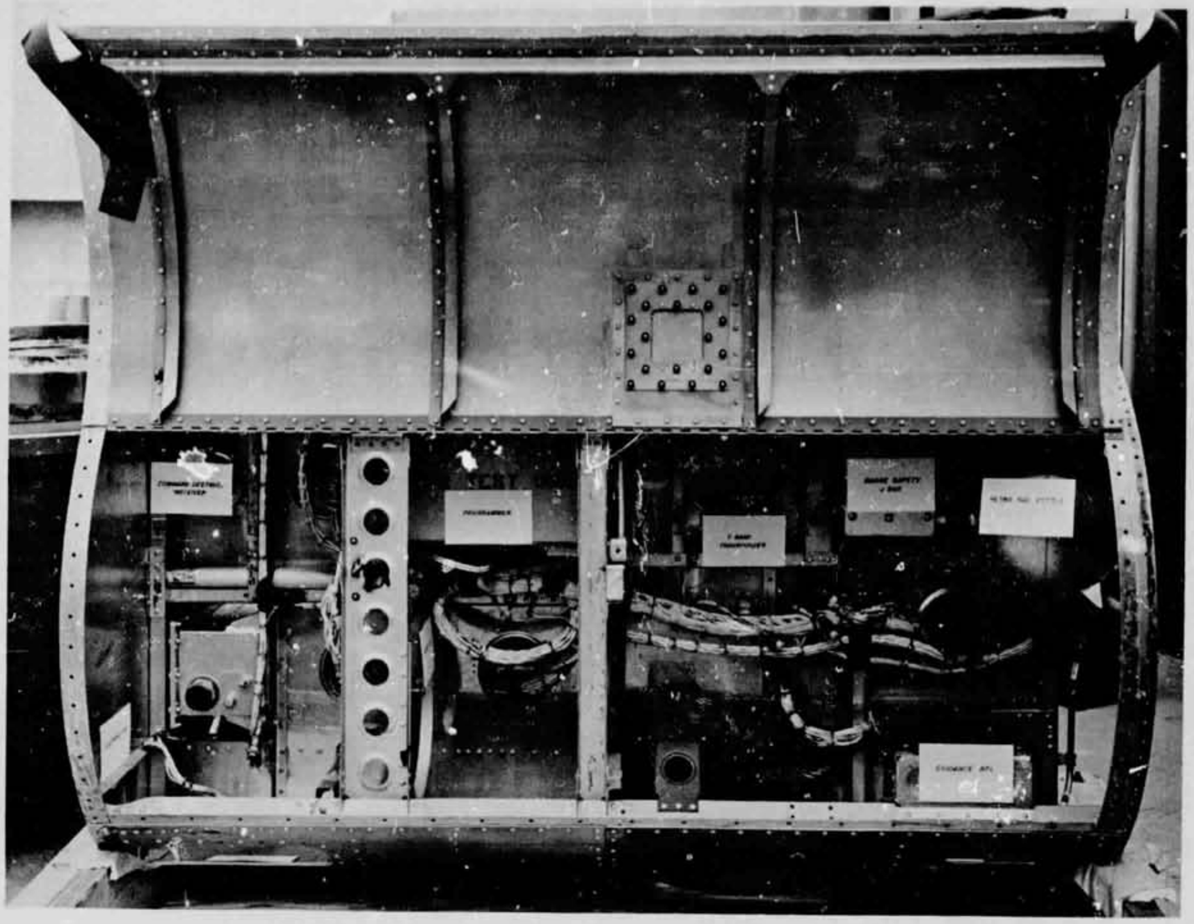

Figure C-4. Second Stage Mock-up

by resistors. The values selected approximate the DC resistance of ordnance/ filter combinations as shown on Figure C-3.

Test Procedure & Equipment: Pulses were applied to the sequence 4 circuits of the mock-ups using an electronic millisecond switch. The switch was set to apply voltage to the circuit under test for a period of 3 milliseconds. A 28v, 6 amp (steady state) power supply was used as the source of pulse power. The pulses were applied to the circuits as described below:

Test A: 2nd Stage

The 3 millisecond pulse was applied to each half of the sequence 4 circuit separately. The pulse was applied first to TB703-18 in the sequence J-Box and then to TB703-19. Vehicle common ground was used as the return connection. The load was a 7.8 ohm resistor connected at the spin tube.

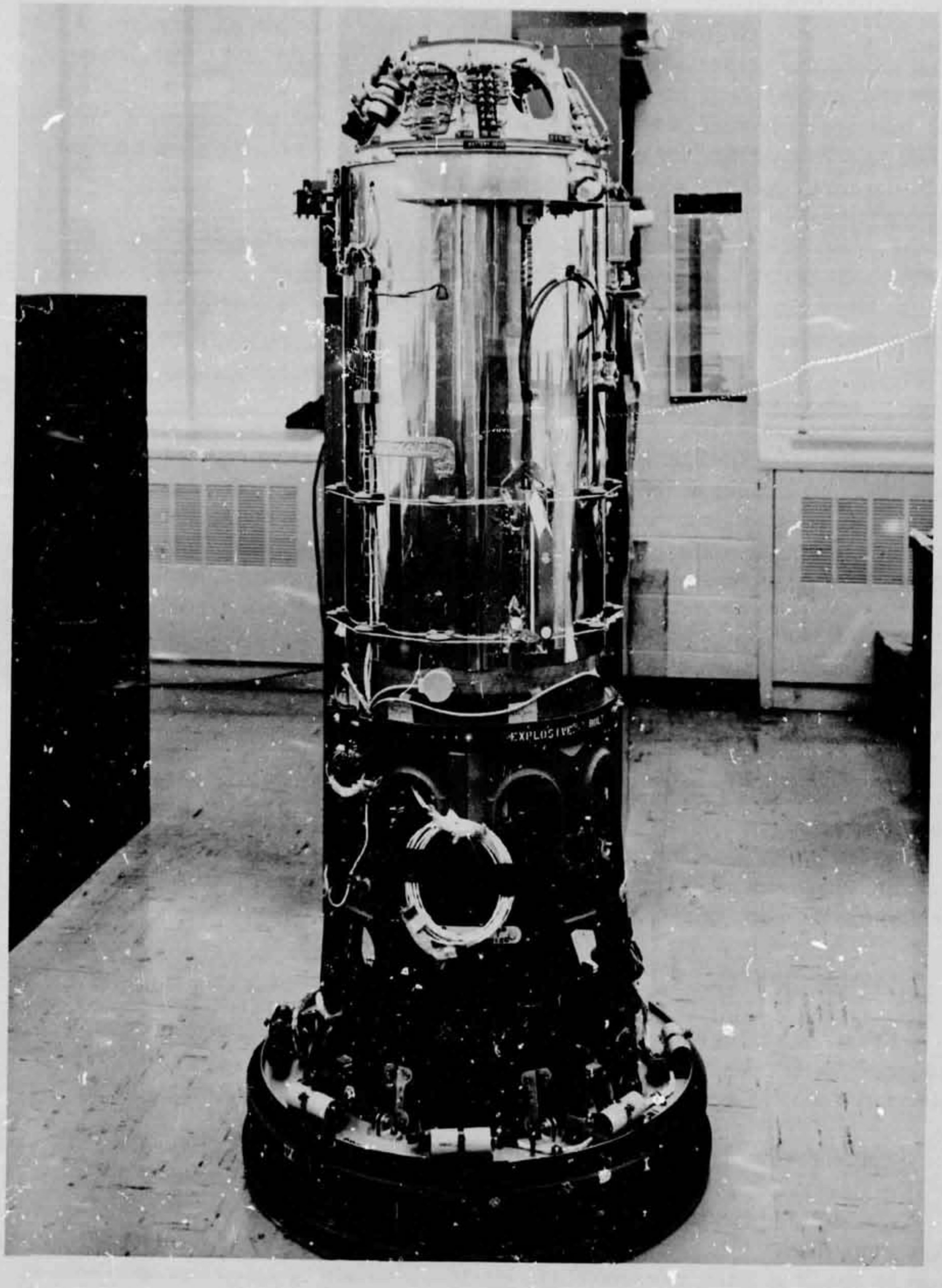

Figure C-5. Third Stage Mock-up

An oscilloscope and camera were used to obtain photographs of the input pulses and pulses across the load resistor at the spin tube. The pulses at input and load points of both halves of the sequence four circuit were identical. Only one set, therefore, was recorded. Photographs were taken at input and load points at a fast sweep rate of the oscilloscope. There photographs enlarge the pulse leading edges for close comparison.

Table C-2 contains Test A photograph data. Column 1 lists the photographs which follow the table; column 2 indicates input or output; column 3 shows where the pulse was recorded; column 4 lists the photograph time scales and column 5 lists the voltage scales.

Test B: 3rd Stage

The 3 millisecond pulse was applied separately to each half of the sequence four circuit at the spin tube connector. An oscilloscope and camera were again used to obtain photographs of the applied pulse and of the pulses appearing across the resistors simulating the ordnance devices. The effect of an RF filter in the circuit was also recorded.

The power supply-pulser combination could not deliver a 28 volt pulse to the very low resistance of the third stage ordnance circuit. Therefore, the pulses applied during Test B were of lower amplitude than the pulses of Test A. These pulses were approximately 17 volts amplitude.

Table C-3 contains Test B photograph data. Column 1 lists the photographs which follow the table; column 2 lists the test points; columns 3 and 4 show the connectors and pins across which the oscilloscope was connected; column 5 lists the resistance values used for simulation, and column 6 lists the scales for the photographs. .

Test Results

From the photographs of input and output pulse waveforms, it is evident that no appreciable distortion occurs. Also, the magnitudes of the outputs at each ordnance location agree with the expected voltage ratios as shown on Table C-4.

Relay Test

A sample of the sequence 4 relay, K703, was tested by the GSFC Quality Assurance Branch to see if contact chatter or closure could be induced by vibration or shock at Delta powered flight levels. It should be noted that the Delta 33 was in an extended coast period prior to the failure. The relay experienced no

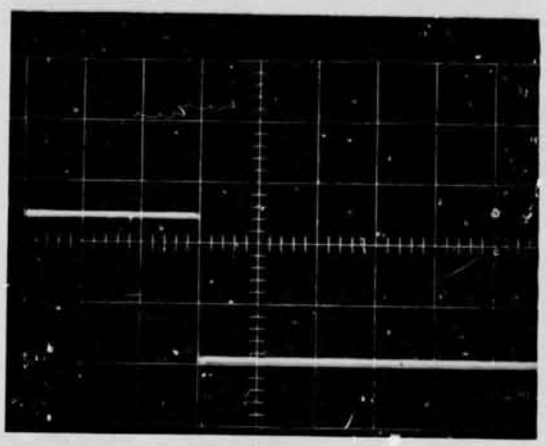

1

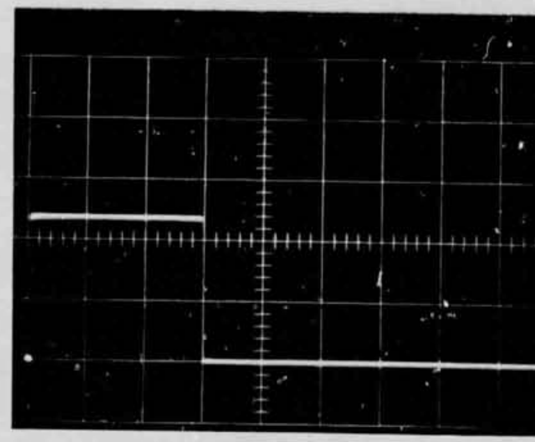

2

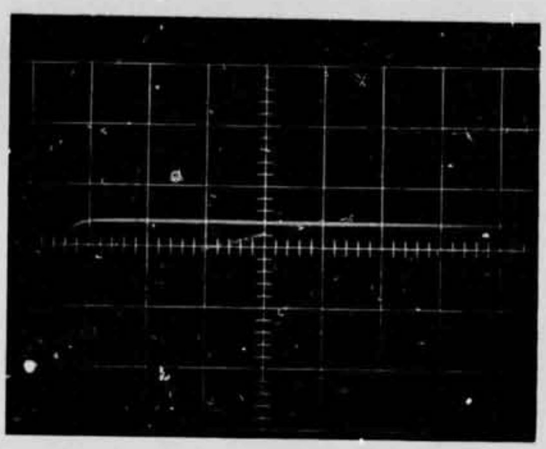

3

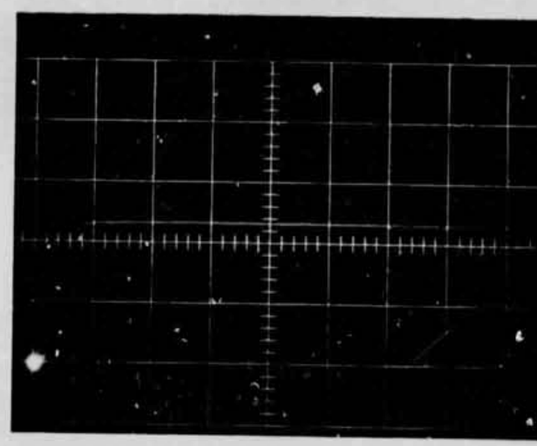

4

TABLE C-2

OSO-C PULSE TEST A PHOTOGRAPH DATA

(1) PHOTO	(2) PULSE	(3) LOCATION	(4) TIME SCALE	(5) VOLTAGE SCALE
1	INPUT	TB703-19	1 MS/CM	10V/CM
2	OUTPUT	P1215-10&8	1 MS/CM	10V/CM
3	INPUT	TB703-19	10 μS/CM	10V/CM
4	OUTPUT	P1215-10&8	10 μS/CM	10V/CM

problems during this test with the monitoring equipment set to detect a chatter level of 100 microseconds.

ANALYSIS

Summary

The sequence 4 circuit and engine battery monitor points were analyzed to determine the time a pulse could be applied to the circuit and be undetected by the instrumentation system. This was determined to be 17 milliseconds.

TABLE C-3

OSO-C PULSE TEST B PHOTOGRAPH DATA

(1) PHOTO #	(2) TEST POINT	(3) CONNECTOR	(4) PIN	(5) RESISTOR	(6) SCALE
1	INPUT	J1215	2-1	0.91	5V/CM
2	SPIN ROCKET #1	J1231	C-B	3.3	1V/CM
3	SPIN ROCKET #2	J1230	C-B	3.3	1V/CM
4	SPIN ROCKET #3	J1229	C-B	3.3	1V/CM
5	SPIN ROCKET #4	J1228	C-B	3.3	1V/CM
6	SPIN ROCKET #5	J1227	C-B	3.3	1V/CM
7	SPIN ROCKET #6	J1226	C-B	3.3	1V/CM
8	SPIN ROCKET #7	J1225	C-B	3.3	1V/CM
9	SPIN ROCKET #8	J1232	C-B	3.3	1V/CM
10	SWITCH S1200	J1237	W-C	2.0	1V/CM
11	DIMPLE MOTOR T424	--	1-2	5.6	1V/CM
12	DIMPLE MOTOR T425	--	1-2	5.6	1V/CM
13	IGNITOR SQUIB	P474	A-B	1.3(W/F)	2V/CM
14	IGNITOR SQUIB	P475	C-D	1.3(W/F)	2V/CM
15	INPUT	J1215	2-1	0.91	5V/CM
16	INPUT	J1215	10-8	0.91	5V/CM
17	SPIN ROCKET #1	J1231	E-D	3.3	1V/CM
18	SPIN ROCKET #2	J1230	E-D	3.3	1V/CM
19	SPIN ROCKET #3	J1229	E-D	3.3	1V/CM
20	SPIN ROCKET #4	J1228	E-D	3.3	1V/CM
21	SPIN ROCKET #5	J1227	E-D	3.3	1V/CM
22	SPIN ROCKET #3	J1226	E-D	3.3	1V/CM
23	SPIN ROCKET #7	J1225	E-D	3.3	1V/CM
24	SPIN ROCKET #8	J1232	E-D	3.3	1V/CM
25	DIMPLE MOTOR T424	--	3-4	5.6	1V/CM
26	DIMPLE MOTOR T425	--	3-4	5.6	1V/CM
27	IGNITOR SQUIB	P474	C-D	1.3 (W/F)	2V/CM
28	IGNITOR SQUIB	P475	A-B	1.3 (W/F)	2V/CM
29	SWITCH S1201	J1237	V-Z	2.0	1V/CM
30	INPUT	J1215	10-8	0.91	5V/CM
31	IGNITOR SQUIB	P470	A-B	2.7 (WO/F)	5V/CM
32	INPUT	J1215	2-1	0.88	5V/CM

TIME SCALE 0.5 MS/CM

(w/f) - with filter
(WO/F) - WITHOUT FILTER

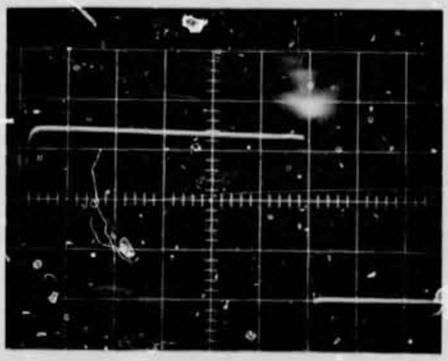

1

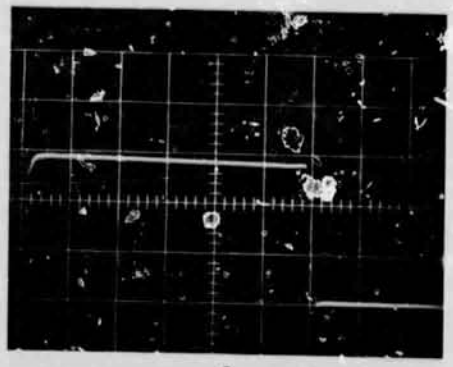

2

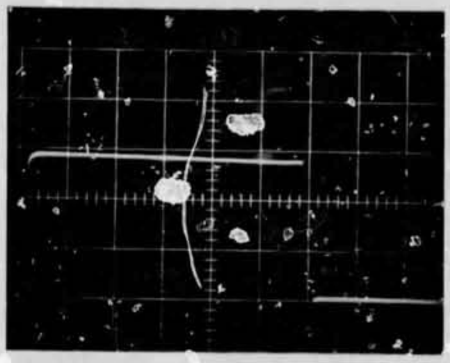

3

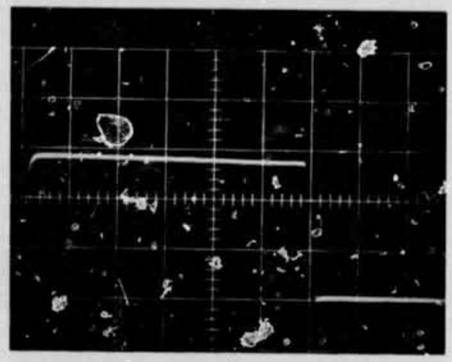

4

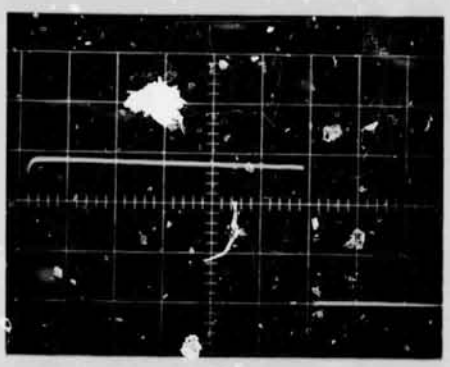

5

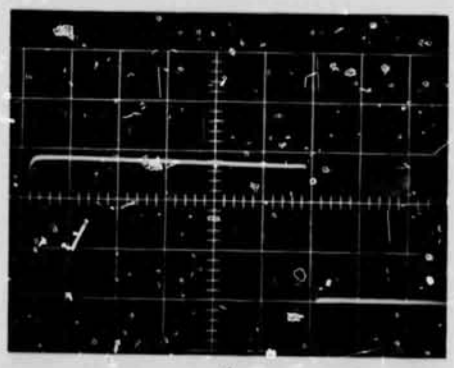

6

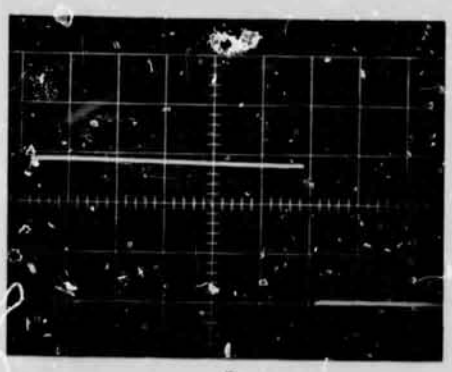

7

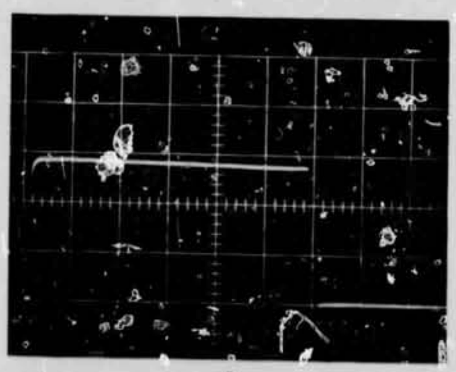

8

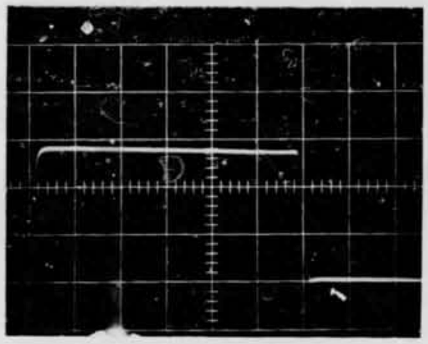

9

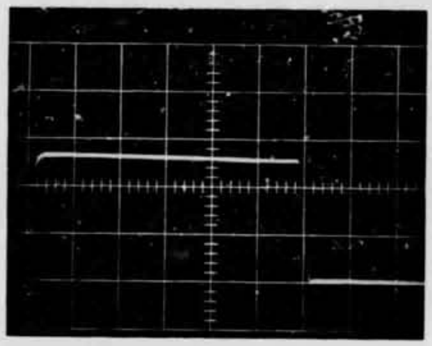

10

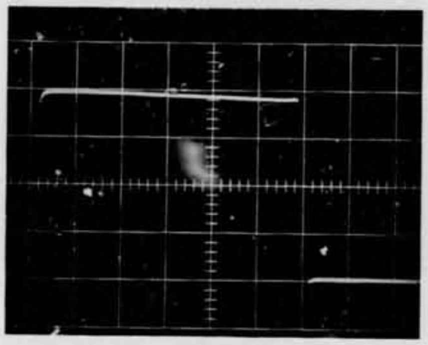

11

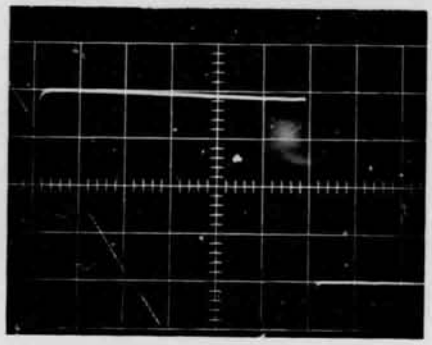

12

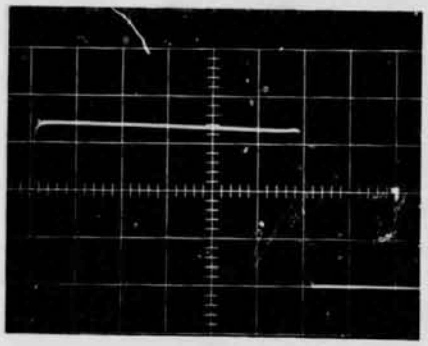

13

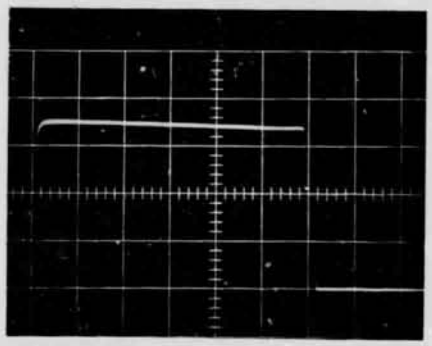

14

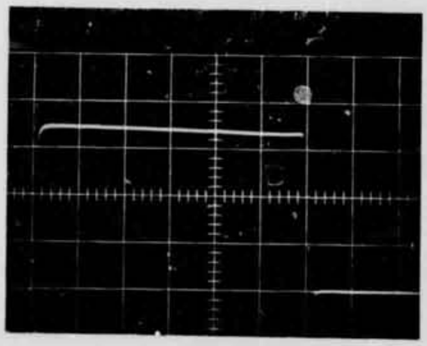

15

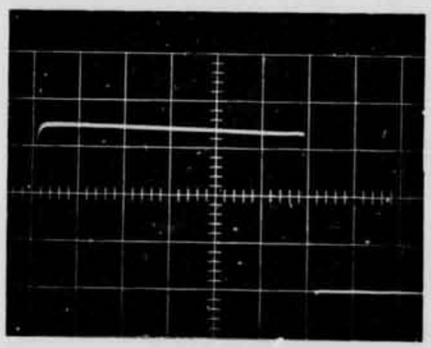

16

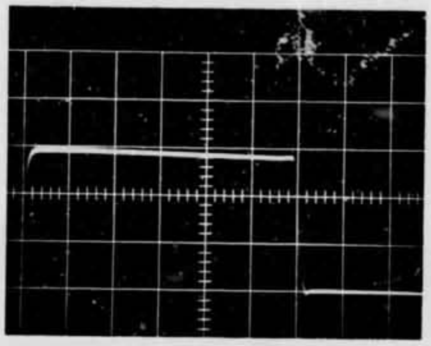

17

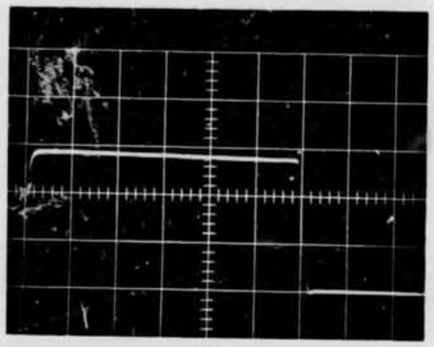

18

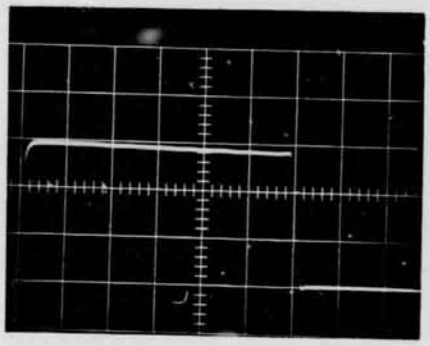

19

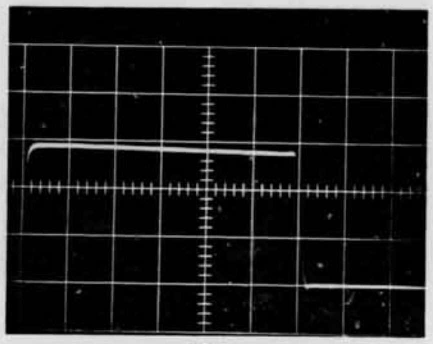

20

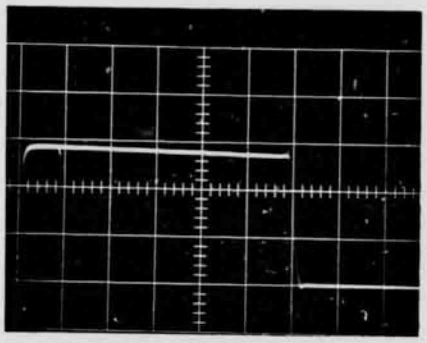

21

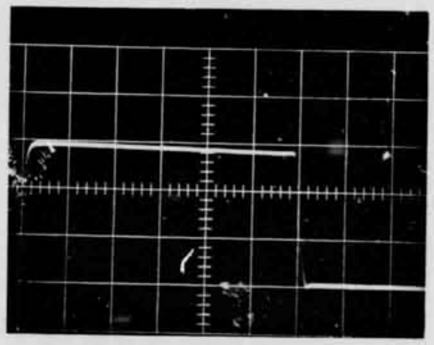

22

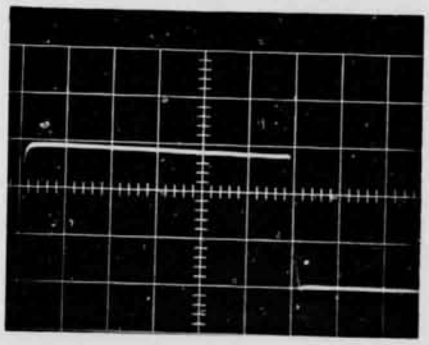

23

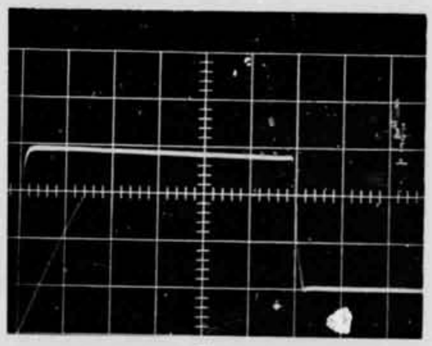

24

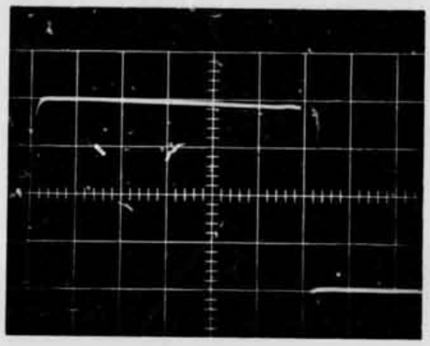
25

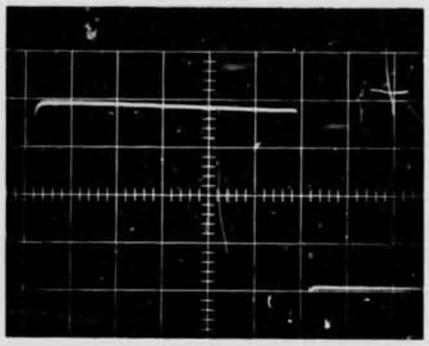
26

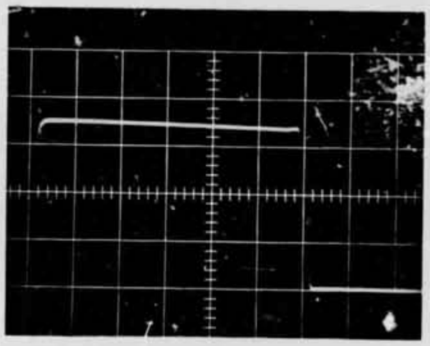
27

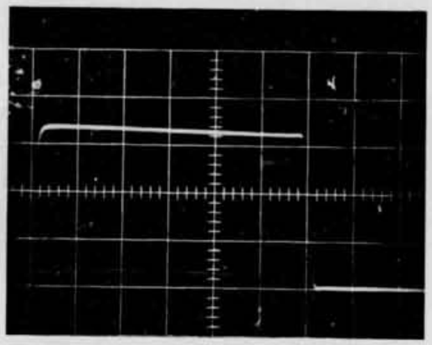
28

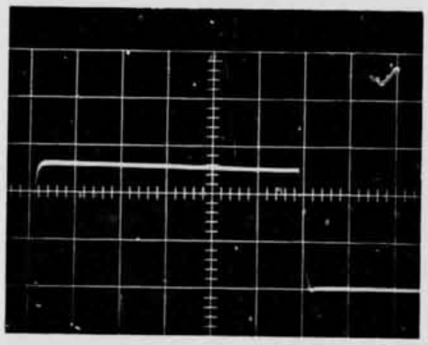
29

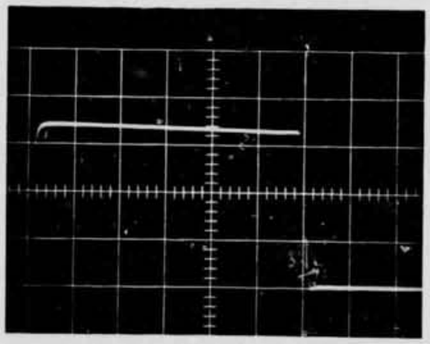
30

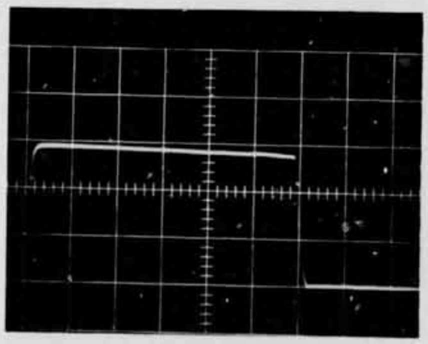
31

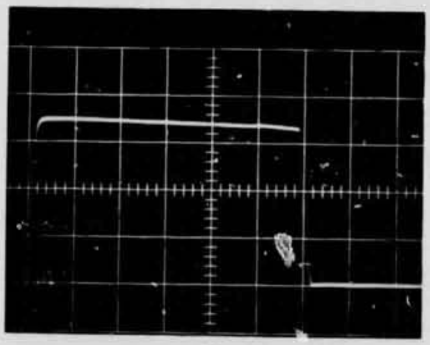
32

TABLE C-4

PULSE AMPLITUDE RATIOS

DEVICE	VOLTAGE OUT AT ORDNANCE/FILTER VOLTAGE IN AT J1215	
	COMPUTED*	MEASURED
SPIN ROCKET	0.20	0.17
SQUIB SWITCH	0.18	0.16
DIMPLE MOTOR	0.29	0.24
IGNITOR SQUIB	0.46	0.41

FOR BOTH SEQUENCE 4 CIRCUITS

* (1) WIRING RESISTANCE NEGLECTED
(2) SUBSTITUED RESISTANCE VALUES APPROXIMATE

A second facet of the electrical system study was the determination of initial current distributions for different circuit conditions. Table C-5 provides a summary of this work.

Engine Battery Voltage Transients at Sequence 4

Following the flight failure of Delta 33, an intensive review of the 2nd stage TM data was begun. Since several ordnance devices are fired from the Engine Battery at the point in time known as Sequence 4, a close look at the engine battery voltage at this time was begun. The results are documented below.

Figure C-6 is a reproduction of the actual telemetry records from Delta 33 showing both the engine battery voltage and the event marker which indicates the occurrence of Sequence 4 or spinup of the third stage. The voltage shows an initial drop, recovery, a decreasing value, then an increasing value terminated by loss of TM signal.

To review, there are 5 classes of ordnance devices of the heated bridgewire type initiated at Sequence 4. These are listed in Table C-5. There are 17 devices having a total of 27 bridgewires which are connected across the engine battery at Sequence 4. These devices are primarily high current devices so that a heavy current drain from the battery would be expected and thus the initial very sharp drop of the battery voltage. Various bridgewires within the squibs

TABLE C-5

DELTA 33
SEQUENCE 4 ORDNANCE DEVICES
ELECTRICAL CHARACTERISTICS

DEVICE	MANUFACTURER	TYPE	BRIDGE WIRE RESISTANCE (OHMS)		NO FIRE ***	MINIMUM *** FIRE	RECOMMENDED ***FOR FIRING	NORMAL ***		SIDE B ONLY ***	SIDE A ONLY ***
			MIN	MAX				SIDE B	SIDE A		
SIX (6) SECOND IGNITER SQUIB	PORT EWEN WORKS HERCULES POWER CO.	SD60A0	1	1.8	1.0	3.5	5-10	L 5.6 R 5.3	5.4 5.3	6.77 6.57	6.72 6.57
ONE (1) SECOND (S1200 & S1201) SQUIB SWITCH	ATLAS CHEMICAL CO.	DM 379-C	1.9	2.5	0.010	**	1.0	1.26	1.26	1.56	1.57
(S703) FOUR (4) SECOND SQUIB SWITCH	ATLAS CHEMICAL CO.	DM 397-C	1.9	2.5	0.010	**	1.0	2.0	N/A	1.66	N/A
DIMPLE MOTOR	ATLAS CHEMICAL CO.	IMT 117	5.0	8.0	0.01	0.3	1.0	.68	.68	.84	.85
SPIN ROCKET	ATLANTIC RESEARCH FLARE NORTHERN DIV.	IKS 40	0.7	1.4	0.25	0.3	1.0	1.03	1.03	1.28	1.29
DIMPLE MOTOR *	HERCULES POWER	DM 25A15	3.0	7.0	0.005	0.050	1.0	N/A	N/A	N/A	N/A

* ALTERNATE - NOT USED ON DELTA 33
** SEE FRANKLIN REPORT F-B2210-3
*** CURRENT IN AMPERES

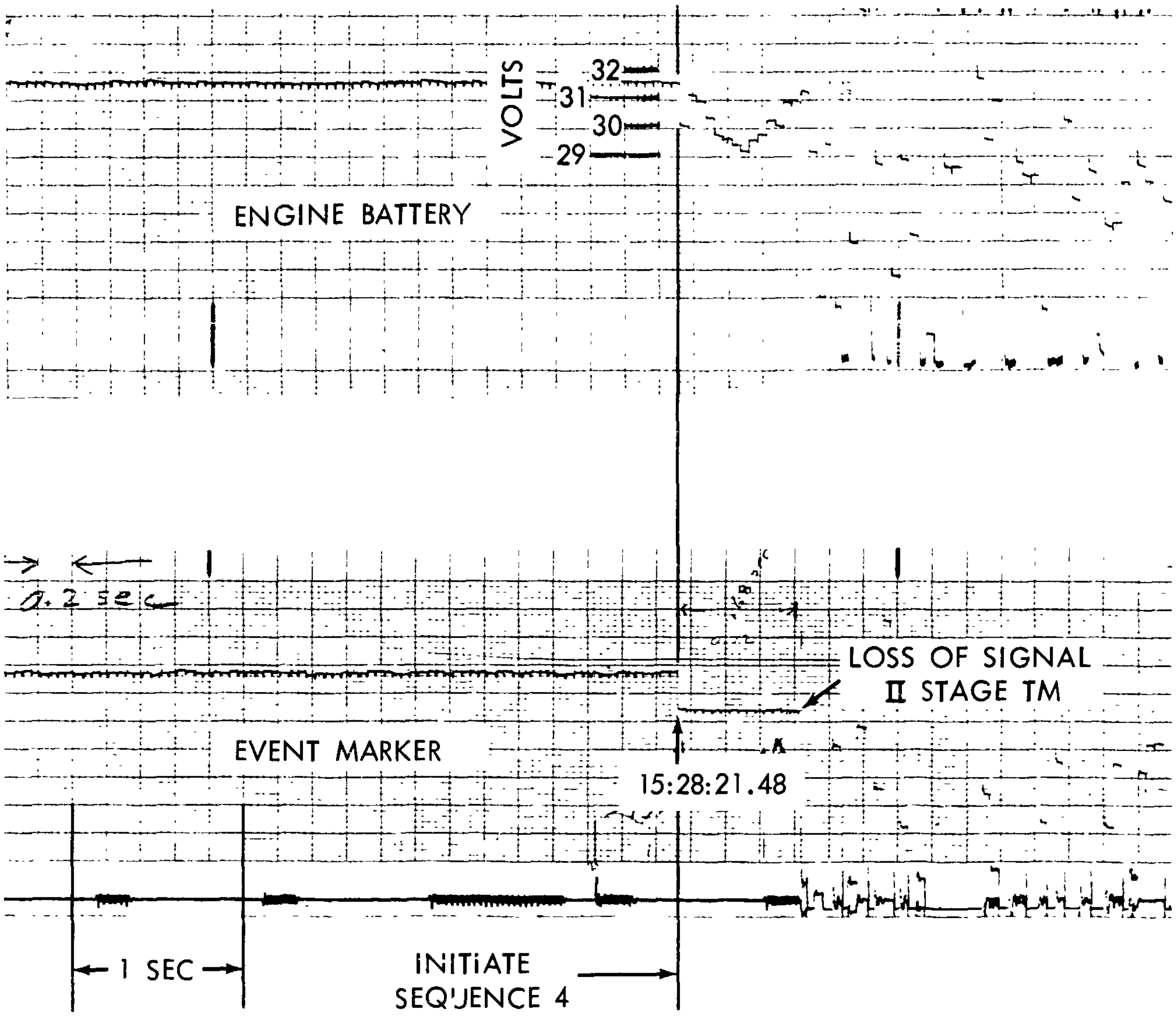

DELTA 33

Figure C-6. Engine Battery Voltage at Sequence 4, Delta 33

may short to case, to each other; they may burn open or carbonize into a high resistance path to ground. This action is comparatively random and thus the varying load on the battery following the initial firing pulse. At 0.7 second after Sequence 4, all 2nd stage TM data was lost. Normally, however, the one (1) second time delay explosive switches would remove the power from the ordnance device and operate the wire cutters and it would be natural to expect a stepwise recovery of the battery voltage.

To determine if the battery voltage signature on Delta 33 was typical, records from past successful Delta launches were examined. These records have been reproduced as Figures C-7, 8, and 9. It should be noted here that the burn time of the spin rockets and the type of third stage timer dimple motors varied from flight to flight. There are 2 classes of battery signatures identifiable.

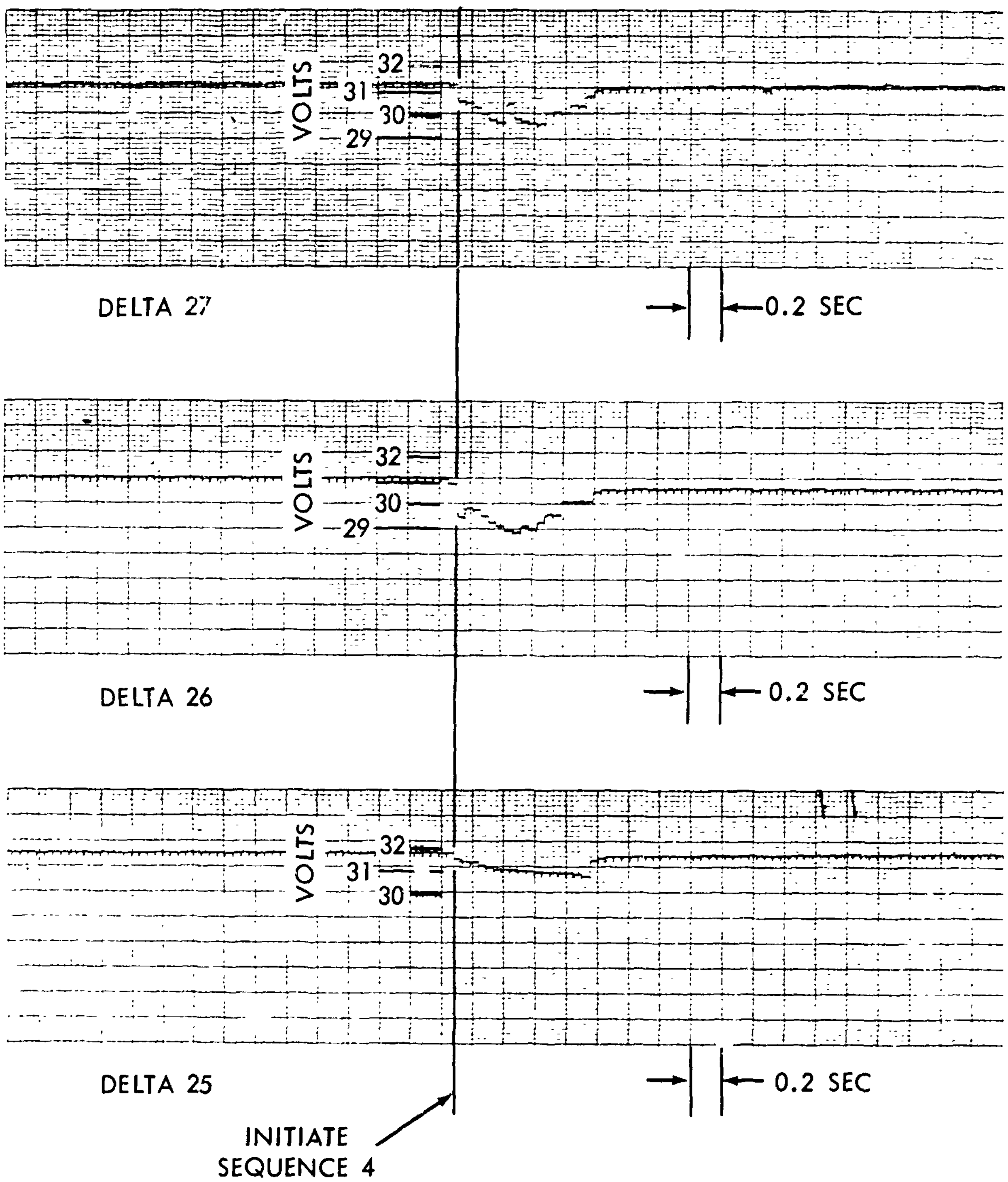

Figure C-7. Engine Battery Voltage at Sequence 4, Delta 25, 26, and 27

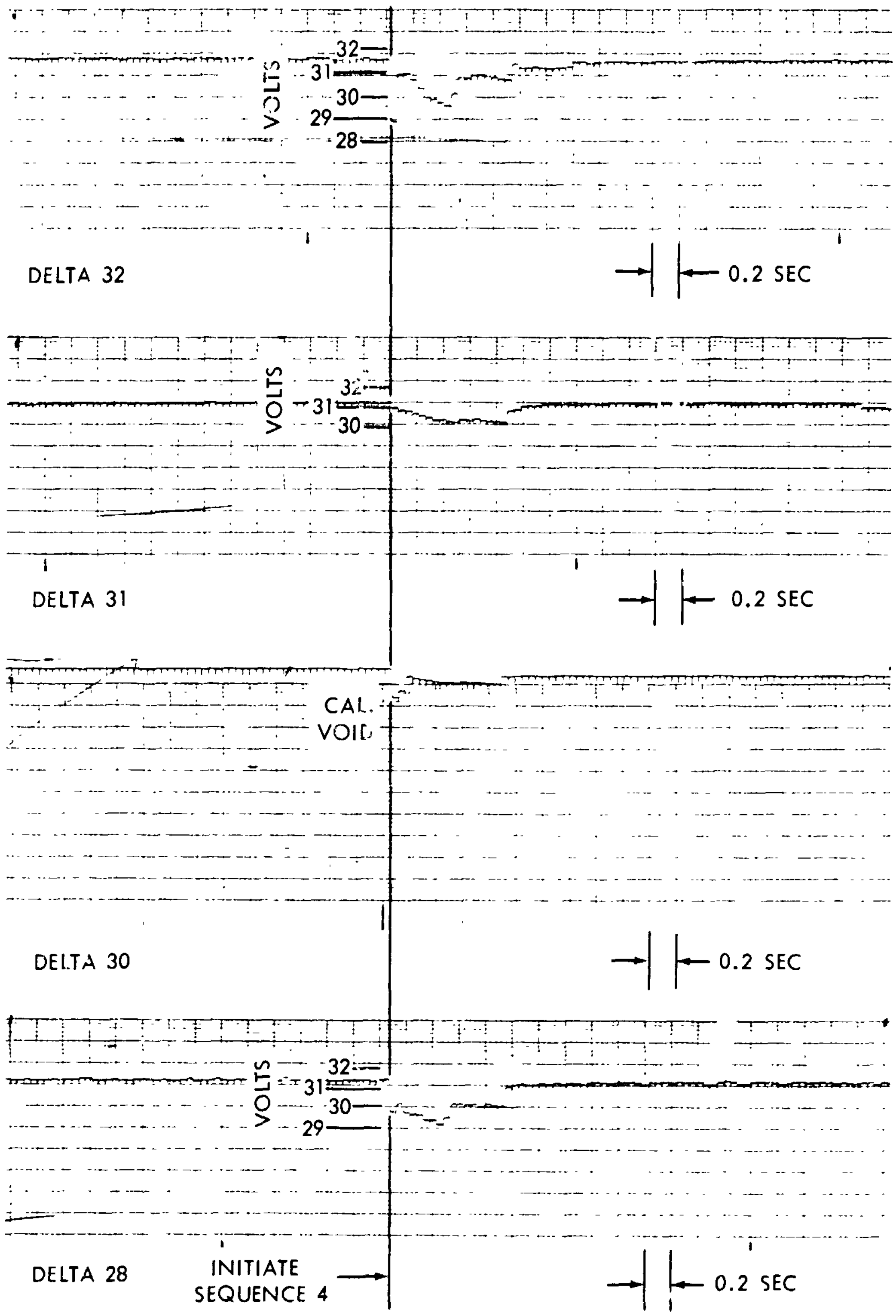

Figure C-8. Engine Battery Voltage at Sequence 4, Delta 28, 30, 31, and 32

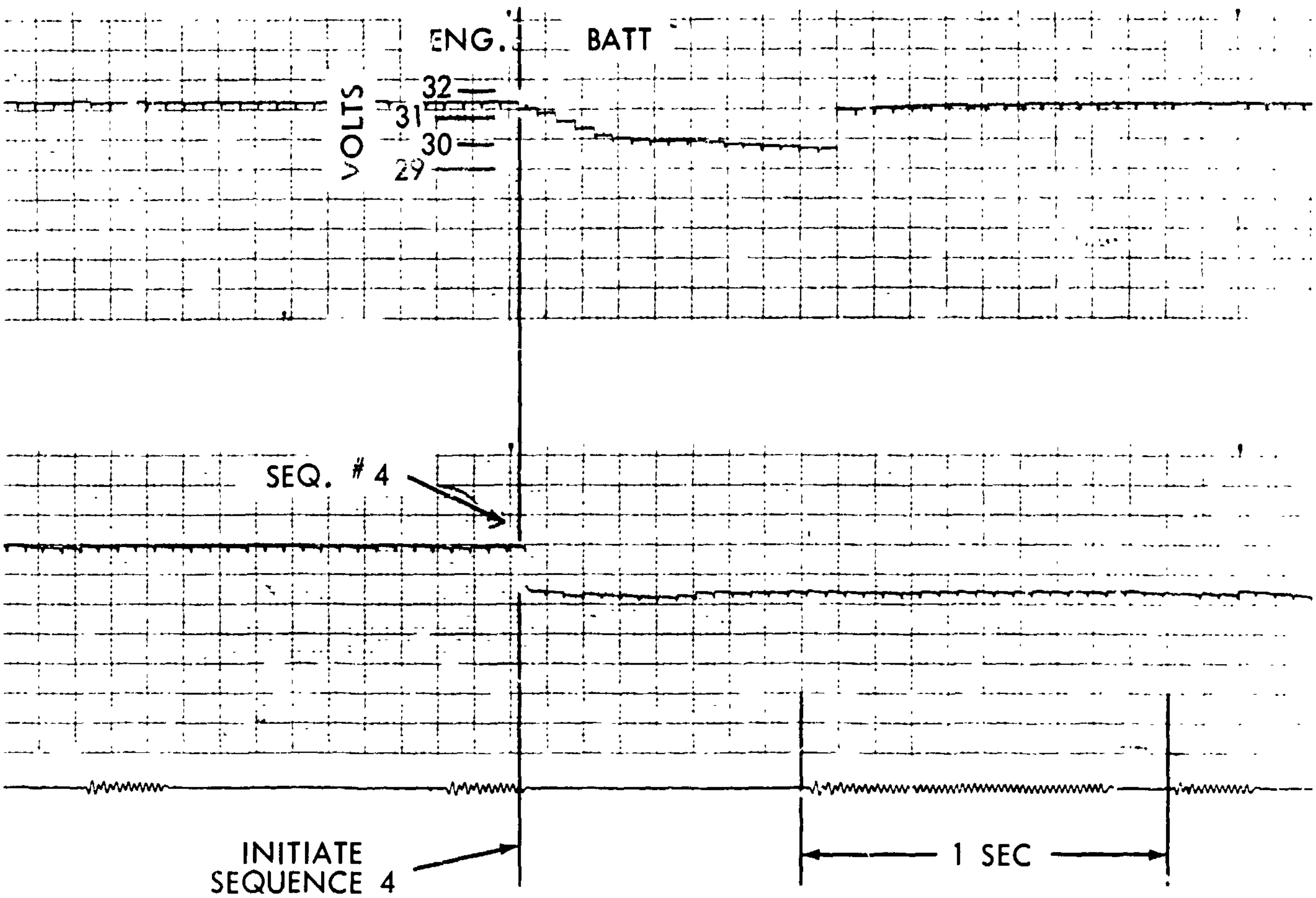

DELTA 29

Figure C-9. Engine Battery Voltage at Sequence 4, Delta 29

Referring to Figure C-7 they are the Delta 25 class and the Delta 26 class. Past flights which fall into the Delta 25 class are Deltas 29, 30, 31, and 25. The remainder are classed with Delta 26, except Delta 28 which appears to be a combination of both 25 and 26. The initial voltage drop, observed in Delta 33 and the Delta 26 class, was not observed in the Delta 25 class probably due to the sampling period of the TM system. The stepwise increase in voltage at 1 second after sequence 4, clearly apparent in the Delta 25 class, is not so clearly visible in the Delta 26 class. The differences may be due only to the random load caused by the spent bridgewire. Specifically, any shorted bridge wires may be "burned clear" prior to the 1 second time so that there was less load to be removed by the explosive switches (S1200/1201). In the records examined, the battery voltage had returned to normal at the end of the 1 second period, indicating that all load was removed by this time.

On Delta 33, the second stage telemetry system contained a PDM (pulse duration modulation) commutator using a standard IRIG 45 × 20 format. The commutator consisted of 45 segments sampled sequentially at the rate of 20 samples per second. Each channel was therefore sampled at 50 millisecond intervals.

The duration of the engine battery voltage transient at Sequence 4 can be estimated with the aid of Figure C-10, which is a representation of the PDM

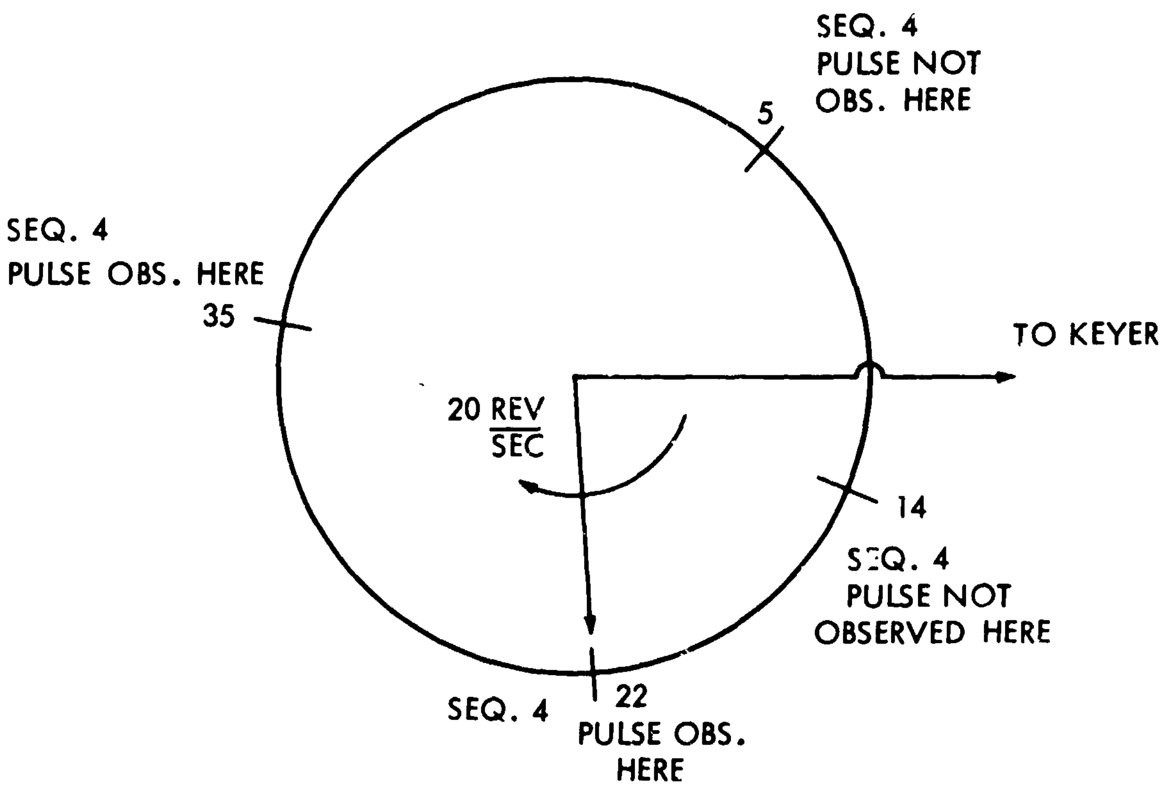

A. SEQ. 4 ORDNANCE LOAD

1. MIMIMUM DURATION OF PULSE - THROUGH 13 CHANNELS @ 1.1 ms = 14 ms

2. MAXIMUM DURATION OF PULSE - (JUST AFTER CH. 14 TO JUST BEFORE CH. 5 = 40 ms

B. POSSIBLE SPURIOUS PULSES

1. MINIMUM DURATION FOR CERTAIN DETECTION - 15 CH. @ 1.1 ms = 17 ms

2. MAXIMUM UNDETECTABLE PULSE WIDTH < 15 CH. = 16.5 ms

Figure C-10. Schematic Representation of PDM Commutator

commutator. Channels 5, 14, 22, and 35 derive their input signal from the engine battery. The initial pulse was observed on channels 22 and 35, but not on 14 and 5. Therefore, the duration of the pulse was between 14 and 40 milliseconds. Further, because of the distribution of the channels around the commutator, a pulse with a duration of 17 milliseconds or more would be observable by the TM system.

With the information above, the conditions for an undetected (TM-wise) premature ignition of the X-258 motor can be listed.

(1) The premature igniting signal must have a duration of less than 17 milliseconds and must occur between the commutation points of the PDM system.

(2) If the premature igniting signal were generated by the 2nd stage programmer, it must be of insufficient duration to operate the Sequence 4 relay K703 (operate time 10-16 milliseconds).

(3) The premature igniting signal must ignite only the X-258 squibs and not the other ordnance devices connected in parallel.

(4) The premature ignition signal must be given six (6) seconds prior to the observed Sequence 4, assuming a nominal igniter delay.

The telemetry data from Delta 33 show the following:

(1) There were no spurious signals recorded by Channels 5, 14, 22, and 35 during the 20 seconds prior to Sequence 4.

(2) The sequence 4 event relay K703 operated at the proper programmed time.

(3) The available TM channels provide positive assurance that the ordnance devices connected across the X-258 squibs were not actuated prior to sequence 4.

(4) There were no spurious pulses on any of the battery channels of six (6) seconds prior to Sequence 4, which could be reasonably interpreted as an X-258 igniter firing pulse.

From the foregoing, the following conclusions can be drawn:

a. The engine battery voltage signature at Sequence 4 was not significantly different than those on past Delta flights. There is nothing to indicate the signature was not normal.

b. If premature ignition of the X-258 motor occurred, it was accomplished without firing the other ordnance devices, which were properly initiated at Sequence 4.

c. There is no evidence to indicate that a motor ignition signal was present prior to Sequence 4.

While this analysis does not pinpoint the cause of the failure on Delta 33, it does tend to eliminate one possible cause, the early (6 second before Sequence 4) ignition.

Current Distribution

The load on the engine battery at sequence 4 was calculated to determine the total current available from the battery. The current distribution was determined from this quantity. Figures C-11 through C-13 depict the load for three conditions of the sequence relay K703. First is the normal operation in which all bridgewires are connected to the engine battery through two contacts of the relay. Then, operation of each contact of the relay is considered. These might correspond to a momentary closure or short circuit. These are summarized in Table C-5.

Three special conditions were considered to determine the power that might be dissipated in the SD60AO squib with various combinations of open and short circuits. Figures C-14, C-15 and C-16 show these connections.

Douglas Aircraft Corp. calculated the initial current distribution when the Delta third stage was changed from the X-248 motor to the X-258 motor. These calculations were based on the use of a 1.5 ohm resistor in series with each bridgewire of the SD60AO squib. Delta 33 had RF filters instead of these resistors. These filters were added to provide additional RF protection for the SD60AO squibs. The earlier Douglas calculations (Table C-6) are presented for comparison to those obtained with the filters.

Third Stage Short Circuit

A third phase in the examination of the electrical system was the distribution of current if the third stage battery should short to the sequence 4 circuit at some point on the attach fitting. The results are shown in Figure C-17, and indicate this to be an unlikely failure mode. The third stage schematic is provided as Figure C-18.

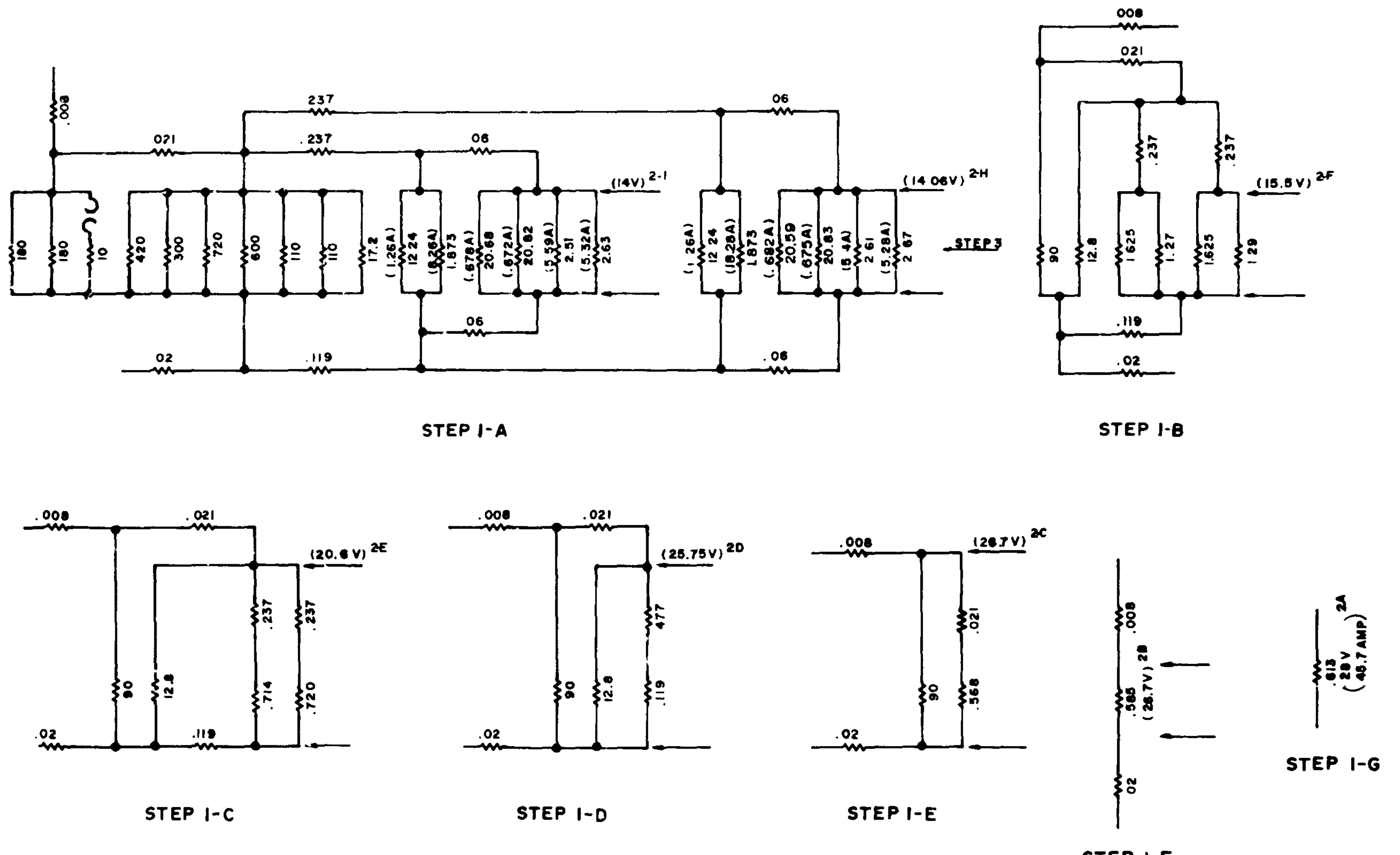

NOTE

ALL RESISTANCE VALUES IN OHMS

Figure C-11. Sequence 4 Initial Current Flow-Normal Operation

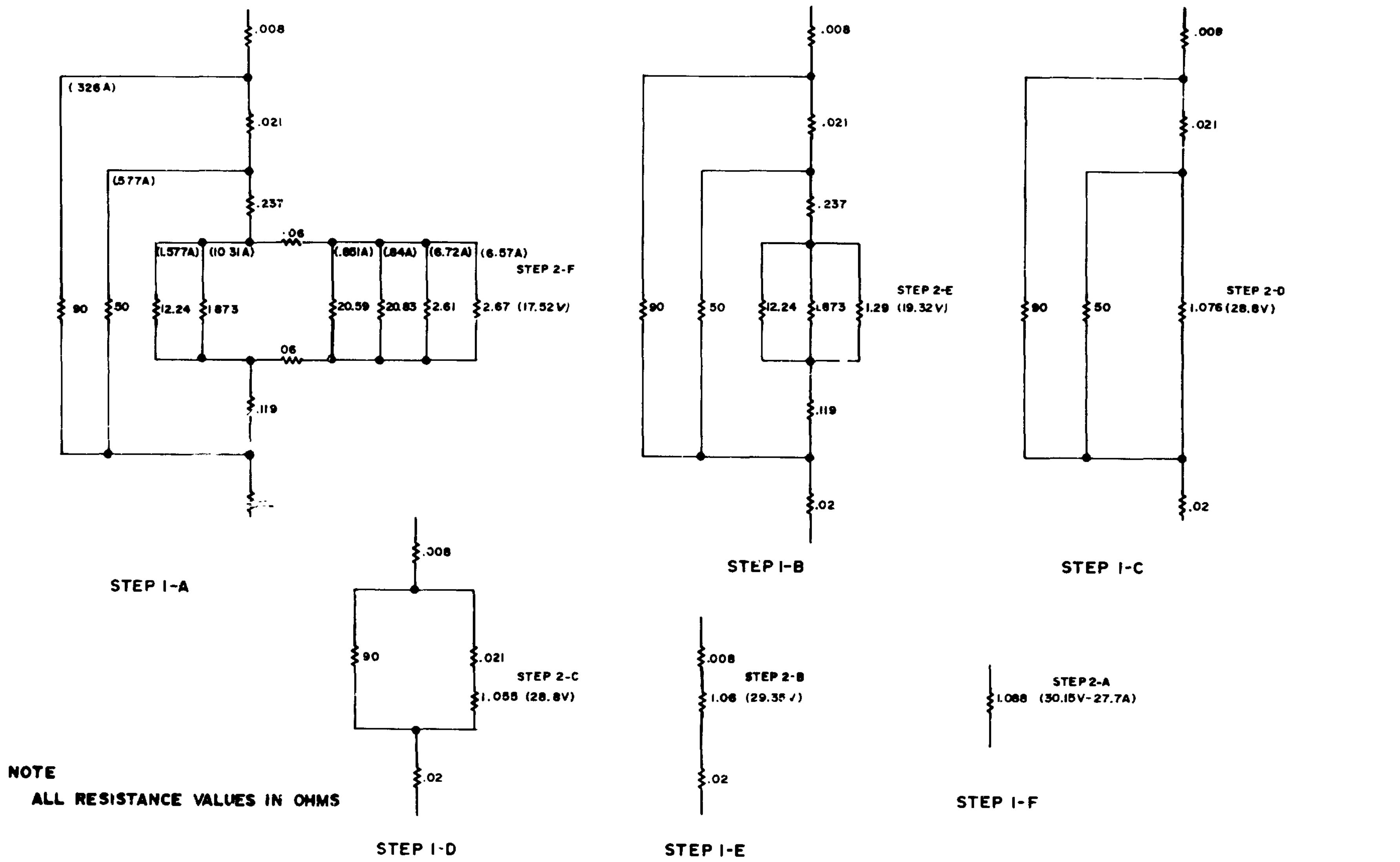

Figure C-12. Sequence 4 Current Flow if ½ of K703 Operates (Side A)

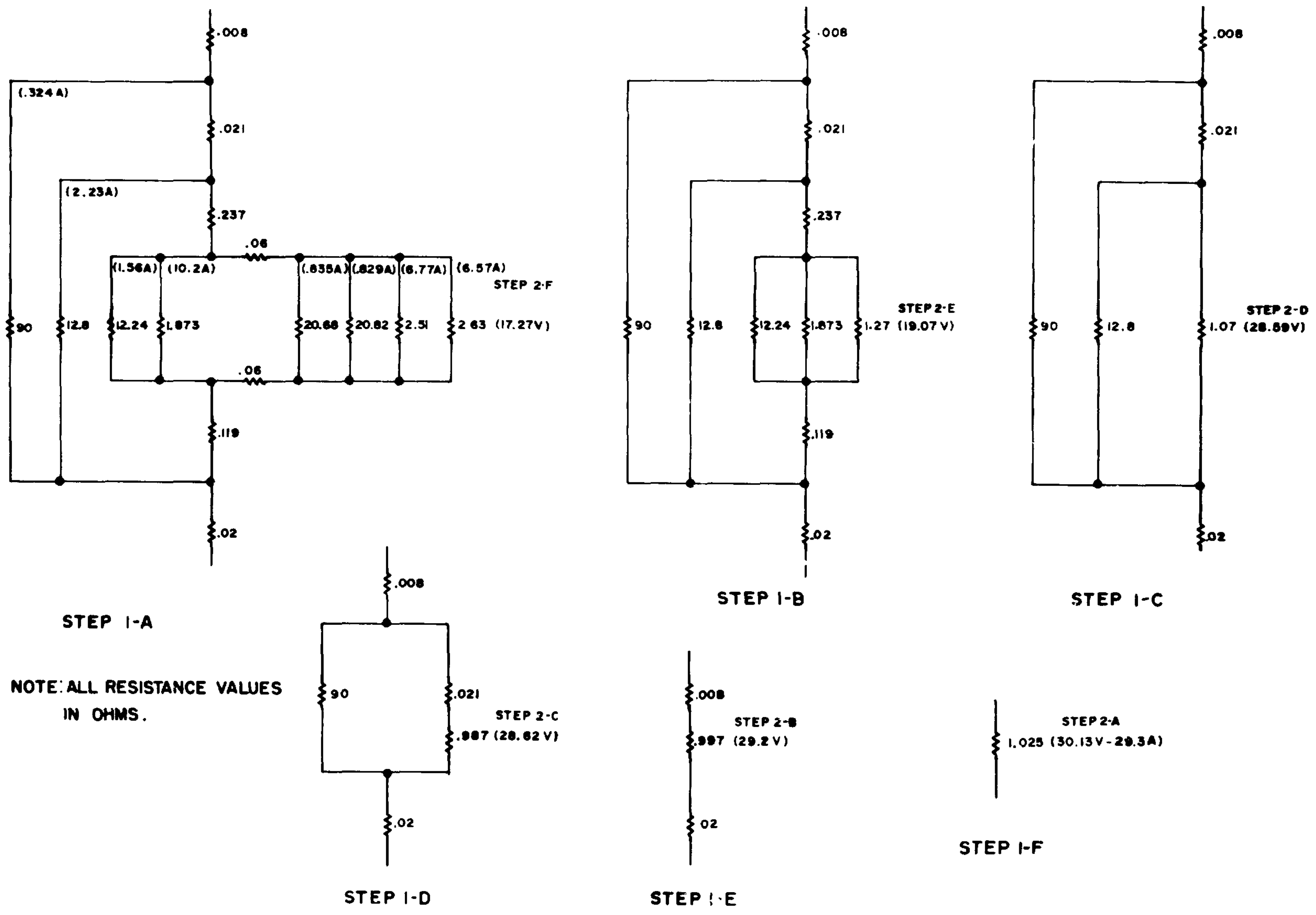

Figure C-13. Sequence 4 Current Flow ½ of K703 Operates Side B with S703

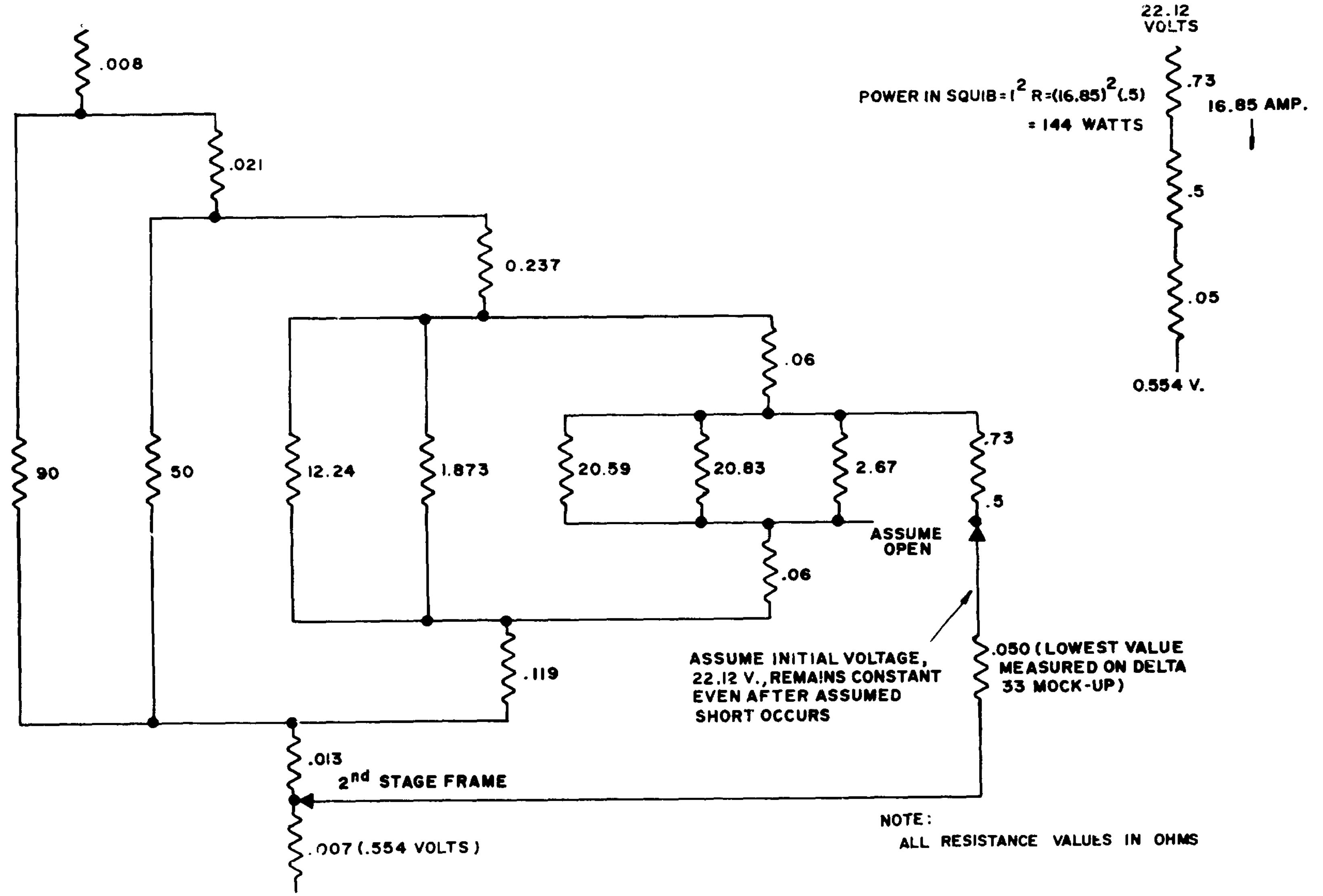

Figure C-14. Special Condition (Assumed Short to 3rd Stage Ground at Squib)

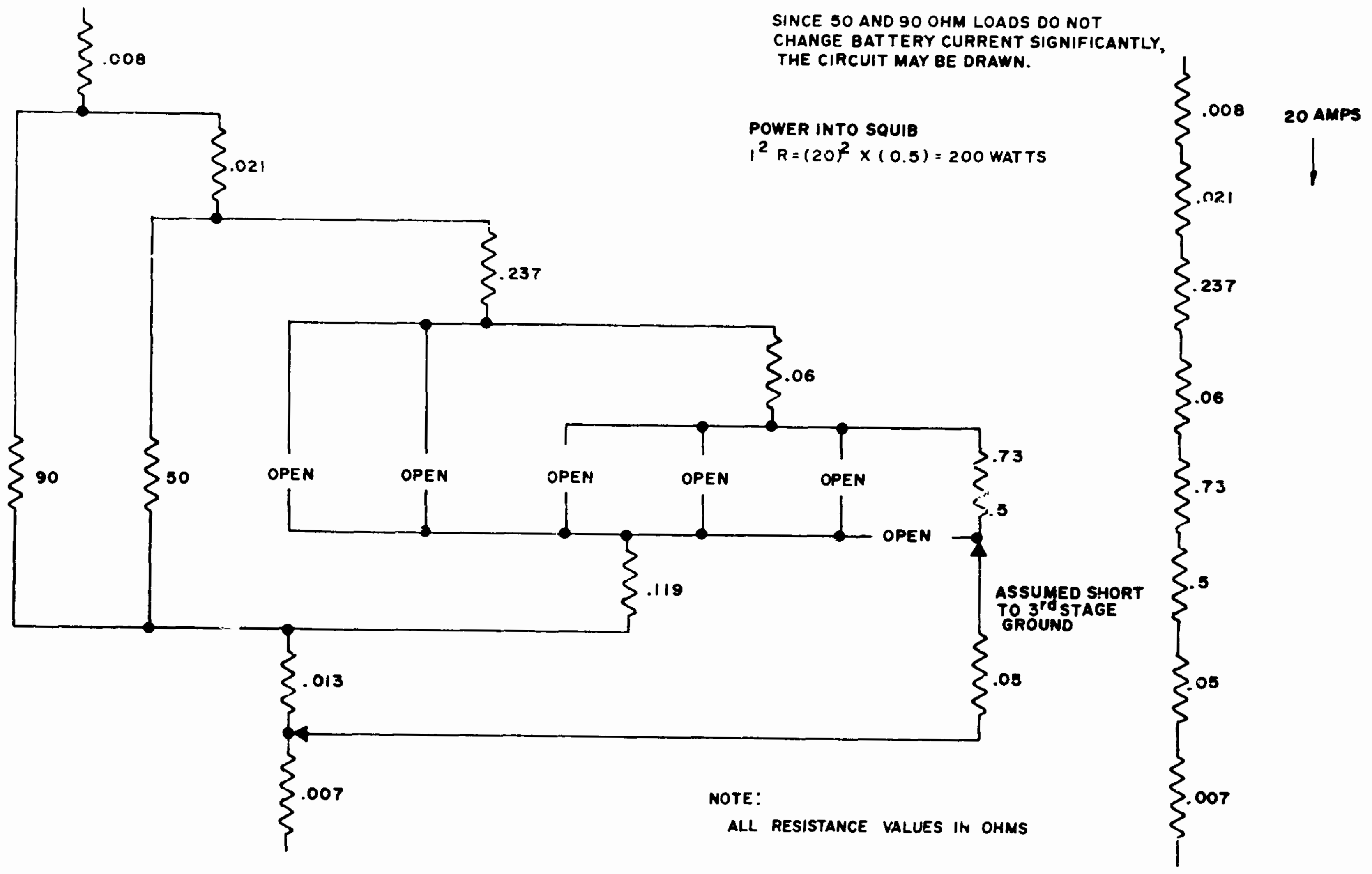

Figure C-15. Special Condition (Assume All Bridgewires Open After Initiation Except One SD60AO Bridgewire)

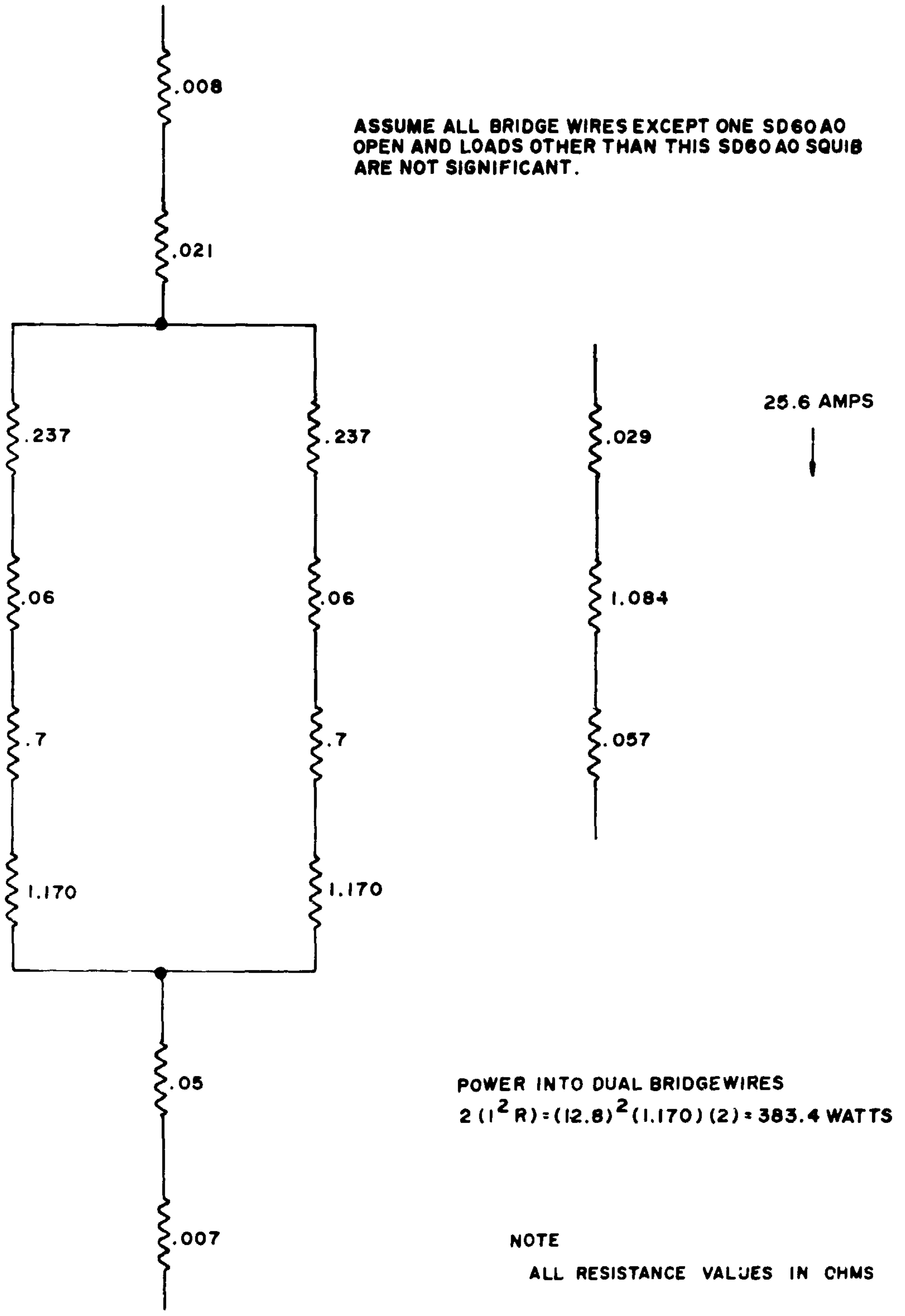

Figure C-16. Special Condition (Assume All Bridgewires Except One SD60AO Open and Loads Other Than This SD60AO Squib are not Significant)

TABLE C-6

	ORIGINAL ANALYSIS		RE-ANALYSIS		CHARACTERISTICS	
PYRO-TECHNIC	WORST CASE (AMPS)	NOMINAL (AMPS)	WORST CASE (AMPS)	NOMINAL (AMPS)	MINIMUM (AMPS)	RECOMMENDED (AMPS)
SPIN ROCKETS	1.08 1.08	1.22 1.185	1.0 0.732	1.12	0.50	1.0
OM 397 SQUIB SWITCH	N/A	1.465	N/A	1.54	0.80	1.0
OM 397 SQUIB SWITCH	1.5	1.72	1.3	1.46	0.80	1.0
DIMPLE MOTORS	0.735	0.91	0.575	0.835	0.25	1.0
X258 IGNITORS	4.93 4.94	6.30	5.0	5.82	4.5	5.0

A mock-up of the second and third stages as well as wiring diagrams and schematics were examined for proximity of power sources, terminals or any deficiency that might provide the means for a short duration pulse to energize the SD60AO squib. None were detected.

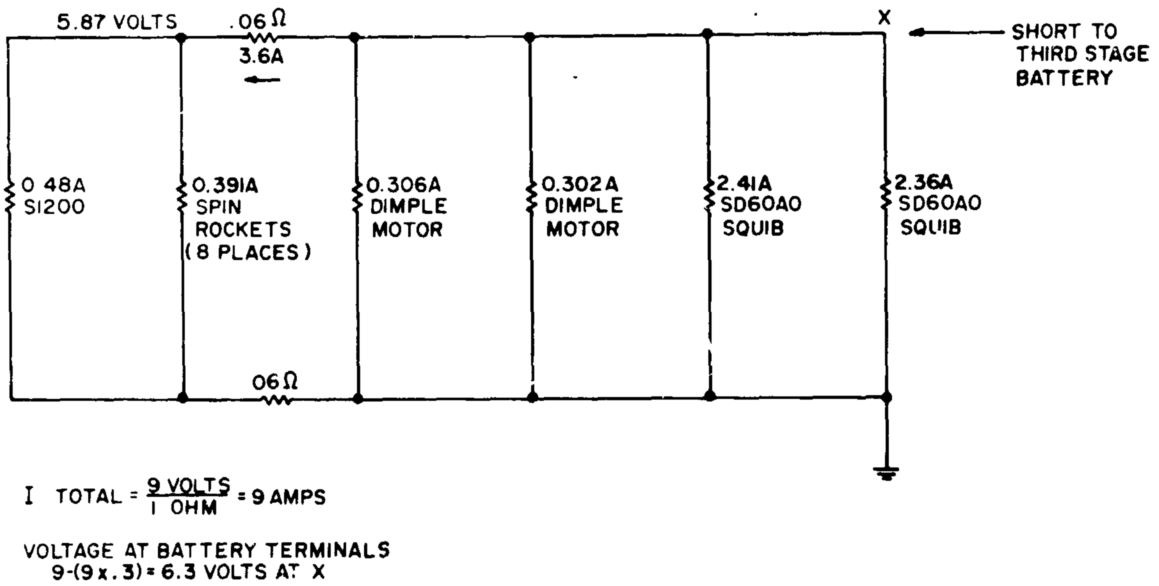

Figure C-17. Sequence 4 Current Distribution — Third Stage Short

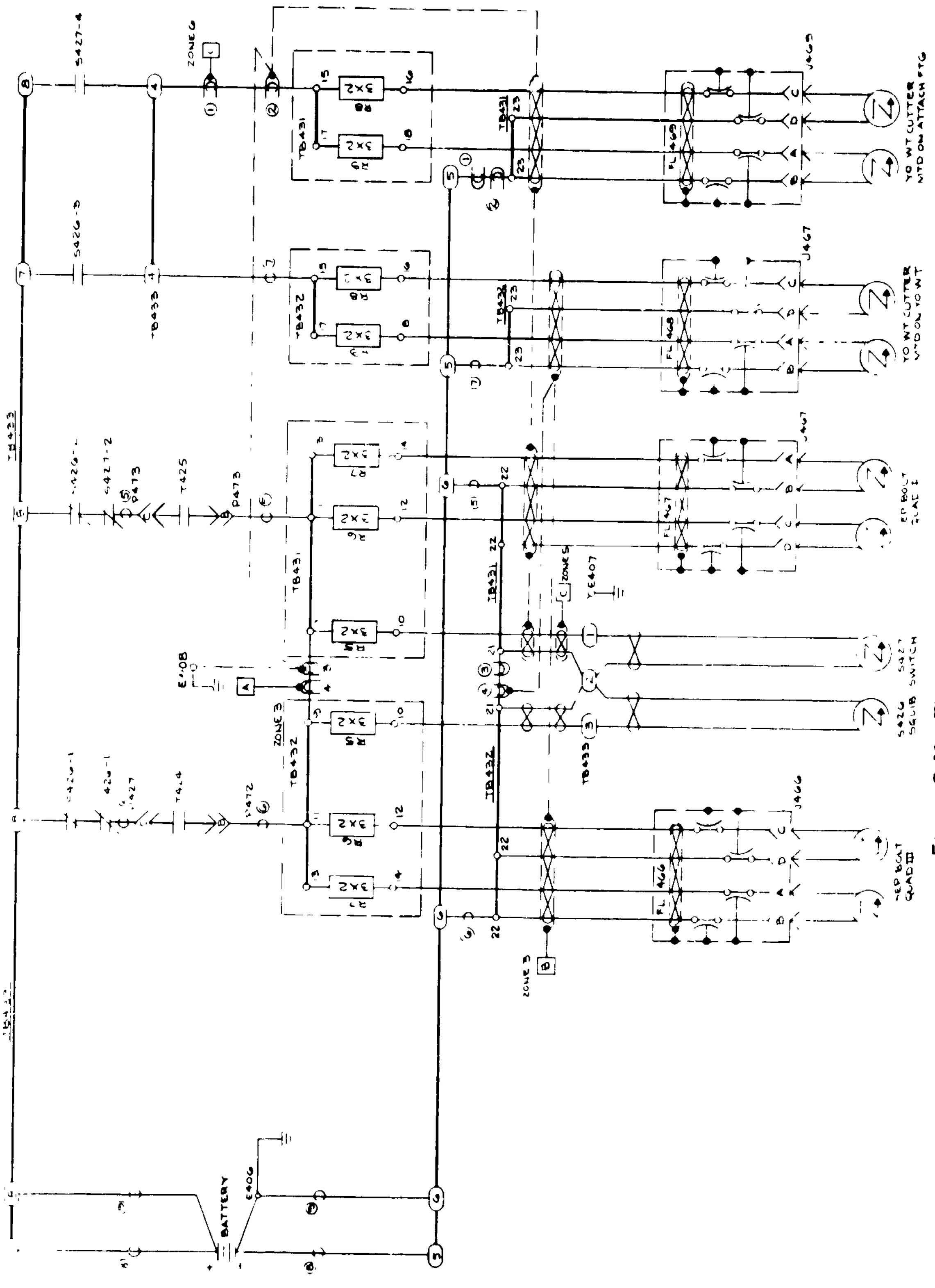

Figure C-18. Third Stage Schematic

APPENDIX C

INDEX TO FIGURES

APPENDIX C

INDEX TO FIGURES (Continued)

INDEX TO TABLES